$12.00
NASA-CR-88121
N67-36235
RE-ORDER NO. 67-347

NATL AERONAUTICS AND SPACE ADM ; NASA-CR-88121
COST ITEM $12.00

Special Report No. 2

May 15, 1967

DO NOT DESTROY
RETURN TO LIBRARY

THE RESULTS OF LONG-TERM STORAGE TESTS FOR COMPATIBILITY OF NITROGEN TETROXIDE WITH VARIOUS SPACECRAFT MATERIALS

Prepared for:

JET PROPULSION LABORATORY
CALIFORNIA INSTITUTE OF TECHNOLOGY
PASADENA, CALIFORNIA 91103

JPL CONTRACT NO. 951581
UNDER NAS7-100

JPL Technical Representative: H. B. STANFORD

15 JUN 1982
MCDONNELL DOUGLAS
RESEARCH & ENGINEERING LIBRARY
ST. LOUIS

By: R. F. MURACA AND J. S. WHITTICK

SRI Project No. ASD-6063

Approved: R. F. MURACA
ANALYSES AND INSTRUMENTATION

REPRODUCED BY
NATIONAL TECHNICAL
INFORMATION SERVICE
U.S. DEPARTMENT OF COMMERCE
SPRINGFIELD, VA. 22161

Copy No. .....

This work was performed for the Jet Propulsion Laboratory, California Institute of Technology, sponsored by the National Aeronautics and Space Administration under Contract NAS7-100.

106

N O T I C E

THIS DOCUMENT HAS BEEN REPRODUCED FROM THE BEST COPY FURNISHED US BY THE SPONSORING AGENCY. ALTHOUGH IT IS RECOGNIZED THAT CERTAIN PORTIONS ARE ILLEGIBLE, IT IS BEING RELEASED IN THE INTEREST OF MAKING AVAILABLE AS MUCH INFORMATION AS POSSIBLE.

RE-ORDER No. 67-3

ACKNOWLEDGMENT

Acknowledgment is made of the labor and contributions of the following chemists of the Department of Analyses and Instrumentation:

Dr. C. A. Crutchfield
Mrs. A. P. Longwell
Miss E. M. McCarthy
Mr. C. H. Martin
Mr. E. Willis

Preceding page blank

RE-ORDER No. 67-347

ABSTRACT

The results of corrosion tests are reported for various metallic and ceramic specimens which have been stored in sealed capsules with nitrogen tetroxide at 110°F for periods of 1-1/2 to 3 years. It was found that the least corroded materials are titanium alloys, iron alloys, cobalt alloys, some nickel alloys, tantalum, and alumina. Corroded materials are: molybdenum, magnesium, and some aluminum and nickel alloys. The materials were prepared and stored in contact with N_2O_4 by the Jet Propulsion Laboratory; terminal analyses were performed by the Stanford Research Institute.

Chemical analysis of the nitrogen tetroxide included determination of water content by a new gas chromatographic procedure, of nitric oxide by a spectrophotometric method, and of chloride content and residue by standard analytical procedures. Examination of solid specimens included determination of change in weight, microphotographic studies of corroded or degraded surfaces, x-ray examination of corrosion products. Gages and fittings used with the storage capsules were also examined in great detail. The results of the chemical and metallurgical determinations are given in tabular form, supplemented by numerous photographs of the surfaces of stored materials.

Conclusions are based on chemical and metallurgical determinations, a review of storage pressure data and procedures, and a computation of corrosion rates.

Preceding page blank

RE-ORDER No. 67-3

CONTENTS

ACKNOWLEDGMENTS iii

ABSTRACT v

TABLES ix

ILLUSTRATIONS xi

I INTRODUCTION 1

II PREPARATION AND STORAGE OF SAMPLES (JPL) 3

III ANALYTICAL PROCEDURES 9

IV GAS CHROMATOGRAPHIC METHOD FOR THE DETERMINATION OF THE WATER CONTENT IN NITROGEN TETROXIDE 19

V RESULTS OF STORAGE TESTS AND DISCUSSION 29

VI RECOMMENDATIONS FOR STORAGE PROCEDURES 95

Appendix A JPL PASSIVATING PROCEDURES 97

Appendix B ALLOY COMPOSITIONS 101

Preceding page blank

RE-ORDER No. 67-34

TABLES

Table 1	Identification of JPL Storage Tests: Treatment, Dimensions, and Storage Data	5
Table 2	Summary of Analyses of N_2O_4 Samples Stored in Contact with Metals Which Were Not Corroded	15
Table 3	Selected Weight Changes ±1 Mgm	16
Table 4	Calibration Data for Determination of H_2O in N_2O_4 by Gas Chromatography	25
Table 5	Relative Error of Gas Chromatographic Determination of H_2O in N_2O_4	25
Table 6	Range of Linearity of Calibration Curves: Gas Chromatographic Determination of H_2O in N_2O_4	25
Table 7	Results of JPL Storage Tests: Corrosion Rates	39
Table 8a	Analyses of N_2O_4 Stored with Titanium Alloys	41
Table 8b	Corrosion of Titanium Alloys Stored with N_2O_4	42
Table 9a	Analyses of N_2O_4 Stored with Aluminum Alloys	43
Table 9b	Corrosion of Aluminum Alloys Stored with N_2O_4	43
Table 10a	Analyses of N_2O_4 Stored with Iron Alloys	44
Table 10b	Corrosion of Iron Alloys Stored with N_2O_4	44
Table 11a	Analyses of N_2O_4 Stored with Nickel Alloys	45
Table 11b	Corrosion of Nickel Alloys Stored with N_2O_4	45
Table 12a	Analyses of N_2O_4 Stored with Various Metals	46
Table 12b	Corrosion of Various Metals Stored with N_2O_4	46
Table 13a	Analyses of N_2O_4 Stored with Alumina Materials	47
Table 13b	Corrosion of Alumina Materials Stored with N_2O_4	47

Preceding page blank

RE-ORDER No. 67-34

ILLUSTRATIONS

Fig. 1 Close-Up View of Storage Capsule (JPL) Showing Typical Specimen and N_2O_4 Content 7

Fig. 2 Typical Variation of Pressure During Nitrogen Tetroxide Compatibility Tests 8

Fig. 3 Photograph of Spectrophotometric Cell for Determination of NO in N_2O_4 17

Fig. 4 Typical Chromatogram 27

Fig. 5 Block Diagram of the Apparatus for the Determination of H_2O in N_2O_4 by Gas Chromatography 27

Fig. 6 Calibration Curve for H_2O in N_2O_4 by Gas Chromatography 28

Fig. 7 Appearance of Test Specimens 0066 to 0073 after Storage 48

Fig. 8 Appearance of Test Specimens 0076 to 0081 after Storage 49

Fig. 9 Appearance of Test Specimens 0082 to 0088 after Storage 50

Fig. 10 Appearance of Test Specimens 0110 to 246 after Storage 51

Fig. 11 Appearance of Test Specimens 247 to 255 after Storage 52

Fig. 12 Appearance of Test Specimens 256 to 262 after Storage 53

Fig. 13 Appearance of Test Specimens 0048, 0089, 0113, and 0117 after Storage 54

Fig. 14 Photomicrographs of Ends of Specimens after Storage (53X). (0066) 410 Stainless Steel; (0067) 416 Stainless Steel 55

Fig. 15 Photomicrographs of Ends of Specimens after Storage (53X). (0069) 430 Stainless Steel; (0070) 19-9 DL Stainless Steel 56

Fig. 16 Photomicrographs of Ends of Specimens after Storage (53X). (0072) 440C Stainless Steel; (0073) 1018 Steel 57

Preceding page blank

RE-ORDER No. 67-34

ILLUSTRATIONS (Continued)

Fig. 17 Photomicrographs of Ends of Specimens after Storage (53X). (0076) A-231C Magnesium Alloy; (0077) Tantalum 58

Fig. 18 Photomicrographs of Ends of Specimens after Storage (53X). (0078) Sintered Molybdenum; (0079) Arc-cast Molybdenum 59

Fig. 19 Photomicrographs of Ends of Specimens after Storage (53X). (0080) Inconel; (0081) Inconel-X 60

Fig. 20 Photomicrographs of Ends of Specimens after Storage (53X). (0082) Hastelloy B; (0083) Stellite Type 6 61

Fig. 21 Photomicrographs of Ends of Specimens after Storage (53X). (0084) Stellite Type 25; (0086) Nickel Span-C 62

Fig. 22 Photomicrographs of Ends of Specimens after Storage (53X). (0087) 6061-T6 Aluminum Alloy; (0088) Nickel, Type A 63

Fig. 23 Photomicrographs of Ends of Specimens after Storage (53X). (0110) 347 Stainless Steel Plus Rulon Coating; (0111) 6Al-4V Titanium Alloy Plus Rulon Coating 64

Fig. 24 Photomicrographs of Ends of Specimens after Storage (53X). (0112) 6061-T6 Aluminum Alloy Plus Rulon Coating; (0115) 6061-T6 Aluminum Alloy Plus Kel-F Grease Coating 65

Fig. 25 Photomicrographs of Ends of Specimens after Storage (53X). (0116) 6Al-4V Titanium Alloy Plus Kel-F Grease Coating; (246) 356-T6 Aluminum Alloy 66

Fig. 26 Photomicrographs of Ends of Specimens after Storage (53X). (247) 356-T6 Aluminum Alloy; (251) 6Al-4V Titanium Alloy 67

Fig. 27 Photomicrographs of Ends of Specimens after Storage (53X). (252) 6Al-4V Titanium Alloy; (253) 6Al-4V Titanium Alloy 68

Fig. 28 Photomicrographs of Ends of Specimens after Storage (53X). (254) 6Al-4V Titanium Alloy; (255) 6Al-4V Titanium Alloy 69

Fig. 29 Photomicrographs of Ends of Specimens after Storage (53X). (256) 6Al-4V Titanium Alloy; (257) 6Al-4V Titanium Alloy 70

RE-ORDER NO. 67

ILLUSTRATIONS (Continued)

Fig. 30 Photomicrographs of Ends of Specimens after Storage (53X). (258) 6A1-4V Titanium Alloy; (259) 6A1-4V Titanium Alloy 71

Fig. 31 Photomicrographs of Ends of Specimens after Storage (53X). (260) 6A1-4V Titanium Alloy; (261) 6A1-4V Titanium Alloy 72

Fig. 32 Photomicrograph of End of Specimen after Storage (53X). (262) 6A-14V Titanium Alloy 73

Fig. 33 Photograph of Typical Deposits Resulting from Corrosion of Kovar Metal Used to Connect the Sample Capsules to the Pressure Gages 74

Fig. 34 Photomicrograph of Kovar Tubing (53X) Showing Mild Attack. (1) inner surface; (2) exterior surface for comparison 75

Fig. 35 Photomicrograph of Kovar Tubing (53X) Showing Moderate Attack. (1) inner surface; (2) exterior surface for comparison 76

Fig. 36 Photomicrograph of Kovar Tubing (53X) Showing Strong Attack. (1) inner surface; (2) exterior surface for comparison. 77

Fig. 37 Photomicrograph of Kovar Tubing (53X) Showing Very Strong Attack. (1) inner surface; (2) exterior surface for comparison 78

Fig. 38 Photograph of Interior Surfaces of Four Kovar Seals Used in Nitrogen Tetroxide Storage Tests, Showing Extent of Corrosion from Mild to Severe . . . 79

Fig. 39 Photomicrographs of Internal and External Surfaces of Bourdon Tube from Test Gage No. 0072 (45X). (1) inner surface; (2) exterior surface for comparison 81

Fig. 40 Photomicrographs of Internal and External Surfaces of Bourdon Tube from Test Gage No. 0078 (45X). (1) inner surface; (2) exterior surface for comparison 82

Fig. 41 Photomicrographs of Internal and External Surfaces of Bourdon Tube from Test Gage No. 0082 (45X). (1) inner surface; (2) exterior surface for comparison 83

Fig. 42 Photomicrographs of Internal and External Surfaces of Bourdon Tube from Test Gage No. 0083 (45X). (1) inner surface; (2) exterior surface for comparison 84

RE-ORDER No. 67-3

ILLUSTRATIONS (Concluded)

Fig. 43 Photomicrographs of Internal and External Surfaces of Bourdon Tube from Test Gage No. 247 (45X). (1) inner surface; (2) exterior surface for comparison 85

Fig. 44 Photomicrographs of Internal and External Surfaces of Bourdon Tube from Test Gage No. 252 (45X). (1) inner surface; (2) exterior surface for comparison 86

Fig. 45 Photomicrographs of Internal and External Surfaces of Bourdon Tube from Test Gage No. 260 (45X). (1) inner surface; (2) exterior surface for comparison 87

Fig. 46 Photomicrographs of Internal and External Surfaces of Bourdon Tube from Test Gage No. 262 (45X). (1) inner surface; (2) exterior surface for comparison 88

Fig. 47 Photomicrographs of Internal and External Surfaces of Bourdon Tube from Gage "A" Not Exposed to N_2O_4 (53X). (1) inner surface; (2) exterior surface for comparison 89

Fig. 48 Photomicrographs of Internal and External Surfaces of Bourdon Tube from Gage "B" Not Exposed to N_2O_4 (53X). (1) inner surface; (2) exterior surface for comparison 90

Fig. 49 Enlarged photomicrograph of Test Specimens after Removal of Corrosion Products (10X). (246) 356-T6 Aluminum Alloy; (247) 356-T6 Aluminum Alloy 91

Fig. 50 Enlarged Photomicrographs of Test Specimens after Removal of Corrosion Products (10X). (0082) Hastelloy B; (0076) Magnesium A231C 92

Fig. 51 Enlarged Photomicrograph of Test Specimens after Removal of Corrosion Products (10X). (0078) Sintered Molybdenum; (0079) Arc-Cast Molybdenum . . . 93

RE-ORDER No. 67-34

I. INTRODUCTION

The program for Advanced Liquid Propulsion Systems (ALPS) at the Jet Propulsion Laboratory, California Institute of Technology, is concerned with the design of liquid propulsion systems which employ storable propellants such as N_2O_4 and N_2H_4. The system is to be operable on command while in the space environment for more than two years. In order to select suitable materials of construction for the N_2O_4-N_2H_4 system, about 2000 samples of commercial alloys and refractories have been stored with nitrogen tetroxide or hydrazine in sealed capsules at 110°F for periods of time in excess of one year.

Under Contract No. 951581 with the Jet Propulsion Laboratory, the Stanford Research Institute has undertaken to analyze a number of the stored samples and propellants (Phase I).

This report summarizes the results of 41 storage tests of various materials in nitrogen tetroxide (N_2O_4). Section II describes the preparation and storage of the samples by JPL.

In Section III, details are given for the procedures used at SRI for the analyses of the test specimens and N_2O_4, and a new gas chromatographic procedure for the determination of water in nitrogen tetroxide is described fully in Section IV.

The results of the analyses are presented in tabular form in Section V; this Section includes photographs of the surfaces of the materials after storage. The interpretation of the results and discussions of storage problems are also presented in this Section, as well as a summary of corrosion rates.

Section VI consists of brief comments on storage procedures.

In the Appendixes are outlines of JPL passivating procedures for specimens prior to storage and the compositions of materials and alloys used in these tests.

RE-ORDER No. 67-34

II. PREPARATION AND STORAGE OF SAMPLES (JPL)

All specimens were cleaned and passivated according to standardized JPL procedures and then weighed on an analytical balance. As shown in Figure 1, the sample specimens were generally of a cylindrical shape and were immersed in about 20 ml of nitrogen tetroxide (Mil-Spec grade) at a depth of one-half to two-thirds their lengths in glass capsules. The capsules were attached to stainless steel Bourdon-type gages (LOX-cleaned and adjusted to read absolute pressure) by means of Kovar-to-glass seals. After introduction of sample and propellant, the capsules were sealed-off under vacuum. The information provided SRI on the materials in the JPL storage tests is summarized in Table 1 and includes weights, dimensions, and storage data. Passivation procedures, listed in Table 1 according to JPL Log Numbers, are described in Appendix A of this report.

The storage times of the test capsules examined during this phase of the work were either 1-1/2 years or more than 3 years. During the long periods of storage at 110 ± 5°F at the Edwards Test Station (Edwards Air Force Base, California), the pressure of each sample was recorded almost daily; the recorded pressures fall within the general range of 34-42 psia with an average pressure of about 38-39 psia, as shown in the pressure curves for two typical storage tests in Figure 2. Because the vapor pressure* of the $N_2O_4 \rightleftharpoons 2\ NO_2$ system is 38.6 psia at 110°F and the limits for bath temperature are ±5°F, the recorded vapor pressure of an unaltered propellant should vary between 34 and 43 psia; excursions of the observed pressures in excess of this range are visible in Figure 2 and must be due to fluctuations in bath temperatures.

---

* Muraca, R.F. et al., "Design Data for Pressurized Gas Systems," Stanford Research Institute, Contract No. NAS7-105, November 1963.

Preceding page blank

On a few occasions, recorded pressures dropped to 16-20 psia but adjustment of the bath temperature brought them back to average storage pressures. Three tests which ranged below the average (26-29 psia) or above (42-47 and 40-44 psia) will be discussed later.

At the termination of the storage tests, the sample capsules were cooled to dry-ice temperature and delivered to SRI at this temperature. Upon receipt of samples at SRI, the capsules were removed from the solid carbon dioxide matrix, wiped with cold isopropyl alcohol to remove condensed water and immediately stored in a deep-freeze cabinet. (The isopropyl alcohol wash also removed vestigial amounts of N_2O_4 originating from broken capsules in the shipments.)

RE-ORDER No. 67-31

Table 1

IDENTIFICATION OF JPL STORAGE TESTS:
TREATMENT, DIMENSIONS, AND STORAGE DATA

JPL TEST NO.	MATERIAL	PASSIVATED, LOG NO.[a]	WEIGHT, g	AREA,[b] cm^2	STORAGE TIME, YR	STORAGE PRESSURE, psia
0048	Sapphire ball (Al_2O_3)	0094	1.8050	2.54	3.4	37-40
0066	410 stainless steel	0090	16.9486	14.97	3.8	36-40
0067	416 stainless steel	0090	16.7660	14.97	3.8	36-40
0069	430 stainless steel	0090	16.7428	14.97	3.8	36-40
0070	19-9 DL stainless steel	0090	17.6032	14.97	3.8	35-38
0072	440C stainless steel	0090	16.7623	14.97	3.8	35-38
0073	1018 steel	0097	17.2793	14.97	3.8	36-40
0076	A-231C magnesium alloy	0092	3.9208	14.97	3.8	36-40
0077	Tantalum	0096	35.3329	14.97	3.8	37-42
0078	Sintered molybdenum	0095	22.4456	14.97	3.8	36-40
0079	Arc-cast molybdenum	0095	22.5626	14.97	3.8	37-40
0080	Inconel	0094	18.6093	14.97	3.8	36-40
0081	Inconel-X	0094	18.2083	14.97	3.3	38-40
0082	Hastelloy B	0094	20.0192	14.97	3.8	37-42
0083	Stellite Type 6	--	18.4350	14.97	3.8	36-41
0084	Stellite Type 25	--	20.0666	14.97	3.8	37-42
0086	Nickel Span-C	0094	16.4977	14.97	3.3	39-40
0087	6061-T6 aluminum alloy	0088	5.9013	14.97	3.8	36-40
0088	Nickel, Type A	0094	19.5195	14.97	3.8	36-40
0089	Ceramic ball, sintered Al_2O_3	--	1.7193	3.14	3.8	37-41
0110	347 stainless steel	0090	17.4959	14.97	3.6	34-38
	+ Rulon coating[c]		0.0027			
0111	6Al-4V titanium alloy	0093	9.0809	14.97	3.2	38-40
	+ Rulon coating[c]		0.0034			
0112	6061-T6 aluminum alloy	0088	5.8720	14.97	3.2	37-38
	+ Rulon coating[c]		0.0026			
0113	Ceramic ball, fused Al_2O_3	--	4.1242	5.31	3.6	36-40
	+ Rulon coating[c]		0.0012			
0115	6061-T6 aluminum alloy	0088	5.8982	14.97	3.1	39-40
	+ Kel-F grease coating		0.0956			

RE-ORDER No. 67-34

Table 1 (Concluded)

JPL TEST NO.	MATERIAL	PASSIVATED, LOG NO.[a]	WEIGHT, g	AREA,[b] cm^2	STORAGE TIME, YR	STORAGE PRESSURE, psia
0116	6Al-4V titanium alloy + Kel-F grease coating	0093	9.1404	14.97	3.1	39-40
0117	Ceramic ball + Kel-F grease coating	--	4.1284 0.0625	5.31	3.6	37-41
246	356-T6 aluminum alloy	--	5.7170	14.97	1.9	40-44
247	356-T6 aluminum alloy	--	5.7848	14.97	1.9	37-40
251	6Al-4V titanium alloy	0093	9.1831	14.97	1.5	36-40
252	6Al-4V titanium alloy	0093	9.174	14.97	1.5	36-40
253	6Al-4V titanium alloy	0093	9.0606	14.97	1.5	36-40
254	6Al-4V titanium alloy	0093	9.2949	14.97	1.5	34-40
255	6Al-4V titanium alloy	0093	9.7432	14.97	1.5	34-39
256	6Al-4V titanium alloy	0093	9.4186	14.97	1.5	26-29
257	6Al-4V titanium alloy	0093	9.3990	14.97	1.5	36-40
258	6Al-4V titanium alloy	0093	9.6275	14.97	1.5	33-38
259	6Al-4V titanium alloy	0093	9.6719	14.97	1.5	42-47
260	6Al-4V titanium alloy	0093	9.5690	14.97	1.5	38-41
261	6Al-4R titanium alloy	0093	9.0596	14.97	1.5	34-39
262	6Al-4V titanium alloy	0093	9.5815	14.97	1.5	36-40

[a] All samples (except the ceramic balls) were cleaned according to JPL Log #0087: degreased by immersion in acetone or by vapor degreasing, followed by air-drying and then passivated d according to the listed Log Nos.; passivating procedures are outlined in Appendix A.

[b] All specimens (except the ceramic balls) were 0.6 cm diameter and 7.65 cm length rods.

[c] Rulon: A fluorocarbon-based spray, Connecticut Hard Rubber Co., New Haven, Conn.

RE-ORDER NO. 67-34

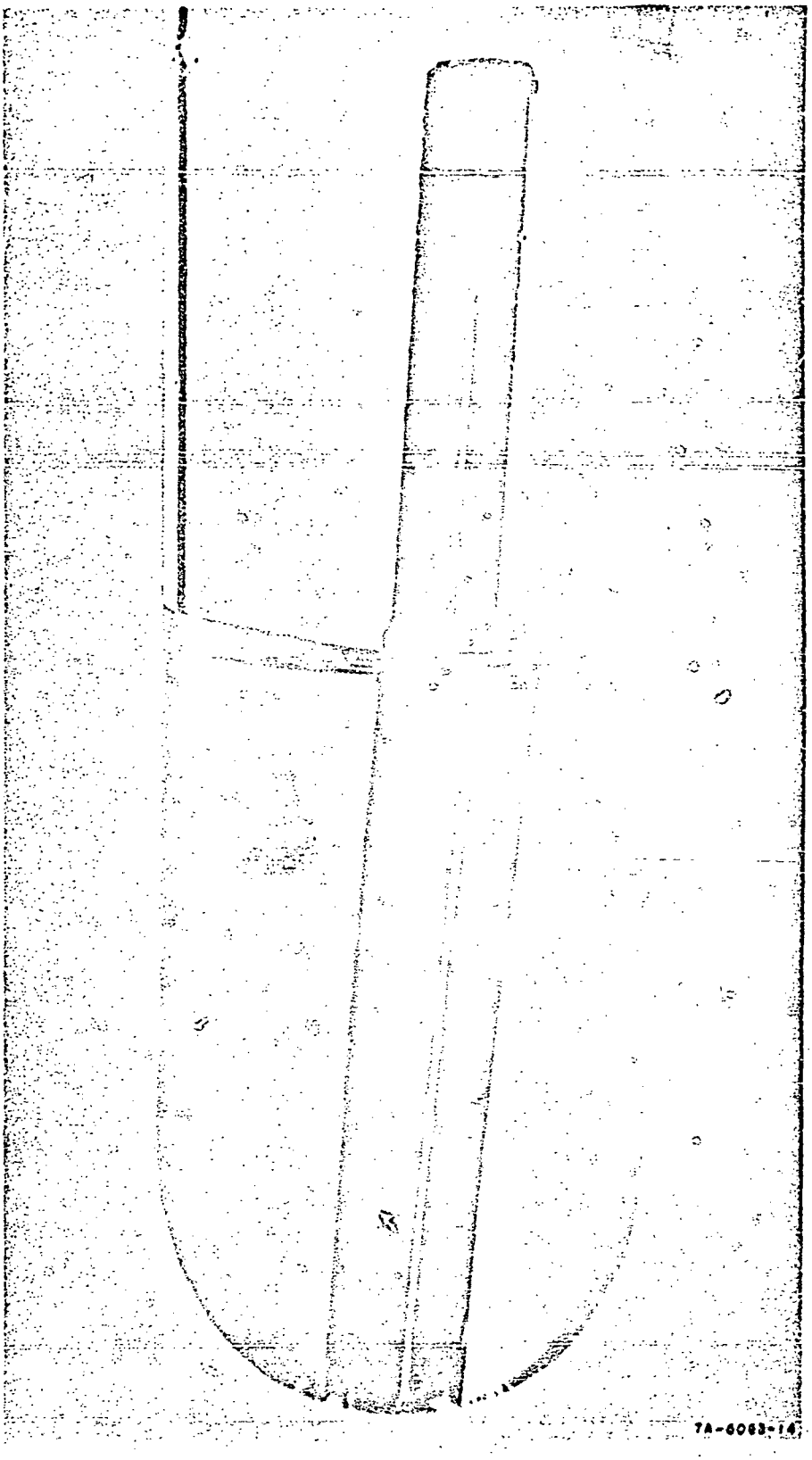

FIG. 1 CLOSE-UP VIEW OF STORAGE CAPSULE (JPL) SHOWING TYPICAL SPECIMEN AND N_2O_4 CONTENT

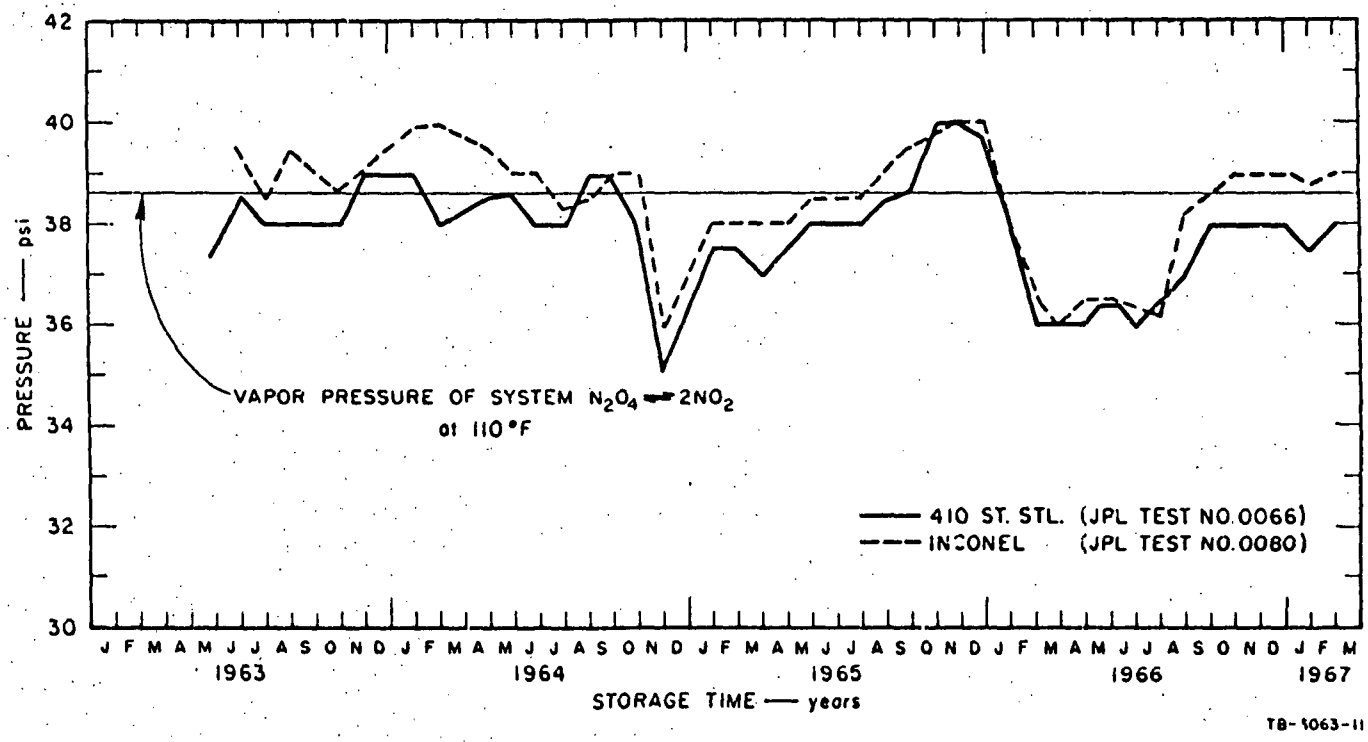
42
40
38
36
34
32
30
PRESSURE — psi
VAPOR PRESSURE OF SYSTEM $N_2O_4 \rightleftharpoons 2NO_2$
at 110°F
410 ST. STL. (JPL TEST NO.0066)
INCONEL (JPL TEST NO.0080)
J F M A M J J A S O N D J F M A M J J A S O N D J F M A M J J A S O N D J F M A M J J A S O N D J F M
1963
1964
1965
1966
1967
STORAGE TIME — years
TB-1063-11

FIG. 2 TYPICAL VARIATION OF PRESSURE DURING NITROGEN TETROXIDE COMPATIBILITY TESTS

RE-ORDER No. 67-347

III. ANALYTICAL PROCEDURES

The capsules received at SRI were stored in a deep-freeze cabinet. Before a capsule was opened, the color of the frozen N_2O_4 was observed and the gage pressure was noted. The contents of the capsules were allowed to thaw partially in order to determine the pressure developed at the melting point of N_2O_4; deviation of the gage pressure from the triple point pressure suggested the evolution of a gas such as O_2, NO, or CO_2 or that the gage had lost calibration. The capsule was then removed to a dry-box and maintained at LN_2 temperature in an atmosphere of dry helium so that its gage could be removed and replaced with a stainless steel valve; stainless steel Swagelok fittings were used.

The capsule was then attached to a stainless steel system to permit sampling of the liquefied propellant for water and nitric oxide. Following these analyses, the capsule was disconnected and returned to the dry-box and N_2O_4 was withdrawn for chloride ion and residue determinations.

The capsule was wiped with isopropyl alcohol and immersed in LN_2 in an atmosphere of dry helium while the neck was broken. The specimen in the capsule was removed and washed thoroughly with ethylene dichloride prior to removal from the dry-box. (Ethylene dichloride dissolves N_2O_4; the washing reduces probability of eventual corrosion of metal samples by reaction of N_2O_4 with atmospheric moisture.) The specimen was bottled, labeled and examined as required. Solid materials clinging to the walls of the capsule were removed and analyzed. Remaining N_2O_4 was evaporated, ashed, and retained.

RE-ORDER No. 67

A. NITROGEN TETROXIDE ANALYSES

Water Content

The new gas chromatographic procedure for the determination of water in nitrogen tetroxide was developed under this contract; it is presented in Section IV so that it may be described in complete detail.

Nitric Oxide

Nitric oxide was determined by a spectrophotometric procedure recently developed by C. M. Wright, A. A. Orr, and W. J. Billing of Hercules Inc. The authors were kind enough to forward their pre-publication paper and complete design drawings for the construction of a special cell; the gift of a calibrated filter is gratefully acknowledged. The spectrophotometric cell (shown in Figure 3) is constructed of materials which are inert to N_2O_4, can be cooled to temperatures near 0°C, is leak-proof under moderate conditions of pressure and vacuum, and has a path length suitable for measuring NO contents in the range of 0% to 1.5%.

The procedure for making the determination is simple and straightforward. Ice-water is circulated through the cooling coils of the cell and then a few milliliters of N_2O_4 are released from the sample container (fitted with a suitable valve) and allowed to flow through the cell. When the cell is thoroughly flushed with N_2O_4 and free of vapor bubbles, all valves are closed in sequence from the outlet valve of the cell to the valve on the sample container. The cell is placed in the sample compartment of a Beckman Model B spectrophotometer, which is purged with nitrogen to prevent fogging of the cell windows. The absorbance is read at 700 mμ and 550 mμ; the difference in the two readings is compared with the calibration chart and read directly as per cent NO.

Chloride Ion

To determine chloride ion, 5 ml of N_2O_4 was introduced into cold, excess 4N KOH solution which was then acidified with nitric acid. Sulfamic acid was added to destroy the resulting nitrous acid (completed

RE-ORDER No. 67-34

when evolution of nitrogen ceased) and the solution was titrated with silver nitrate solution (potentiometric end point).

Residue

Nonvolatile material was determined by evaporating about 5 ml of N_2O_4 in a platinum crucible at 100°C and weighing the residue. The residue was then ignited at 500°C to remove organic matter and to convert inorganic salts to oxides. No further analysis was made of the final residues since they seldom exceeded 0.01% and were generally less than 0.001%. The weight of residue obtained by evaporation at 100°C is an indication of the organic matter dissolved or suspended in the N_2O_4 sample.

Because of the sampling techniques required for the determination of NO, H_2O, Cl^-, and soluble residue, only qualitative information was obtained for sludge and other insoluble matter which were present in several of the samples. These materials were analyzed by x-ray fluorescence for major elemental composition.

Initial N_2O_4 Composition

It is of interest to determine the effect on N_2O_4 composition brought about by its attack on various materials. Ordinarily, corrosion studies are set up so that a large body of the corroding fluid is used for an extended series of tests and the composition of the fluid is determined accurately at the start; following exposure, the composition of the fluid in contact with specimens is then re-determined. By inclusion of suitable "blanks" in the test series, the effect of the test environment on the corroding fluid is easily assessed.

No "blanks" were shipped to SRI from the JPL test site, and samples of the original N_2O_4 used to fill the test capsules are not available.

In order to provide a norm for determining the changes in N_2O_4 composition brought about by its attack on specimens, the values indicated in Table 2 were collected from the analytical results

obtained from test capsules in which no (or trifling) corrosion of the test specimen was observed. As indicated in Table 2, the values visibly fall into two categories, corresponding to the two loadings of test capsules, and strongly suggest that two batches of N_2O_4 were involved (or that a 1-1/2 year storage of one batch resulted in its giving H_2O and NO). The close grouping of the results for H_2O and NO about the average indicates that the filling of the test capsules was effected under rigid control.

The average values for H_2O, NO, and Cl^- for the 1-1/2 and the 3-year batches given in Table 2 are used as norms in this report.

B. SPECIMEN ANALYSES

Weight Change and Corrosion Rate

The specimens were weighed to ±0.2 mg and the weight compared with the original value provided by JPL in order to compute the extent of corrosion. Specimens which showed an increase in weight of more than 1 mg were re-weighed after the removal of corrosion products or foreign matter by washing with water and rubbing with a soft cloth. Then, corrosion values were computed from the loss of weight of the specimen; it was assumed that corrosion had taken place uniformly over the entire surface of the specimen.

Since there is always the question of accuracy of weighing by different operators using different balances, specimens with weight changes differing only by less than 1 mg were isolated so that the values could be examined in related groups; these are listed in Table 3. Since the values for the 1.5-year storage tests are predominantly negative and those for the 3-year tests are positive, it becomes necessary to examine the possibility that the bias originates in the setting or calibration of the balances.

The first grouping in Table 3 (titanium alloys) indicates a definite trend to a loss in weight averaging about -0.0003 g, a rather small number which might be considered as balance-operator differences. However, the N_2O_4 remaining (5-10 ml) after the primary analyses had been evaporated, ashed and retained; thus, a number of residues were available for subsequent qualitative analyses which definitely proved the presence of titanium in these residues, which could derive only from the loss of titanium from the specimens. Hence, the loss in weight is meaningful and a corrosion rate can be calculated. If the average calculated corrosion rate for titanium alloys were re-computed on the basis of a ±0.2 mg difference between balances and operators,* the value might be expressed as ±50% (abs.), still a small number.

The second class of materials listed in Table 3 are iron alloys; for these specimens, there is a definite increase in weight. Whereas titanium alloys may form soluble (in N_2O_4) substances, corrodible iron alloys are more apt to be converted into nitrates which adhere to the specimens and cause increases in weight. One specimen, showing a 0.2 mg increase in weight after storage, was washed with distilled water and polished with a soft cloth; the resulting final weight loss of about 0.2 mg is equivalent to a corrosion rate of about 0.2 µin/yr, commensurate with the rate computed from the increase of weight as being due to an adherent nitrate. The same correlation has been shown between calculated weight-loss based on the adherence of 2-20 mg of corrosion products on other alloys and metals and the actual loss in weight recorded after the products were removed.

In view of the above findings, it may be assumed that the differences listed in Table 3 are significant and that the maximum deviation between samples weighed at JPL and at SRI is of the order of ±0.2 mg.

---

* National Bureau of Standards, Circular No. 3, 1918.

RE-ORDER No. 67-3

Microscopy and Photography

All specimens were examined under a microscope for evidence of corrosion or irregular features. Photomicrographs of the ends of the cylindrical specimens immediately after initial weighing were taken on Polaroid film (PN55) with a Graflex 4 x 5 camera; the ceramic balls were not amenable to this type of photography. In order to obtain depth of field, photomicrographs of several specimens were made at low magnifications after the removal of corrosion products, and then enlarged photographically to show the extent of corrosion.

Full-size photographs were taken of all specimens so that their original appearance upon removal from the N_2O_4 might be recorded.

Corrosion Products

The major components of the corrosion products were determined by x-ray diffraction and fluorescence.

C. ANALYSES OF FITTINGS AND GAGES

Observations were made of the internal surfaces of the Kovar tubing and the Bourdon tubes in the pressure gages which had been attached to the test capsules. Evidences of corrosion were sought, where possible, by the techniques described for specimen analyses, that is, microscopy, photomicrography, and x-ray diffraction and fluorescence analyses.

RE-ORDER NO. 67-347

Table 2

SUMMARY OF ANALYSES OF N_2O_4 SAMPLES STORED IN CONTACT WITH METALS WHICH WERE NOT CORRODED

STORAGE TIME	JPL TEST NO.	H_2O	NO	Cl^-
1-1.2	251	0.060	0.014	0.0010
years	253	0.070	0.014	0.0010
	254	0.070	0.015	0.0007
	255	0.052	0.018	0.0007
	256	0.057	0.015	< 0.0005
	257	0.060	0.013	< 0.0005
	261	0.046	0.015	< 0.0005
	262	0.052	0.015	< 0.0005
	$\bar{X}$ =	0.058	0.015	0.0007
	σ =	15.0%	12.0%	27.0%
	One-sigma =	(0.047%-0.067%)	(0.013%-0.017%)	(0.0005%-0.0009%)
3+	0087	0.020	0.017	0.0010
years	0112	0.034	0.016	< 0.0005
	0069	0.010	0.044	0.0005
	0073	0.020	0.015	< 0.0005
	0111	0.034	0.060	< 0.0005
	0086	0.022	0.040	< 0.0005
	0083	0.010	0.031	< 0.0005
	0084	0.025	0.054	< 0.0005
	0089	0.027	0.040	< 0.0005
	0113	0.027	0.059	0.0010
	$\bar{X}$ =	0.022	0.037	0.0006
	σ =	33.5%	38.7%	28.0%
	One-sigma =	(0.015%-0.029%)	(0.023%-0.051%)	(0.0004%-0.0008%)

RE-ORDER No. 67-3

Table 3

SELECTED WEIGHT CHANGES, ±1 MGM

ALLOY CLASS	STORAGE, YEARS	JPL TEST NO.	S. WT., g JPL	WT. CHANGE, g, SRI
Titanium	1.5	25₁	9.1831	-0.0006
		252	9.174	-0.0005
		253	9.0606	-0.0007
		254	9.2949	-0.0003
		255	9.7432	-0.0006
		256	9.4186	-0.0002
		257	9.3990	-0.0003
		258	9.6275	-0.0006
		259	9.6719	+0.0004
		260	9.5690	+0.0002
		261	9.0596	-0.0006
		262	9.5815	-0.0004
Iron	3.8	0066	16.9486	+0.0003
		0067	16.7660	+0.0004
		0069	16.7428	+0.0002
		0070	17.6032	+0.0001
		0072	16.7623	+0.0009
		0073	17.2793	-0.0003

Reproduced from best available copy.

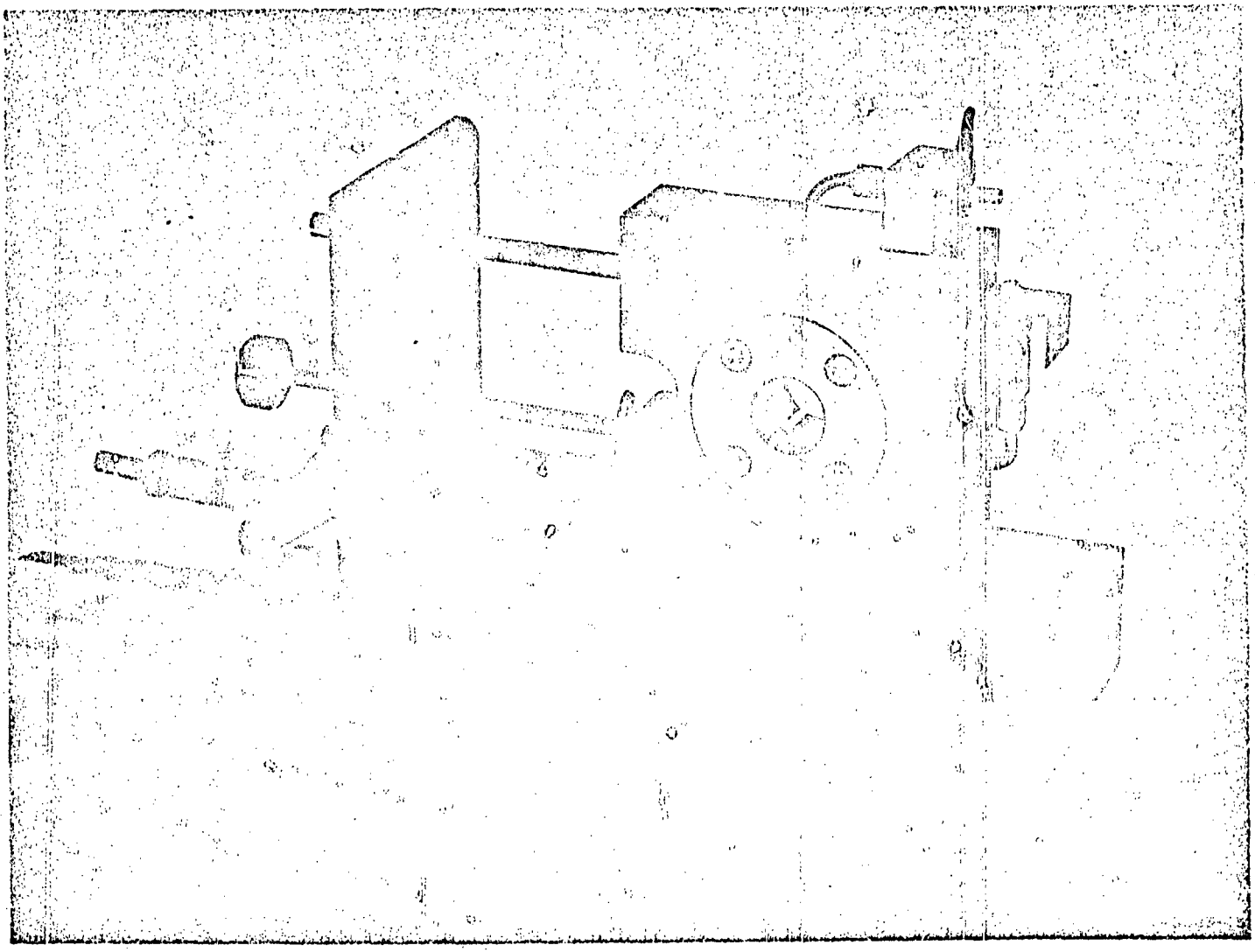

FIG. 3 PHOTOGRAPH OF SPECTROPHOTOMETRIC CELL FOR DETERMINATION OF NO IN N_2O_4.

RE-ORDER NO. 67-34

(Page 18, 19)

This page was missing from the report when received by NTIS. Repeated efforts to obtain a replacement page have been unsuccessful.

This report is being made available in its present form with the hope it will be of sufficient value to justify its announcement and distribution.

RE-ORDER No. 67-34

Numerous papers (e.g., 3,4,5,6) have appeared in the literature on gas chromatographic analysis of the impurities in N_2O_4, but a successful method for the direct determination of water has not been reported. Although GLC columns coated with an organic substrate separate water cleanly, the oxidizing nature of N_2O_4 precludes direct determination with these columns. On the other hand, columns prepared from inert materials, such as silica gel and molecular sieves, are too polar and lead to excessive tailing of the water peak; hence, it is not possible to make quantitative measurements of the water content in N_2O_4 even with these columns.

It has been found that the problems posed by the reactive nature of N_2O_4 can be circumvented by passing it over hot copper before it reaches the gas chromatograph, whereupon it and the nitric acid content are converted quantitatively to nitrogen and water; the free water content simply passes through. A typical chromatogram showing the retention times of the nitrogen peak and the water peak on a Porapak-T column is shown in Figure 4; equations of the reactions leading to the final products of nitrogen and water are given below.

When water is present, the following equilibria exist below the boiling point of N_2O_4 (21°C);

$$2\,N_2O_4 + 2\,H_2O \rightleftharpoons 2\,HNO_3 + 2\,HNO_2 \qquad (1)$$

$$2\,HNO_2 \rightleftharpoons H_2O + N_2O_3 \qquad (2)$$

$$N_2O_3 \rightleftharpoons NO_2 + NO \qquad (3)$$

$$N_2O_3 + HNO_3 \rightleftharpoons 2\,N_2O_4 + H_2O \qquad (4)$$

and the net over-all reaction gives:

$$N_2O_4 + H_2O \rightleftharpoons HNO_2 + N_2O_3 + HNO_3 \rightleftharpoons NO + NO_2$$

Preceding page blank

A certain amount of water of equilibrium must exist, but the law of mass action suggests that the amount will be small in the presence of a great excess of N_2O_4. Thus, it can be readily deduced that, for all practical considerations, the greater portion of the water added to an N_2O_4 sample is present as nitrous and nitric acid. If oxygen is present, N_2O_3 and NO will be oxidized and only nitrous and nitric acid can exist.

If the temperature is above the boiling point of N_2O_4, certain species predominate and other species may be formed:

Equilibrium	Temperature Range	
$N_2O_4 \rightleftharpoons 2\ NO_2$	0°-140°C	(5)
$2\ NO_2 \rightleftharpoons 2\ NO + O_2$	150°-620°C	(6)
$2\ HNO_3 \rightleftharpoons H_2O + 2\ NO_2 + 1/2\ O_2$	>86°C	(7)

As implied by equation (7), oxygen may be formed by decomposition of the HNO_3 in N_2O_4 which has been contaminated by water. Hence, N_2O_4 for use in rocketry should have low HNO_3 content to prevent pressure build-up during storage at elevated temperatures. The role of excess HNO_3 and its oxidizing properties (both as a supplier of free oxygen and as a reagent for NO) as indicated in equation (4) has not been properly evaluated; it may furnish the key for the problem of stress-corrosion cracking.

At temperatures greater than 620°C, a mixture of N_2O_4 and water responds as follows, regardless of the equilibrium species which may be present:

$$N_2O_4 + H_2O \longrightarrow H_2O + NO + O_2 \qquad (8)$$

and in the presence of hot copper the reaction becomes:

$$N_2O_4 + H_2O + 4\ Cu \xrightarrow{>620^\circ} N_2 + H_2O + 4\ CuO \qquad (9)$$

RE-ORDER No. 67-34

EXPERIMENTAL

Apparatus

A block diagram of the apparatus is given in Figure 5. The gas chromatograph is a dual-column F&M Model 810 with a thermal conductivity detector operating at a filament current of 200 ma. The GC column is made from 6 feet of 1/4" stainless steel tubing and is packed with Porapak T (Waters Associates); it is operated at 170°C (isothermal). The injection port and detector temperatures are held at 230°C, and helium is used as the carrier gas. The helium gas is purified by passage over a moisture-hydrocarbon trap (F&M Part No. 2-3660).

The reduction system is a Dumas-type furnace containing a quartz tube packed with copper wire and operated at 780°C; it is connected to the gas chromatograph by means of stainless steel Swagelok fittings.

The sampling block is maintained at 2°C by circulating ice-water, and was fabricated from aluminum to fit the liquid sampling valve (Wilkens Cat. No. 57-040 with core No. 57-049) which ensures reproducibility of 2-µl samples.

Standard Samples

Calibration vessels of about 75 cc were fabricated from thick-walled Pyrex glass fitted with Teflon stopcocks and terminated with glass-to-Kovar seals to which stainless steel Swagelok fittings were affixed. The vessels were dried, evacuated, weighed, and attached to a steel cylinder of N_2O_4 (Matheson Company) by means of stainless steel tubing and fittings. The connecting line was evacuated and then approximately 50 cc of N_2O_4 were introduced into the sample vessel. After re-weighing the sample vessel, the N_2O_4 content was frozen with liquid nitrogen in a dry-box and a measured quantity of water was added from a syringe through the stopcock. Then the vessel was evacuated, warmed to room temperature, and re-weighed. (Standards prepared in this way may be maintained for a long time without change in water content.)

The calibration points below 0.03% water were obtained directly from water-ethanol mixtures since the water content of the available N_2O_4 was too high (0.052%). The ethanol-water mixture was introduced directly into the gas chromatograph since combustion of the mixture in the reduction furnace would lead to the formation of large quantities of water from the ethanol diluent.

Procedure

Conditions of operation are adjusted as described under apparatus: A sample vessel is attached to the system by stainless steel fittings; when thermal equilibrium is established in the chromatograph, reduction furnace, and sample cooling block, a small amount of N_2O_4 from the sample vessel is vented through the sampling valve to force any air bubbles out of the line between it and the sampling vessel. Then the valve is turned to introduce N_2O_4 into the analyzing system and allowed to pass over the hot copper. The resulting gases are swept by helium into the GC column where they are separated as nitrogen and water. The integrated area of the water peak is then compared with areas from a calibration curve.

RESULTS AND DISCUSSION

The calibration data shown in Table 4 are plotted in Figure 6. The data points are linear; the line passes through zero, and is straight over a wide range--this is shown by the analysis of an 0.78% H_2O-N_2O_4 mixture, determined by extrapolation of the calibration curve (Table 6). The coefficient of variation is about 1% (Table 5) shown by four replicates of 0.092% water content in N_2O_4.

In order to verify the hypothesis suggested by equation (9), an 1% solution of 90% HNO_3 in N_2O_4 was analyzed and the resulting chromatogram displayed only two peaks, whose retention time corresponded with

RE-ORDER No. 67-347

nitrogen and water, respectively. The water peak obtained corresponded exactly to the calculated total proton content of the sample.

As indicated in Figure 4, carbon dioxide is also determinable. Carbon dioxide may be present per se in N_2O_4 or be formed from dissolved or suspended organic matter.

RE-ORDER No. 67-347

Table 4

CALIBRATION DATA FOR DETERMINATION OF H_2O IN N_2O_4 BY GAS CHROMATOGRAPHY

% H_2O	AREA, INTEGRATOR COUNTS
0.01	40
0.015	60
0.017	76
0.020	90
0.025	100
0.0405	175
0.122	525

Table 5

RELATIVE ERROR OF GAS CHROMATOGRAPHIC DETERMINATION OF H_2O IN N_2O_4

% H_2O	AREA, INTEGRATOR COUNTS
0.092	392
0.092	390
0.092	396
0.092	390
Mean	393 ±3.3
Relative Error	0.84%

Table 6

RANGE OF LINEARITY OF CALIBRATION CURVES: GAS CHROMATOGRAPHIC DETERMINATION OF H_2O IN N_2O_4

% H_2O ADDED	AREA, INTEGRATOR COUNTS	% H_2O FOUND
0.78	3020	0.71

RE-ORDER No. 67-3

REFERENCES

1. Mil-Spec P-26539B.

2. Sutton, N. V., et al., "Chemical Analysis of Corrosive Oxidizers," Advanced Propellant Chemistry, American Chemical Society No. 54, 1966, p. 231.

3. Trowell, J. M., Anal. Chem., 37, 1152 (1965).

4. Hagstrom, R. A., "Gas Chromatographic Methods for Liquid Propellant Analysis," AFRPL-TR-66-20, January 1966.

5. Smith, R. N., et al. Anal. Chem., 30, 1217 (1958).

6. Huillet, F. D., and Urone, P., J. Gas. Chromat., 4, 249 (1966).

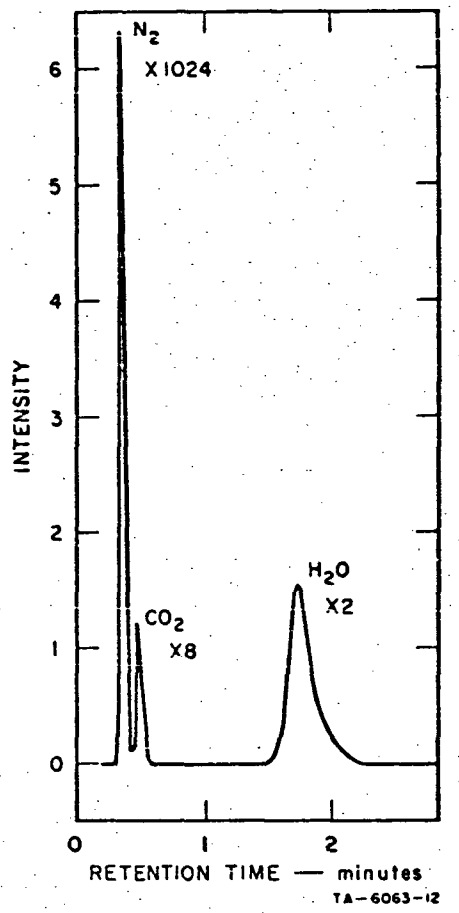

FIG. 4 TYPICAL CHROMATOGRAM

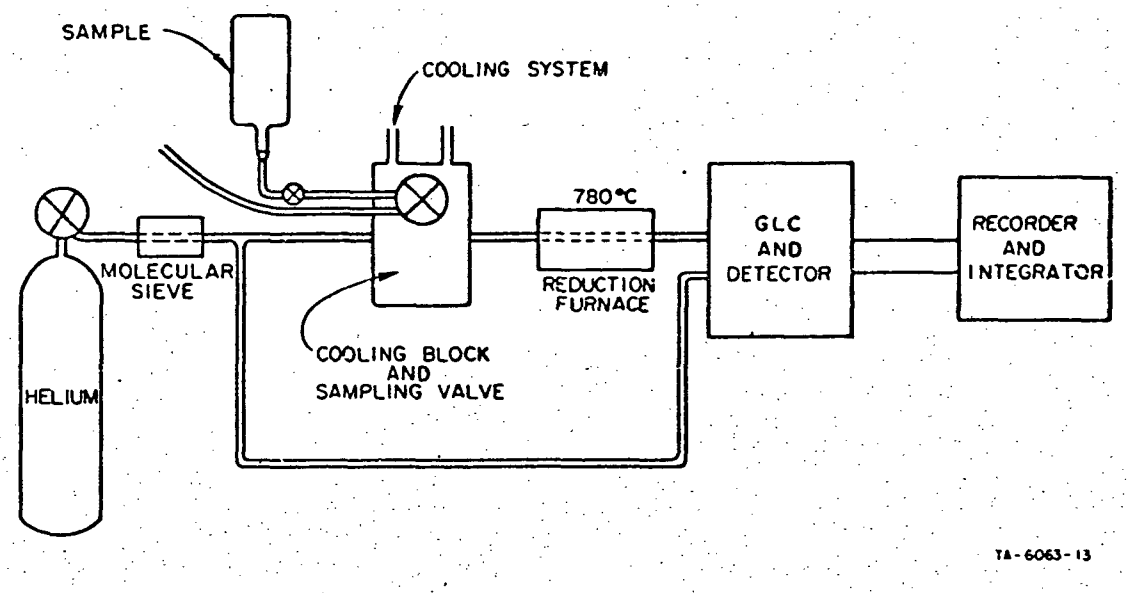

FIG. 5 BLOCK DIAGRAM OF THE APPARATUS FOR THE DETERMINATION OF H_2O IN N_2O_4 BY GAS CHROMATOGRAPHY

RE-ORDER NO. 67-5

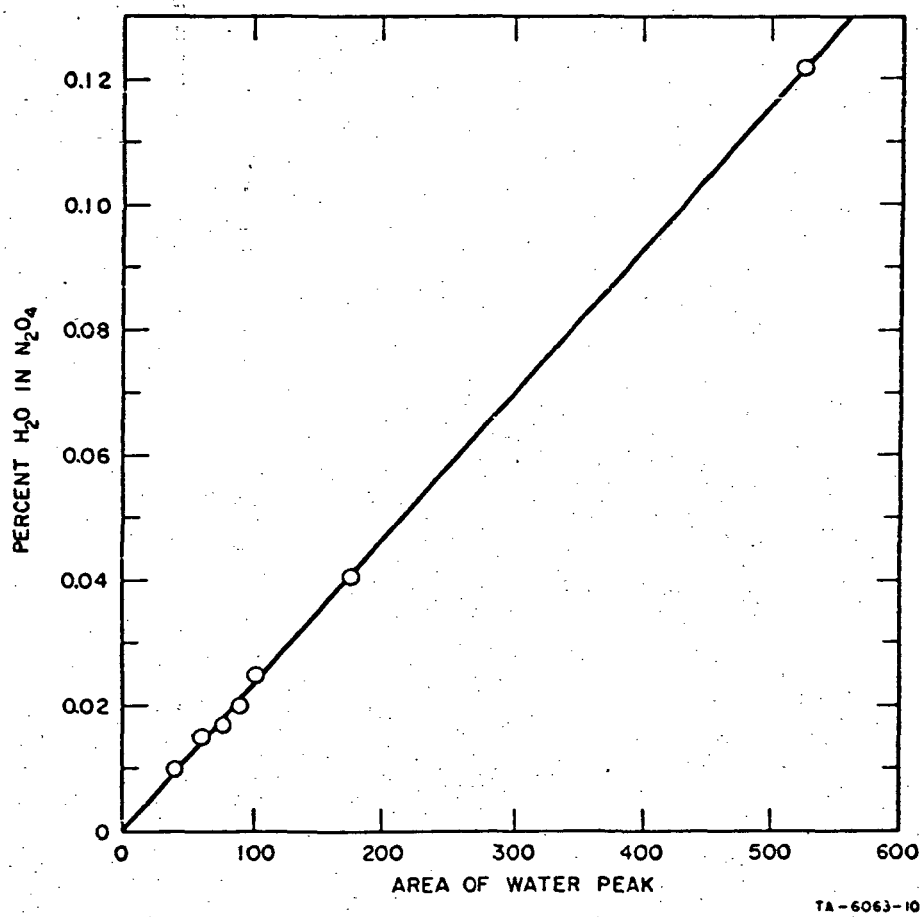

FIG. 6 CALIBRATION CURVE FOR H_2O IN N_2O_4 BY GAS CHROMATOGRAPHY

RE-ORDER No. 67-347

V. RESULTS OF STORAGE TESTS AND DISCUSSION

The results of the storage tests indicate that the materials which are most resistant to N_2O_4 in a sealed system at 110°F are titanium alloys, iron alloys, cobalt alloys, some nickel alloys, tantalum, and Al_2O_3 materials. Materials such as molybdenum, magnesium, and some aluminum and nickel alloys are least resistant. A summary of corrosion rates is given in Table 7. An attempt has been made to rate the materials in order of excellence; a rating of 1 is based on a corrosion rate of <1 μin/yr, no apparent pitting or etching of the specimen, and no decomposition of N_2O_4.

No decrease in corrosion rates was apparent because of the use of coatings of Kel-F grease or Rulon. The coatings of grease on several specimens lost adherence during storage and contaminated the N_2O_4 with heavy, flocculent particles. The Rulon coatings (fluorocarbon) were more adherent, but they also became loose and portions of the metal surfaces were openly subjected to attack by the N_2O_4.

It is interesting to note that even in cases of "severe corrosion" of specimens, the composition of the residual N_2O_4 is not significantly different from the original material; also, the storage pressure of the $N_2O_4 \rightleftharpoons 2\ NO_2$ system was unaffected. In the few instances where deviations in N_2O_4 composition occur, organic impurities are suspected as the cause.

It appears that the 3- to 4-year compatibility tests were initiated with extreme care with regard to treatment of specimens and maintenance of anhydrous conditions of the N_2O_4 and test capsules. The 1-1/2 to 2-year test show some indications of fingerprint markings on the specimens and other organic contamination. In two instances, water or organic contamination probably is responsible for higher-than-average storage pressures and impurity content of the N_2O_4.

RE-ORDER No. 67

It was found that the Kovar metal used to connect the glass capsules to the pressure gages was not completely inert, and in some instances there was deposition of corrosion products of Kovar on the capsule walls and specimens. The Bourdon tubes of the pressure gages were not visibly attacked by N_2O_4.

The analytical data for the tests after storage are summarized in Tables 8a/8b to 13a/13b. The tables are divided (a-b) in order to permit convenient separation of N_2O_4 analyses from specimen analyses and are grouped, in general, according to material type, e.g., iron alloys, so that effects of alloy composition on corrosion may be readily identified.

The appearance of the metal specimens after storage is shown in the photographs in Figures 7 through 12, which are arranged according to JPL test numbers; in many instances, the interface between the immersed metal (1/2 to 2/3 of length) and the metal in the vapor phase is readily discernible. The sapphire and ceramic balls are shown in Figure 13.

Photomicrographs of the ends of the cylindrical rods are given in Figures 14 through 32; they are arranged according to JPL test numbers. Additional documentation will be found in Figures 33 to 51.

Kovar Metal Tubing

Prime sources of contamination in these storage tests are the corrosion products of the Kovar metal used to link the glass capsules to the metal pressure gages. The amount of such solid materials on the walls of the capsules ranged from unobservable to readily-apparent quantities; this is illustrated by the photographs of several Kovar-to-glass seals (Figure 33) after they had been broken away from the capsules. In order to show the extent of storage corrosion, the Kovar tubing was split and opened so that the interior walls could be examined microscopically (see Figure 33). Photomicrographs of the interior surfaces (and the external surfaces for comparison) are shown in Figures 34 to 37. A (color) photograph of the interior surfaces is shown in Figure 38.

Sufficient deposit could be removed (for analysis by x-ray fluorescence) from test capsule Nos. 0067, 0072, 246, and 247, all containing alloy specimens, and from No. 0048, containing only a sapphire ball. Positive identification was made for iron, nickel, and cobalt in all of these deposits.* In no instance is cobalt present in the test specimens in a quantity greater than 0.25% except, of course, in the Stellite alloys. Cobalt was not detected (by wet chemical analysis) in the Bourdon tube metal.

Since the test capsules were maintained in an upright position from the time of filling and all through storage (JPL), the corrosion products of the Kovar tubing apparently flaked off and fell into the capsule, assisted by the refluxing action of NO_2 between the capsule and the cooler areas near the gage.

Bourdon Tube (Gages)

Eight pressure gages (chosen at random) were cut apart so that the internal walls of the Bourdon tubes could be examined microscopically; photomicrographs of the internal and external surfaces of the Bourdon tubes are reproduced in Figures 39-46, and suggest that intergranular corrosion has taken place inside the tubes. Two gages, LOX-cleaned in the same way at the same time for the storage tests, but not used in the tests, were also cut apart. As shown in Figures 47 and 48, the same kind of corrosion is apparent although these gages were never exposed to N_2O_4. Thus, it can be surmised that the Bourdon tubes were etched during the manufacturing process or by a cleaning cycle, but certainly not by exposure to N_2O_4.

Titanium Alloys

Analytical data for the titanium alloys are given in Table 8a/8b. Eleven out of 12 storage tests of 6Al-4V titanium alloy (Nos. 251-258

* Kovar metal is an alloy of 54% iron, 29% nickel, and 17% cobalt.

and 260-262) showed only the barest evidence of attack (discoloration and infrequent, spotty coatings) during 1-1/2 years of storage (Figures 11 and 12). Microscopic examination revealed no evidence of corrosion (see Figures 26-32). Careful examination of all the evidence indicates that the amount of corrosion is minor (weight changes less than 1 mg), and also that organic matter (fingerprints, grease) is contributory to slight variations in analytical data.

The average storage pressure in Test No. 259 was in the range of 42-47 psia (compared with an average storage pressure of 36-40 psia). Gage pressure of the test capsule (after storage) at -11°C was 10 psia (vs 2.7 psia theo.); when the capsule was cooled at liquid nitrogen temperature, the gage pressure fell to zero, indicating absence of noncondensable gases such as N_2 and O_2 (or CO) and that the gage had not lost its calibration. The color of the frozen N_2O_4 was blue, and subsequent analysis showed excesses of H_2O (0.108%) and NO (0.101%). The residue of 0.16% at 100°C was decreased by a factor of 100 by ignition at 500°C, thus suggesting the presence of organic matter (unidentified). The direct addition of water to the test capsule is also suspected. The appearance of the test specimen (Figure 12) is more mottled than the neighboring alloys of the same composition, and the presence of a spotty coating is quite obvious in the photomicrograph shown in Figure 30; however, no etching or pitting is apparent. The sample actually suffered a net increase of weight during storage (+0.0004 g) in contrast with the replicate specimens which incurred losses only.

The low average pressure reported during storage for Test No. 256 (26-29 psia) was traced to a change of calibration of the gage as indicated in the table below:

Actual Pressure, psia	Pressure Indicated by Gage #256, psia
0	0
14.7	14.5
24.7	15.5
34.7	20.5
44.7	33.0

RE-ORDER No. 67-347

Test specimen No. 0111 was prepared with an 0.0034-g coating of Rulon (sprayed-on fluorocarbon). During the storage period of 3.2 years, 0.0023 g of the coating was removed, leaving an unevenly coated surface. The analysis of N_2O_4 is consistent with that for the N_2O_4 from tests stored for 1-1/2 years. The appearance of the specimen is shown in Figure 10, and in Figure 23 the loosening of the coating is quite evident. An attempt to loosen and remove the coating by heating and quenching was unsuccessful, but the final weight of the sample and its remaining coat indicates that very little corrosion occurred.

Test specimen No. 0116 was prepared with an 0.1518-g coating of Kel-F grease. During the storage period of 3.4 years, 0.0512 g of the grease was loosened and was found floating in the N_2O_4; this accounts for the large residue of 0.342% at 100°C. Other than the residue, the analysis of the N_2O_4 is quite consistent with that stored with the other titanium alloys for 1-1/2 years. The appearance of the specimen is shown in Figure 10, and flecks of remaining grease can be seen in the photomicrograph shown in Figure 25. After washing off the grease with solvents, only a minor increase in weight over initial was noted.

The results of all tests show that the titanium alloys are quite stable in N_2O_4 (with respect to corrosion) and that protective coatings are loosened and may interfere with the propellant system operation because of the liberation of particles which can clog valving systems and filters. Since all the measured corrosion rates were small, it is impossible to ascertain whether grease or fluorocarbon coatings reduce attack of the metal; it is certain they do not measurably accelerate corrosion.

Aluminum Alloys

Analytical data for the aluminum alloys are given in Table 9a/9b. On the basis of one test (0087), the 6061-T6 alloy was not attacked by the N_2O_4 during a storage period of 3.8 years. The appearance of the test specimen (shown in Figure 9) is quite clean and only very few stains are apparent under the microscope. The localized, circular

RE-ORDER No. 67-3

markings (or coatings) on the end of the specimen as shown in a photomicrograph (Figure 22) look more like liquid splashes than corrosive coatings. It is assumed that a small amount of contamination was present on the specimen when it was sealed in the capsule.

The alloy 6061-T6 also was covered with coatings of Kel-F grease or Rulon and stored for 3.2 years. The grease on specimen No. 0015 was loosened during storage and found in the N_2O_4 as heavy, flocculent particles. The remaining grease was removed from the metal specimen with solvents; a very small gain in weight was recorded.

Attempts to remove the remaining Rulon from specimen No. 0012 were unsuccessful. The estimated corrosion rates for Nos. 0015 and 0012 do not differ noticeably from the computed rate for No. 0087, indicating that little if any benefit was derived from the use of coatings and that the coatings did not measurably accelerate corrosion.

The results of storage tests for duplicate specimens of 356-T6 aluminum stored for 1.9 years are so diverse and contaminated as to preclude any confident evaluation of this material. There was much cyrstalline material on the walls of both test capsules, identified with the corrosion of the Kovar connecting tubes, i.e., iron, nickel, and cobalt salts. As shown by the appearance of the specimens (test Nos. 246 and 247) in Figures 10 and 11, corrosion of the specimens has occurred primarily in the vapor phase but at radically different rates. The difference is readily discernible in the photomicrographs of the ends of the specimens shown in Figures 25 and 26; the coatings were identified as aluminum nitrate. Photomicrographs at 2X of the cylindrical surfaces of the specimens after the removal of the nitrate coatings have been enlarged to 10X in Figure 49 in order to show the extent of corrosion.

The average storage pressure was 40-44 psi for No. 246 (above the over-all average of 36-40) and 37-40 psia for No. 247 (normal). As expected, the terminal pressure of No. 246 at -11°C was found to be 10 psia. The excess pressure and the analysis of the N_2O_4 for No. 246

is quite similar to that noted for the incongruous titanium alloy test capsule in a batch of 12 replicates (No. 259); there is suspicion of organic contamination but there is also the probability of direct addition of water to the capsule.

Iron Alloys

Analytical data for iron alloys stored for 3.8 years are given in Table 10a/10b. Contamination from the Kovar tubing was evident in test capsule Nos. 0067 and 0072; however, cobalt was not detected in the deposit from No. 0072, but the quantity of available material was very small and it can only be surmised (on the basis of all other tests) that the residue had its origin from Kovar. The appearance of the test specimens 0066 to 0072 (Figure 7) shows clean surfaces except for mild staining in the vapor phase. No. 0073 appears more susceptible to attack, but the computed corrosion rate is not outside of the average range for the iron alloys. The water content of No. 0066 is in excess of the norm for these storage tests (Table 2), but apparently is not due to corrosion of the specimen as indicated by other data. Photomicrographs of the test specimens (Figures 14-16) show no evidence of attack except for a faint coating on No. 0073.

Storage pressures of all the test capsules were within the overall average of 36-40 psia, and in only one instance was an abnormal pressure noted after storage at -11°C (5 psia for No. 0069 vs 2.7 psia theo.). Except for No. 0066, all impurity levels in the N_2O_4 stored with the various specimens are within one-sigma limits established for this storage period (see Table 2). On the basis of one specimen for each alloy, it can be concluded that these steels are resistant to N_2O_4.

Nickel Alloys

Analytical data for nickel alloys stored for 3.3 years to 3.8 years are given in Table 11a/11b. Analysis of the N_2O_4 stored with these specimens shows that it is within the limits of one-sigma variation for the propellant stored (Table 2) except for Inconel-X (No. 0081);

however, infrequent flecks of deposit are noticeable on No. 0081, and in view of the high residue at 100°C, this may possibly be attributed to organic contaminants. The appearance of the specimens 0080-0082, 0086, and 0088 is shown in Figures 8 and 9. The most severe attack was on Hastelloy B (No. 0082); corrosion is also evident for Nickel Type A (No. 0088). Photomicrographs of the ends of the specimens are shown in Figures 19-21; no evidence of corrosion is noted in Test No. 0080 (Inconel). The extensive coating, identified as nickel nitrate, is quite evident in No. 0082 (Hastelloy B) and evidences of etching are noticeable in No. 0088 (Nickel Type A). The etched surface of No. 0082 is apparent in the enlarged photomicrograph taken after the removal of the coating (Figure 50).

On the basis of one test for each type of alloy, it is concluded that the resistance of Inconel alloys and Nickel Span-C to N_2O_4 is excellent; Nickel Type A is somewhat resistant, but Hastelloy B is not recommended.

Miscellaneous Metals

Analytical data for miscellaneous metals and alloys are given in Table 12a/12b.

Magnesium A231C (test No. 0076)* was severely attacked during 3.8 years of storage as shown by the appearance of the specimen in Figure 8 and the photomicrograph of the end of the specimen in Figure 17; the coating was identified as magnesium nitrate. An enlarged photomicrograph of the cylindrical surface after the removal of the coating (Figure 50) shows the extent of etching and pitting. Analysis of the N_2O_4 revealed high values for NO. Although this alloy is not recommended, storage pressures did not exceed that of the vapor pressure of N_2O_4 at 110°F.

---

* Possibly a typographical error in test data; magnesium AZ31C is recorded in the alloy registers.

RE-ORDER No. 67-347

Tantalum metal (No. 0077), stored for 3.8 years apparently suffered little attack as shown by the appearance of the specimen in Figure 8; however, a rare instance of coating is visible in the photomicrograph (Figure 17). The residue at 100°C is somewhat high, but it is unchanged at 500°C, thus indicating lack of organic matter in the N_2O_4. The specimen suffered a gain in weight, and the high value for ignited residue points to minor corrosion. Nevertheless, the metal is considered to be resistant to N_2O_4.

Both molybdenum metal samples (Nos. 0078 and 0079) stored for 3.8 years were corroded. As shown by the appearance of the specimens in Figure 8, they are darkened in the liquid phase and grayish coatings are discernible in the vapor phase. The photomicrographs shown in Figure 18 reveal more clearly the presence of the coatings, identified as "molybdenum oxides." (During removal of the coating by washing with water, it was noted that an under-layer of "molybdenum blue," another oxide, was tightly adherent to the metal.) Photomicrographs taken after the removal of the corrosion products (Figure 51) show clearly a definite transition at the interface of the liquid and vapor phases and also an etched groove about the circumference of the arc-cast molybdenum (0079) at the interface. Analyses of the N_2O_4 stored with these samples showed impurity levels to be within one-sigma variation (Table 2) for the tests. However, on the basis of metal attack, these materials are not considered to be resistant to N_2O_4.

Two cobalt alloys (test Nos. 0083 and 0084) stored for 3.8 years appear to be resistant to N_2O_4. The appearance of the specimens in Figure 9 shows little evidence of attack; this is confirmed by the clean appearance of the ends of the specimens as shown in the photomicrographs in Figures 20 and 21. Only moderate staining of the specimens was noted, and the analysis of the N_2O_4 stored with these specimens is not much different from the norm for these storage tests (Table 2).

RE-ORDER No. 67-3

Alumina Materials

Analytical data for alumina materials are given in Table 13a/13b, and the appearance of the specimens are shown in Figure 13.

The sapphire ball (No. 0048) stored for 3.4 years incurred no corrosion as evidenced by the clean appearance in the photograph and the analyses of the N_2O_4 with which it was stored. This test was contaminated by the corrosion products of Kovar metal which were quite evident as clear, hygroscopic, crystalline deposits on the walls of the test capsule. The analysis of the N_2O_4 in contact with the sapphire showed a higher water content than the majority of test specimens, outside of the limits established in Table 2; because other impurities and residue were below average, the sapphire is considered resistant to N_2O_4.

The same resistance to N_2O_4 is granted for the ceramic ball (Al_2O_3), test No. 0089. This specimen was stored also for 3.8 years; however, the N_2O_4 impurity level has remained within the limits indicated in Table 3.

The Rulon (fluorocarbon) coating on the ceramic ball specimen No. 0013 was partially removed during the storage tests, evident by the spotty appearance of the surface of the ball under the microscope; the ball itself showed no staining or etching. Impurity limits of the N_2O_4 were within acceptable variations (Table 2).

The Kel-F grease coating on the ceramic ball specimen No. 0017 was almost entirely removed and thence dispersed in the liquid phase, as shown by the high residue content of the N_2O_4 at 100°C. Again, however, the ball itself showed no indication of corrosion under microscopic examination. Impurity limits of the N_2O_4 (except for the 100°C) residue were within one-sigma variation (Table 2) for the stored propellant.

RE-ORDER No. 67-347

Table 7

RESULTS OF JPL STORAGE TESTS
CORROSION RATES

JPL TEST NO.	MATERIAL	STORAGE TIME, YR	CORROSION, μ IN/YR	RATING[a]
0048	Sapphire ball (Al_2O_3)	3.4	< 2.0	1
0066	410 stainless steel	3.8	< 0.1	1
0067	416 stainless steel	3.8	< 0.1	1
0069	430 stainless steel	3.8	< 0.1	1
0070	19-9 DL stainless steel	3.8	< 0.1	1
0072	440C stainless steel	3.8	0.1	1
0073	1018 steel	3.8	0.2	1
0076	A-231C magnesium alloy	3.8	1.7	3
0077	Tantalum	3.8	0.1	1
0078	Sintered molybdenum	3.8	1.7	3
0079	Arc-cast molybdenum	3.8	2.2	3
0080	Inconel	3.8	< 0.1	1
0081	Inconel-X	3.3	0.1	1
0082	Hastelloy B	3.8	7.4	3
0083	Stellite Type 6	3.8	0.2	1
0084	Stellite Type 25	3.8	0.2	1
0086	Nickel Span-C	3.3	0.2	1
0087	6061-T6 aluminum alloy	3.8	2.1	2
0088	Nickel, Type A	3.8	2.1	2
0089	Ceramic ball, sintered Al_2O_3	3.8	< 2.0	1
0110	347 stainless steel	3.6	0.2	1
0111	6Al-4V titanium alloy + Rulon coating	3.2	1.9	2
0112	6061-T6 aluminum alloy + Rulon coating	3.2	2.0	1
0113	Ceramic ball, fused Al_2O_3 + Rulon coating	3.6	0.6	1
0115	6061-T6 aluminum alloy + Kel-F grease coating	3.1	2.0	1

Reproduced from best available copy.

RE-ORDER No. 67-

Table 7 (Concluded)

JPL TEST NO.	MATERIAL	STORAGE TIME, YR	CORROSION, μ IN/YR	RATING[a]
0116	6Al-4V titanium alloy + Kel-F grease coating	3.1	< 1.0	2
0117	Ceramic ball + Kel-F grease coating	3.6	0.6	1
246	356-T6 aluminum alloy	1.9	invalid	--
247	356-T6 aluminum alloy	1.9	8.3	3
251	6Al-4V titanium alloy	1.5	2.4	2
252	6Al-4V titanium alloy	1.5	2.1	2
253	6Al-4V titanium alloy	1.5	2.8	2
254	6Al-4V titanium alloy	1.5	1.2	2
255	6Al-4R titanium alloy	1.5	2.4	2
256	6Al-4V titanium alloy	1.5	0.8	2
257	6Al-4V titanium alloy	1.5	1.2	2
258	6Al-4V titanium alloy	1.5	2.4	2
259	6Al-4V titanium alloy	1.5	invalid	--
260	6Al-4V titanium alloy	1.5	0.8	2
261	6Al-4V titanium alloy	1.5	2.4	2
262	6Al-4V titanium alloy	1.5	1.6	2

[a] 1 = Excellent, < 1.0 μ in/yr; attack limited to staining or extremely thin adherent coating; no decomposition of N_2O_4.

2 = Good; 1-3 μ in/yr; attack limited to staining or thin coating; no apparent etching or pitting; no decomposition of N_2O_4.

3 = Not recommended; > 1 μ in/yr; visible coating and flaking; apparent etching and/or pitting; possible decomposition of N_2O_4.

Reproduced from best available copy.

RE-ORDER No. 67-34

Table 8a

ANALYSES OF N_2O_4 STORED WITH TITANIUM ALLOYS

JPL TEST NO.	SPECIMEN	IMPURITIES, WT-%			RESIDUE, WT-%		REMARKS
		H_2O	NO	Cl^-	@ 100°C	@ 500°C	
0111	6Al-4V titanium + Rulon coating	0.034	0.06	< 0.0005	0.0008	< 0.0001	--
0116	6Al-4V titanium + Kel-F grease	0.034	0.03	< 0.0005	0.342	0.0139	Numerous small, heavy flocculent particles
251	6Al-4V titanium	--	--	--	--	--	Capsule broken in shipment
252	6Al-4V titanium	0.060	0.014	0.0010	0.0003	0.0001	P = < 3 psia at -11°C
253	6Al-4V titanium	0.070	0.014	0.0010	0.0052	0.0001	P = < 3 psia at -11°C
254	6Al-4V titanium	0.070	0.015	0.0007	0.0015	0.0002	P = < 3 psia at -11°C
255	6Al-4V titanium	0.052	0.018	0.0007	0.0015	0.0002	P = < 3 psia at -11°C
256	6Al-4V titanium	0.057	0.015	< 0.0005	0.0062	0.0009	P = < 3 psia at -11°C
257	6Al-4V titanium	0.060	0.013	< 0.0005	0.0051	0.0023	P = < 3 psia at -11°C
258	6Al-4V titanium	0.060	0.001	< 0.0005	0.0081	0.0047	P = < 3 psia at -11°C
259	6Al-4V titanium	0.108	0.101	< 0.0005	0.1600	0.0011	P = 10 psia at -11°C and 0 psia at -195°C; frozen color blue
260	6Al-4V titanium	--	--	--	--	--	Capsule broken in shipment
261	6Al-4V titanium	0.046	0.015	< 0.0005	0.0016	0.0006	P = < 3 psia at -11°C
262	6Al-4V titanium	0.052	0.015	< 0.0005	0.0065	0.0009	P = < 3 psia at -11°C

RE-ORDER No. 6

Table 8b

CORROSION OF TITANIUM ALLOYS STORED WITH N_2O_4

JPL TEST NO.	MATERIAL	WEIGHT CHANGE, g	APPEARANCE	REMARKS
0111	6Al-4V titanium + Rulon coating	< 0.0010	Slight etch on sides, attributed to loss of Rulon	Rulon wt., init, 0.0031 g; final, 0.0011g
0116	6Al-4V titanium + Kel-F grease	<+0.0002	Dark, irregular stain	Kel-F wt., init, 0.1518 g; final, 0.1006g
251	6Al-4V titanium	-0.0006	No apparent etch or pitting; some lengthwise stains	Capsule broken in shipment
252	6Al-4V titanium	-0.0005	Fingerprint stains	---
253	6Al-4V titanium	-0.0007	Fingerprint stains	---
254	6Al-4V titanium	-0.0003	No apparent stains	---
255	6Al-4V titanium	-0.0006	No apparent stains	---
256	6Al-4V titanium	-0.0002	Apparent light stain	---
257	6Al-4V titanium	-0.0003	Fingermarks	---
258	6Al-4V titanium	-0.0006	Spotty, light-brown stains	---
259	6Al-4V titanium	+0.0004	Light grey stains; coating visible under microscope	---
260	6Al-4V titanium	-0.0002	No apparent stains	Capsule broken in shipment
261	6Al-4V titanium	-0.0006	Few spotty stains	---
262	6Al-4V titanium	-0.0004	Many small spotty stains	---

RE ORDER No. 67-3

Table 9a

ANALYSES OF N_2O_4 STORED WITH ALUMINUM ALLOYS

JPL TEST NO.	MATERIAL	IMPURITIES, WT-%			RESIDUE, WT-%		REMARKS
		H_2O	NO	Cl^-	@ 100°C	@ 500°C	
0087	6061-T6 aluminum	0.020	0.017	0.0010	0.0023	< 0.0001	--
0112	6061-T6 aluminum + Rulon coating	0.034	0.016	< 0.0005	0.0007	< 0.0001	--
0115	6061-T6 aluminum + Kel-F grease	0.030	0.07	< 0.0005	0.256	0.0114	Numerous small, heavy, flocculent particles
246	356-T6 aluminum	0.108	0.174	< 0.0005	0.0677	0.0050	P = 10 psia at -11°C, and 0 psia at -195°C; frozen material blue; much crystalline material on walls containing Fe, Ni, Co.
247	356-T6 aluminum	0.065	0.017	< 0.0005	0.0024	0.0008	P = < 3 psia at -11°C; much crystalline material on walls containing Fe, Ni, Co.

Table 9b

CORROSION OF ALUMINUM ALLOYS STORED WITH N_2O_4

JPL TEST NO.	MATERIAL	WEIGHT CHANGE, g	APPEARANCE	REMARKS
0087	6061-T6 aluminum	-0.0003	Very few stains	--
0112	6061-T6 aluminum + Rulon coating	< +0.0005	Etch on end attributed to loss of Rulon	Rulon wt., init, 0.0026 g, final, 0.0009 g.
0115	6061-T6 aluminum + Kel-F grease	< +0.0005	Considerable stain at one end	Kel-F wt., init, 0.0956 g, final, 0.0009 g.
246	356-T6 aluminum	0.0000	Very thin grey deposit on upper end; light yellow-green spots	Coating identified as aluminum nitrate; light etch marks in liquid phase
247	356-T6 aluminum	-0.0015	Much grey deposit on upper end; small black spots on lower	Coating identified as aluminum nitrate; intergranular corrosion, especially at interface and in vapor phase

RE-ORDER No. 67-3

Table 10a

ANALYSES OF N_2O_4 STORED WITH IRON ALLOYS

JPL TEST NO.	MATERIAL	IMPURITIES, WT-%			RESIDUE, WT-%		REMARKS
		H_2O	NO	Cl^-	@ 100°C	@ 500°C	
0066	410 stainless steel	0.061	0.017	< 0.0005	0.0306	0.0025	--
0067	416 stainless steel	0.020	0.054	< 0.0005	0.0211	0.0032	Residue on walls of capsule contains Fe, Ni, Co
0069	430 stainless steel	0.010	0.044	0.0005	0.0025	0.0008	P = 5 psia at -11°C; frozen color greenish
0070	19-9 DL stainless steel	0.04	< 0.02	< 0.0005	0.0233	0.0008	--
0072	440C stainless steel	0.020	0.027	0.0001	0.0037	0.0042	Slight residue on walls of capsule containing Fe, Ni, and Co
0072	1018 steel	0.020	0.015	< 0.0005	0.0012	< 0.0001	--
0110	347 stainless steel + Rulon	0.017	0.003	0.0010	0.0054	0.0013	P = < 3 psia at -11°C

Table 10b

CORROSION OF IRON ALLOYS STORED WITH N_2O_4

JPL TEST NO.	MATERIAL	WEIGHT CHANGE, g	APPEARANCE	REMARKS
0066	410 stainless steel	+0.0003	Slight stain, especially at liquid-vapor interface and vapor phase	--
0067	416 stainless steel	+0.0004	Slight stain, especially at liquid-vapor interface	--
0069	430 stainless steel	+0.0002	Slight staining, especially just below interface	--
0070	19-9 DL stainless steel	+0.0001	No stains or etching	--
0072	440C stainless steel	+0.0009	Moderate stain, especially in vapor phase	Some matter on upper end
0073	1018 steel	-0.0003	Rusty stains	Small particles adherent to surface
0110	347 stainless steel + Rulon	< +0.0012	Very light stains; Rulon probably cause of etched appearance	Rulon wt, init, 0.0029 g, final, 0.0009 g

RE-ORDER No. 67-34

Table 11a

ANALYSES OF N_2O_4 STORED WITH NICKEL ALLOYS

JPL TEST NO.	MATERIAL	IMPURITIES, WT-%			RESIDUE, WT-%		REMARKS
		H_2O	NO	Cl^-	@ 100°C	@ 500°C	
0080	Inconel	--	--	--	0.0083	< 0.0001	Capsule broken in handling
0081	Inconel-X	0.033	< 0.02	< 0.0005	0.0642	0.0001	--
0082	Hastelloy B	0.010	0.029	0.0007	0.0013	0.0026	--
0086	Nickel Span C	0.022	0.04	< 0.0005	0.0007	0.0002	--
0088	Nickel, Type A	0.015	0.062	0.0006	0.0019	0.0007	P = < 3 psia at -11°C

Table 11b

CORROSION OF NICKEL ALLOYS STORED WITH N_2O_4

JPL TEST NO.	MATERIAL	WEIGHT CHANGE, g	APPEARANCE	REMARKS
0080	Inconel	+0.001	Black stain in vapor phase; light stain in liquid phase	--
0081	Inconel-X	+0.0006	Slight stain on one side	--
0082	Hastelloy B	-0.0089	Severe attack; yellow-green coating over total surface, especially in liquid phase	Coating identified as nickel nitrate; pitting and etching over entire surface, severe in liquid phase
0086	Nickel Span-C	+0.0006	No unusual stains or features	--
0088	Nickel, Type A	-0.0026	Slight over-all stain; some possible pitting	--

RE-ORDER NO. 67-3

Table 12a

ANALYSES OF N_2O_4 STORED WITH VARIOUS METALS

JPL TEST NO.	MATERIAL	IMPURITIES, WT-%			RESIDUE, WT-%		REMARKS
		H_2O	NO	Cl^-	@ 100°C	@ 300°C	
0076	A231C magnesium	0.020	0.093	< 0.0005	0.0006	0.0015	--
0077	Tantalum	0.010	0.026	< 0.0005	0.0162	0.0165	--
0078	Sintered molybdenum	0.015	0.033	< 0.0005	0.0034	0.0007	--
0079	Arc-cast molybdenum	0.020	0.029	0.0010	0.0012	0.0025	--
0083	Stellite, Type 6	0.010	0.031	< 0.0005	0.0025	0.0007	P = < 3 psia at -11°C
0084	Stellite, Type 25	0.025	0.054	< 0.0005	0.0016	0.0022	--

Table 12b

CORROSION OF VARIOUS METALS STORED WITH N_2O_4

JPL TEST NO.	MATERIAL	WEIGHT CHANGE, g	APPEARANCE	REMARKS
0076	A231C magaesium	- 0.0044	Severe attack; white coating over entire surface	Coating identified as magnesium nitrate; severe pitting on surface
0077	Tantalum	+ 0.0005	Few stains; appear to be fingermarks	--
0078	Sintered molybdenum	- 0.0025	Thin white deposit in vapor phase, dark-grey in liquid	Coating identified as molybdenum oxide; pronounced etch pits at interface, light etching in liquid phase
0079	Arc-cast molybdenum	- 0.0032	Thin, white deposit in vapor phase, dark grey in liquid	Coating identified as molybdenum oxide; etch pits at interface and in liquid
0083	Stellite, Type 6	0.0000	Moderate staining; very thin coating	Only moderate staining under coating
0084	Stellite, Type 25	+ 0.0002	Slight, spotty staining	--

RE-ORDER No. 67-317

Table 13a

ANALYSES OF N_2O_4 STORED WITH ALUMINA MATERIALS

JPL TEST NO.	MATERIAL	IMPURITIES, WT-%			RESIDUE, WT-%		REMARKS
		H_2O	NO	Cl^-	@ 100°C	@ 500°C	
0048	Sapphire ball (Al_2O_3)	0.101	< 0.02	< 0.0005	0.0000	0.0000	Hygroscopic, crystalline material on capsule walls, containing Fe, Ni, Co
0089	Sintered ceramic ball (Al_2O_3)	0.017	0.040	< 0.0005	0.0083	0.0007	--
0113	Fused ceramic ball, Al_2O_3 + Rulon coating	0.027	0.059	0.0010	0.0036	0.0000	P = < 3 psia at -11°C
0117	Ceramic ball + Kel-F grease	0.012	0.016	0.0007	0.101	0.0056	P = < 3 psia at -11°C (glass ball-holder broken)

Table 13b

CORROSION OF ALUMINA MATERIALS STORED WITH N_2O_4

JPL TEST NO.	MATERIAL	WEIGHT CHANGE, g	APPEARANCE	REMARKS
0048	Sapphire ball (Al_2O_3)	+ 0.0007	Mirror surface, no stains	--
0089	Sintered ceramic ball, Al_2O_3	+ 0.0007	Glassy surface; some medium gray areas	--
0113	Fused ceramic ball, Al_2O_3 + Rulon coating	+ 0.0009	Glassy to dull; no stains	Rulon wt, init, 0.0012 g, final, 0.0008 g
0117	Ceramic ball + Kel-F grease	+ 0.0002	Glassy; no apparent attack	Kel-F wt, init, 0.0025 g, final, 0.0001 g

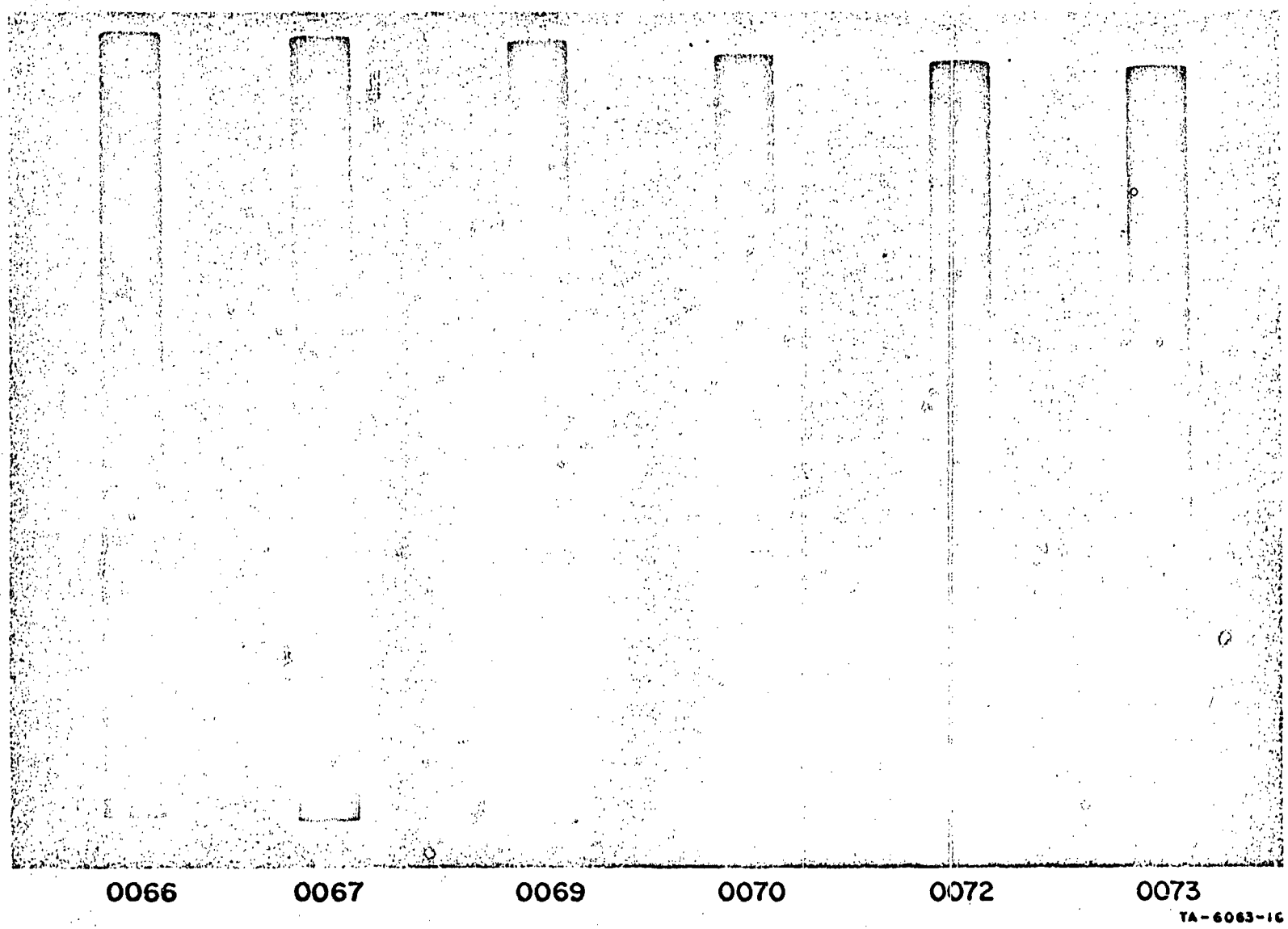

FIG. 7 APPEARANCE OF TEST SPECIMENS 0066 TO 0073 AFTER STORAGE. (See Table 1 for identification.)

RE-ORDER NO. 67-347

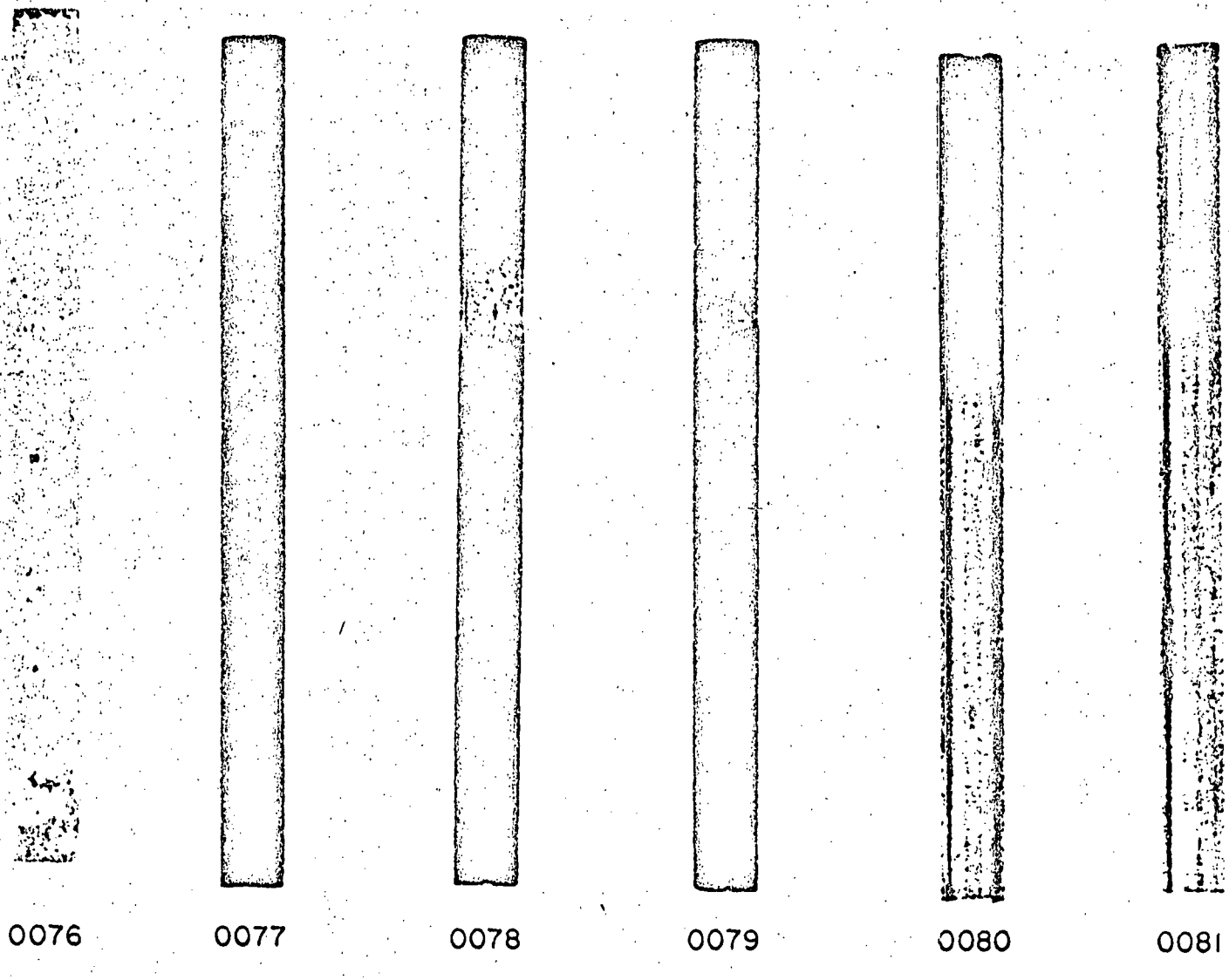

FIG. 8 APPEARANCE OF TEST SPECIMENS 0076 TO 0081 AFTER STORAGE. (See Table 1 for identification.)

RE-ORDER NO. 67-347

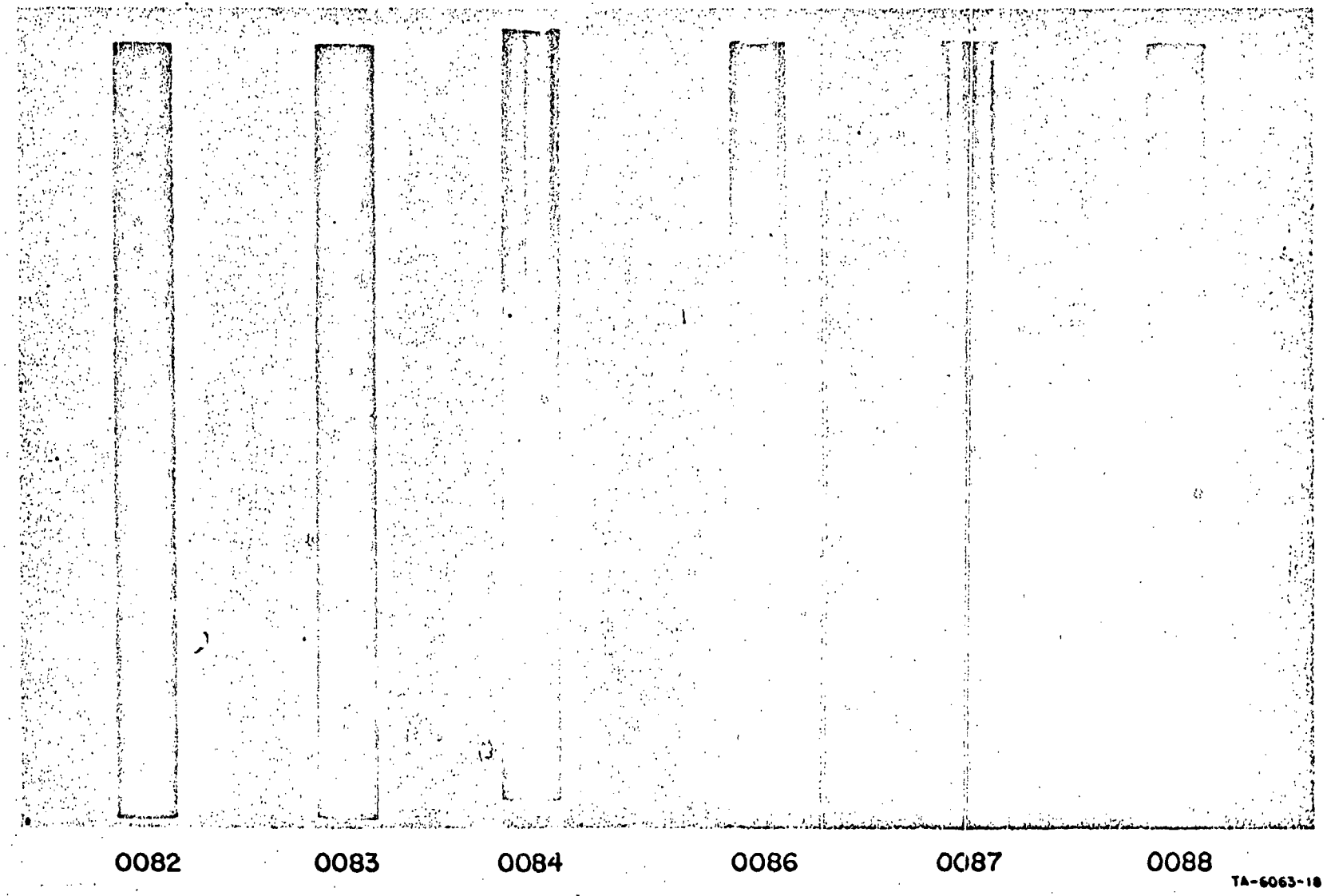

FIG. 9 APPEARANCE OF TEST SPECIMENS 0082 TO 0088 AFTER STORAGE. (See Table 1 for identification.)

RECORDED IN DOCKET NO. 67-317

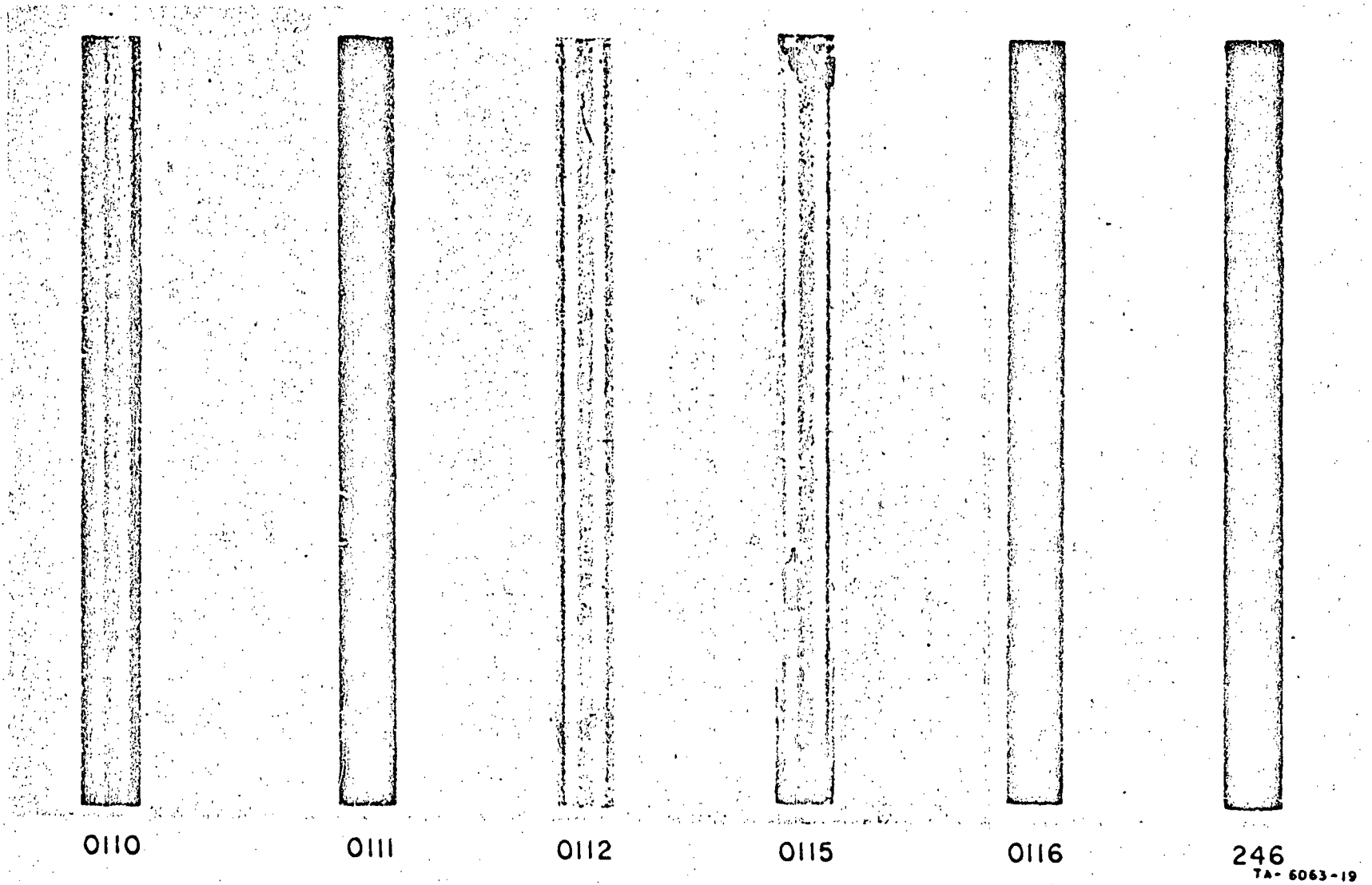

FIG. 10 APPEARANCE OF TEST SPECIMENS 0110 TO 246 AFTER STORAGE. (See Table 1 for identification.)

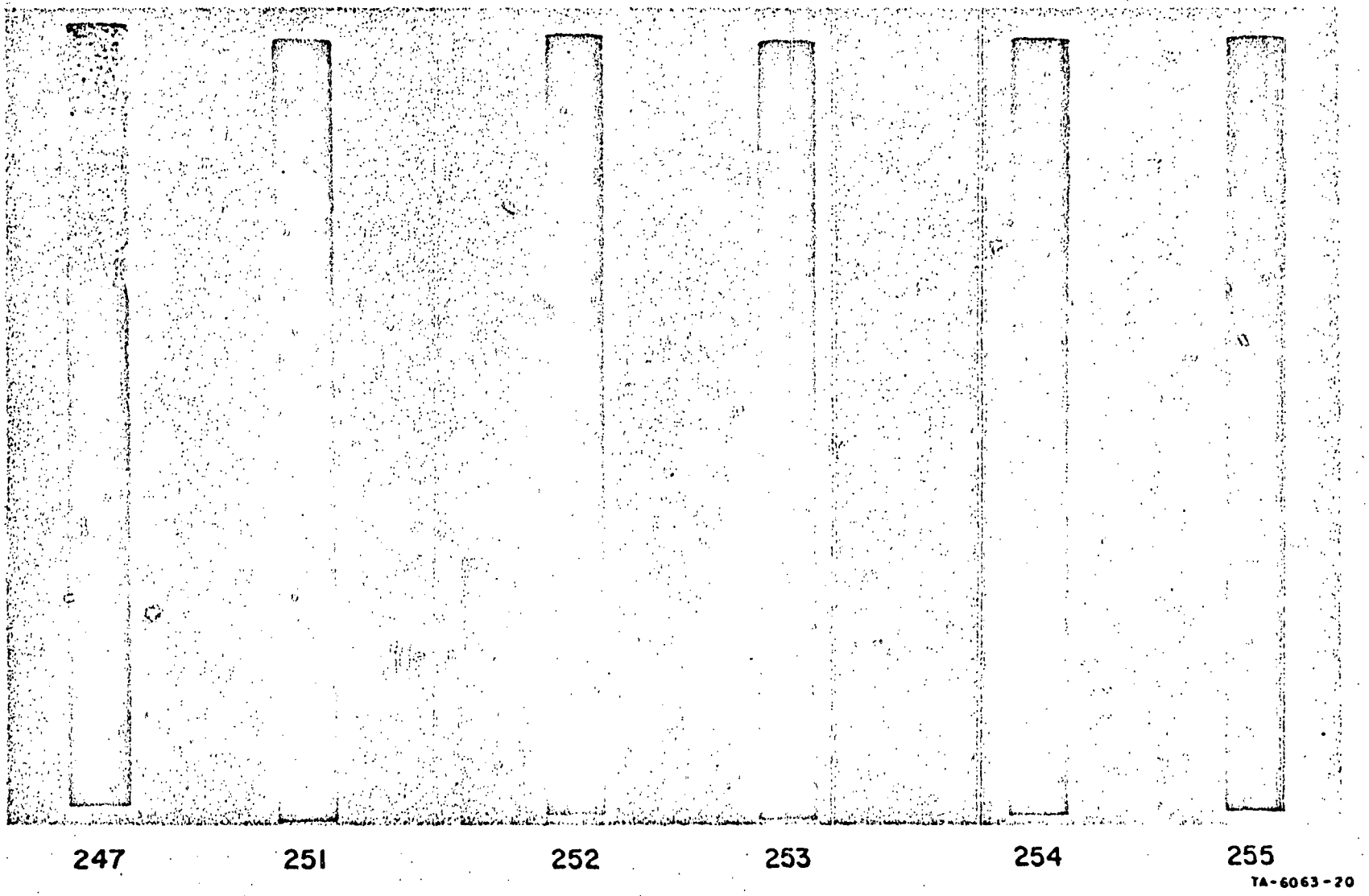

FIG. 11 APPEARANCE OF TEST SPECIMENS 247 TO 255 AFTER STORAGE. (See Table 1 for identification.)

RE-ORDER NO. 67-3

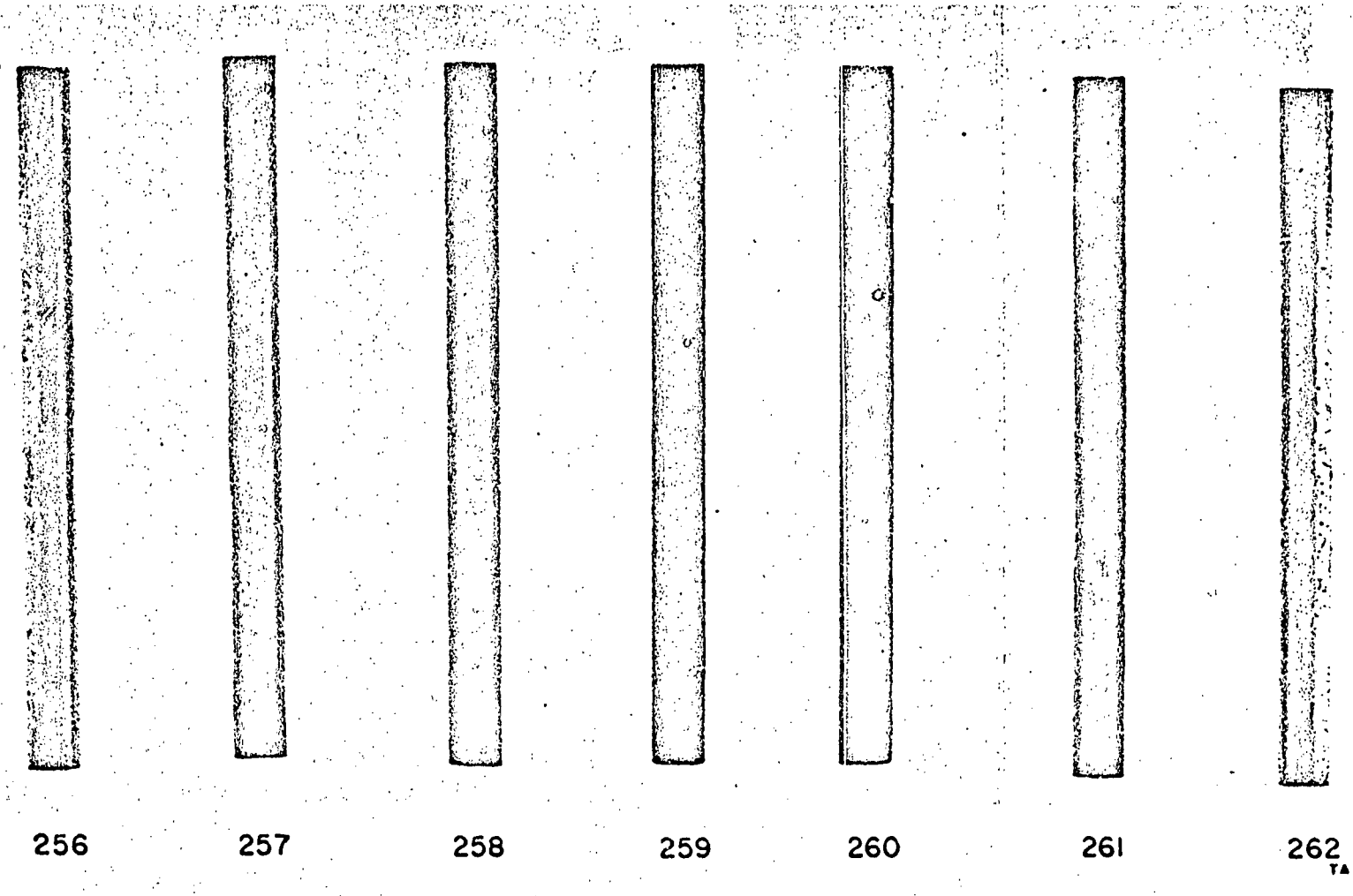

FIG. 12 APPEARANCE OF TEST SPECIMENS 256 TO 262 AFTER STORAGE. (See Table 1 for identification.)

RE-ORDER NO. 67-347

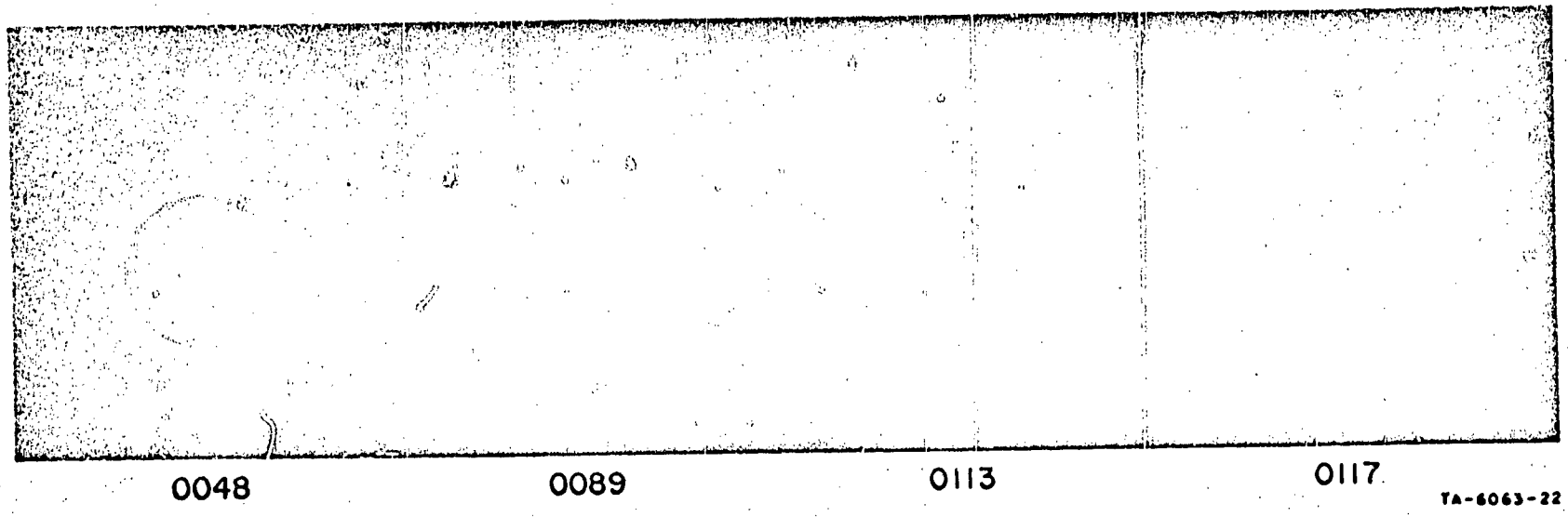

FIG. 13 APPEARANCE OF TEST SPECIMENS 0048, 0089, 0113, AND 0117 AFTER STORAGE.
(See Table 1 for identification.)

RE-ORDER NO. 67-3

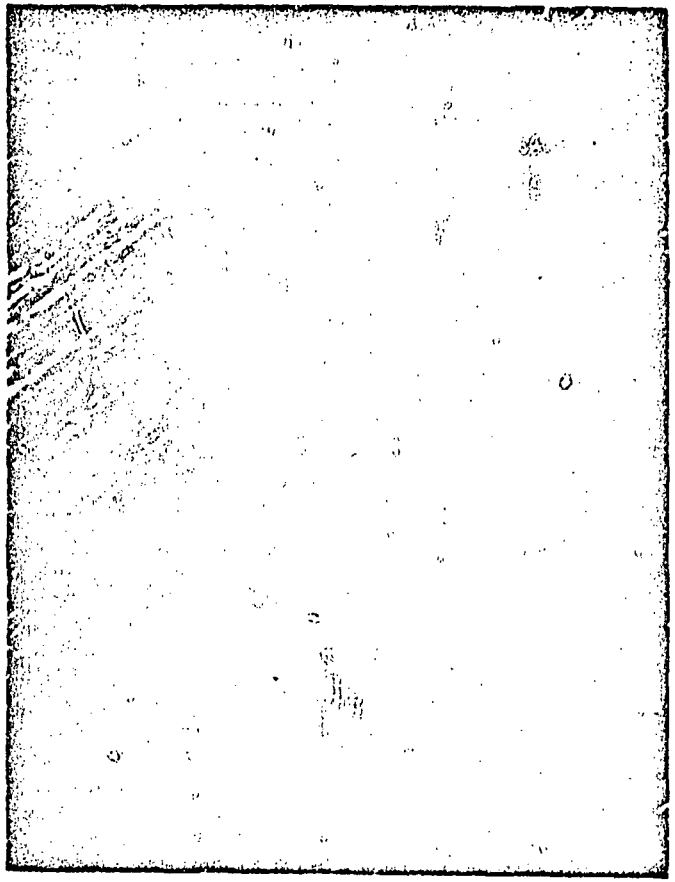

0066

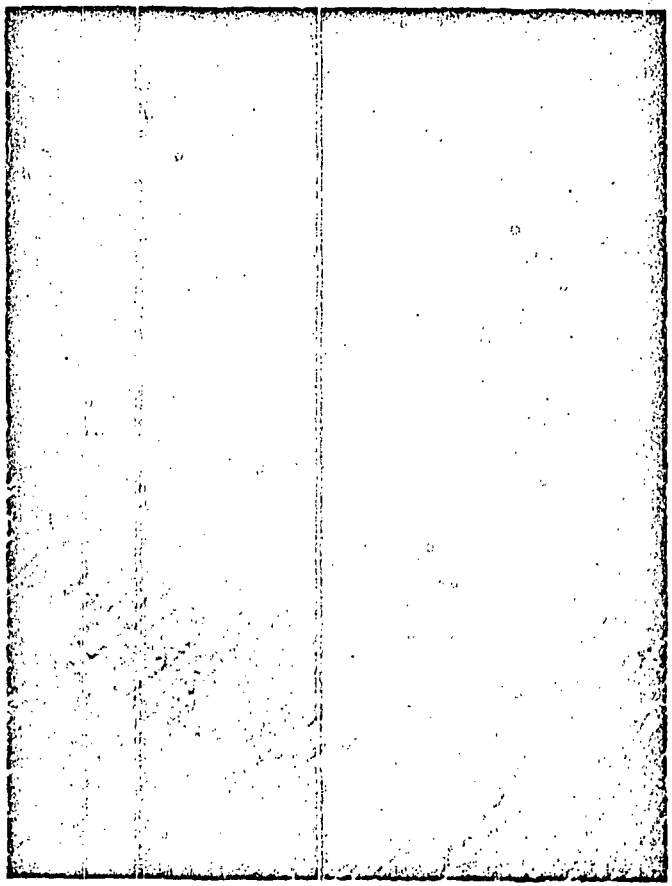

0067

TA-6063-23

FIG. 14 PHOTOMICROGRAPHS OF ENDS OF SPECIMENS AFTER STORAGE (53X). (0066) 410 stainless steel; (0067) 416 stainless steel.

RE-ORDER NO. 67-347

0069

0070

TA-6065-24

FIG. 15 PHOTOMICROGRAPHS OF ENDS OF SPECIMENS AFTER STORAGE (53X).
(0069) 430 stainless steel; (0070) 19-9 DL stainless steel.

RE-ORDER NO. 67-317

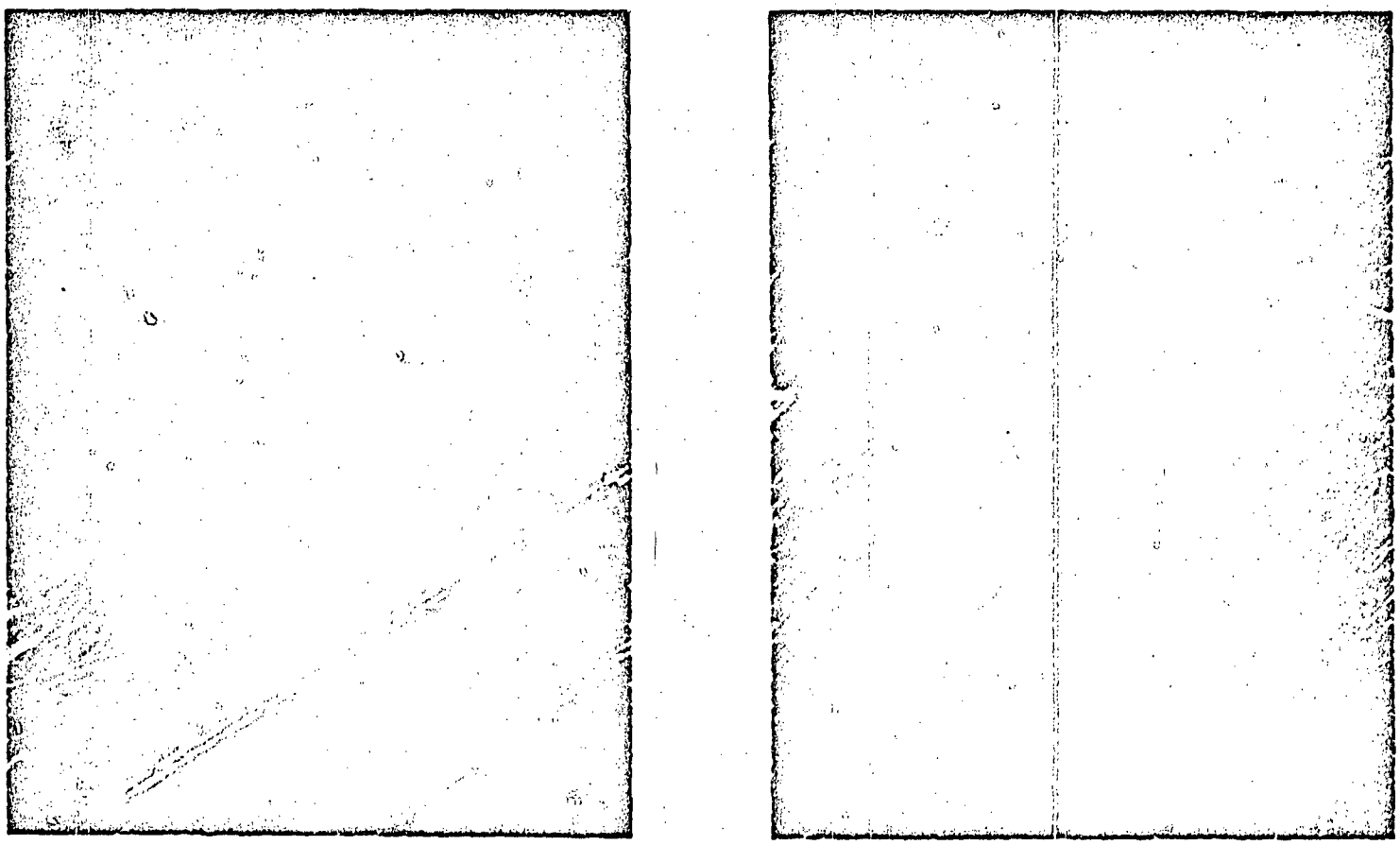

FIG. 16 PHOTOMICROGRAPHS OF ENDS OF SPECIMENS AFTER STORAGE (53X).
(0072) 440C stainless steel; (0073) 1018 steel.

RE-ORDER No. 67-347

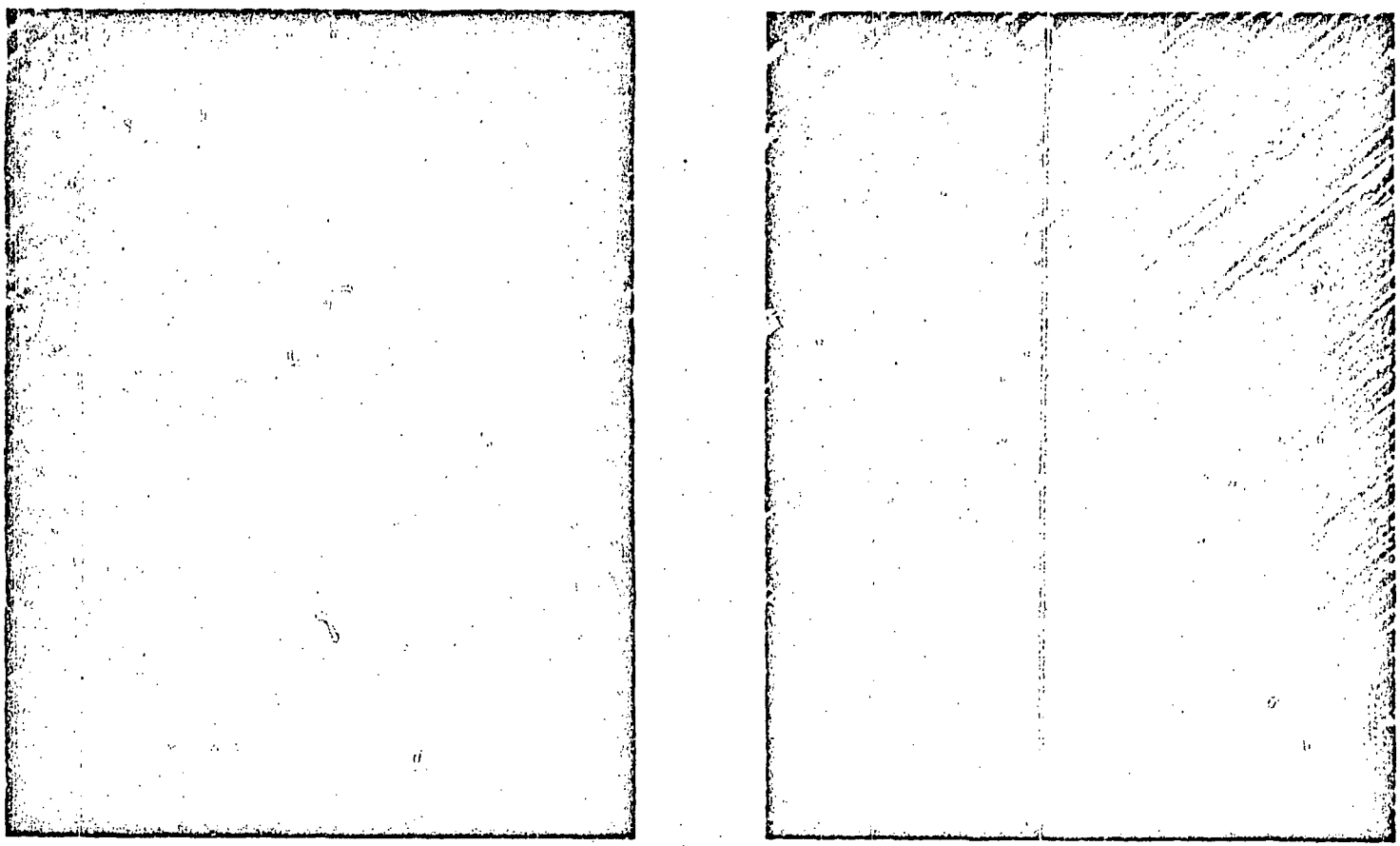

0076

0077

TA-6063-26

FIG. 17 PHOTOMICROGRAPHS OF ENDS OF SPECIMENS AFTER STORAGE (53X). (0076) A-231C magnesium alloy; (0077) Tantalum.

RE-ORDER NO. 67-341

0078

0079

TA-6063-27

FIG. 18 PHOTOMICROGRAPHS OF ENDS OF SPECIMENS AFTER STORAGE (53X).
(0078) Sintered molybdenum; (0079) Arc-cast molybdenum.

RE-ORDER No. 67-347

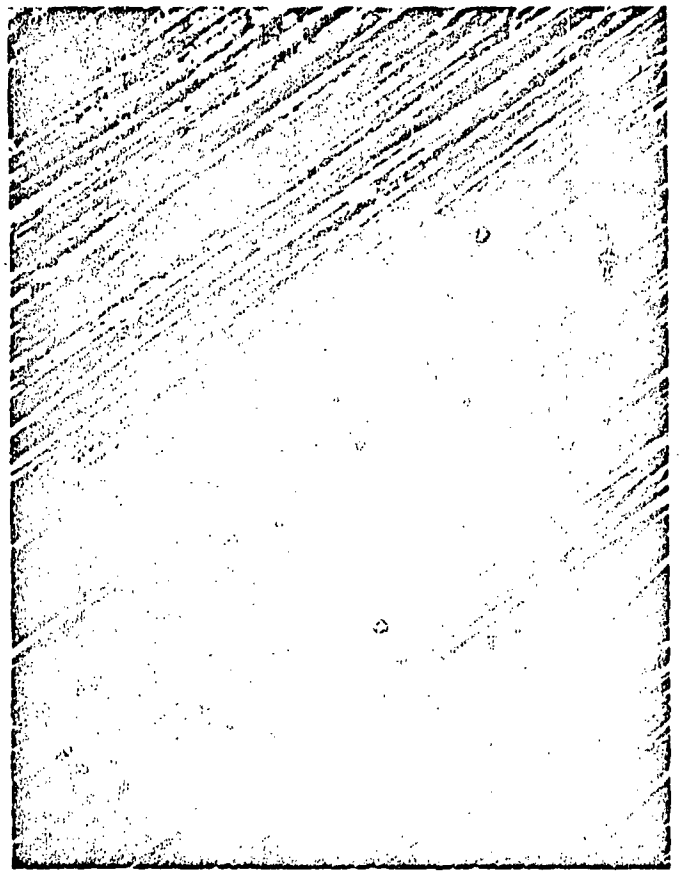

0080

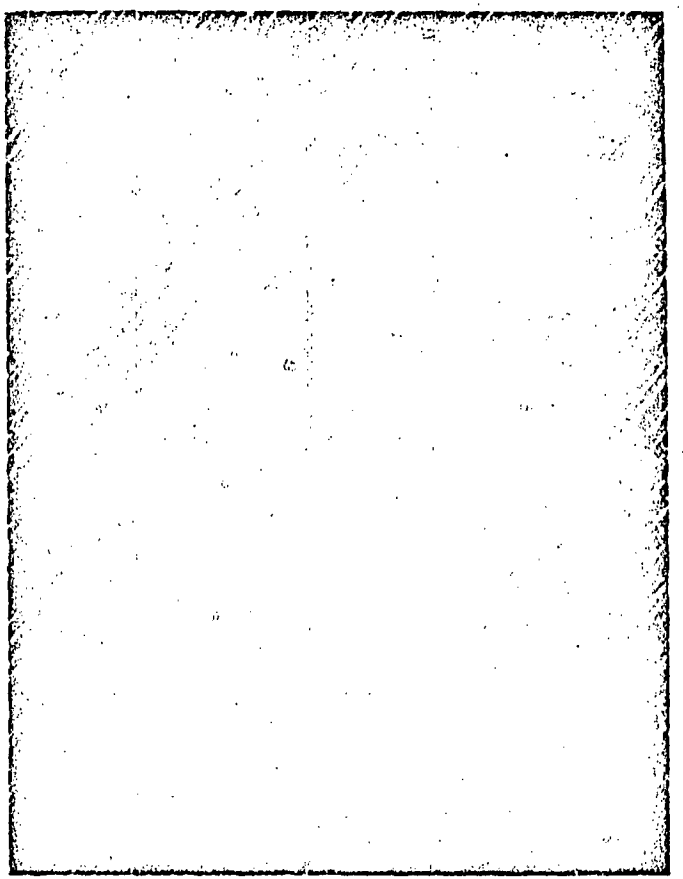

0081

TA-6063-28

FIG. 19 PHOTOMICROGRAPHS OF ENDS OF SPECIMENS AFTER STORAGE (53X).
(0080) Inconel; (0081) Inconel-X.

RE-ORDER NO. 67-34

0082

0083

TA-6063-29

FIG. 20 PHOTOMICROGRAPHS OF ENDS OF SPECIMENS AFTER STORAGE (53X). (0082) Hastelloy B; (0083) Stellite Type 6.

RE-ORDER No. 67-347

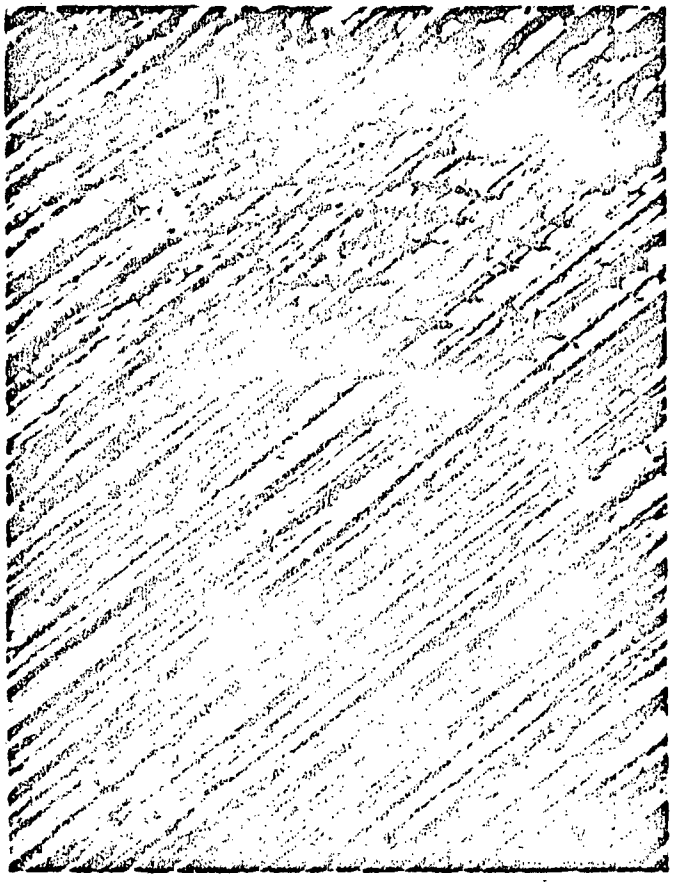

0084

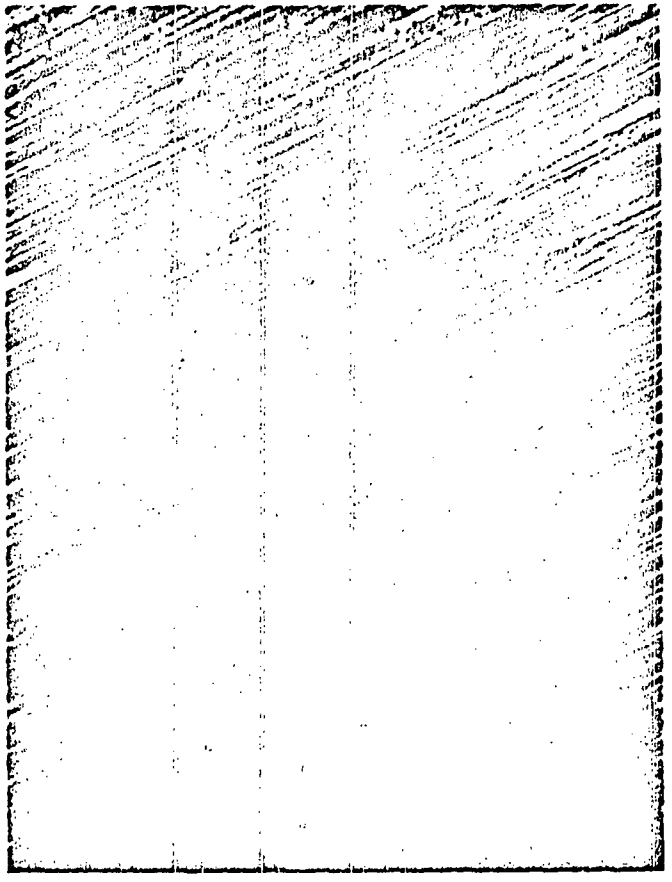

0086

TA-6063-30

FIG. 21 PHOTOMICROGRAPHS OF ENDS OF SPECIMENS AFTER STORAGE (53X).
(0084) Stellite Type 25; (0086) Nickel Span-C.

RE-ORDER NO. 67-3

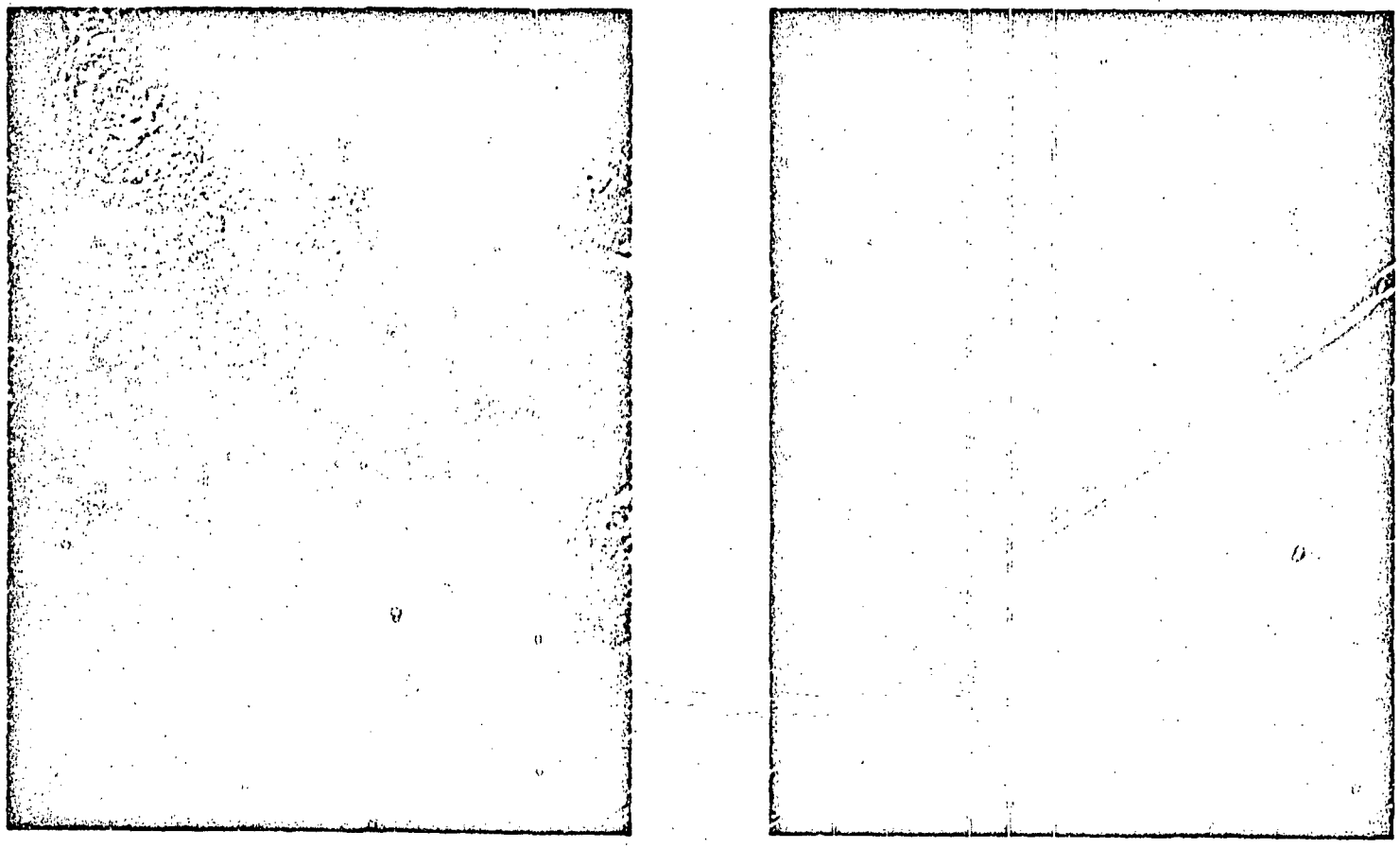

0087

0088

TA-6063-31

FIG. 22 PHOTOMICROGRAPHS OF ENDS OF SPECIMENS AFTER STORAGE (53X).
(0078) 6061-T6 aluminum alloy; (0088) Nickel, Type A.

RE-ORDER No. 67-347

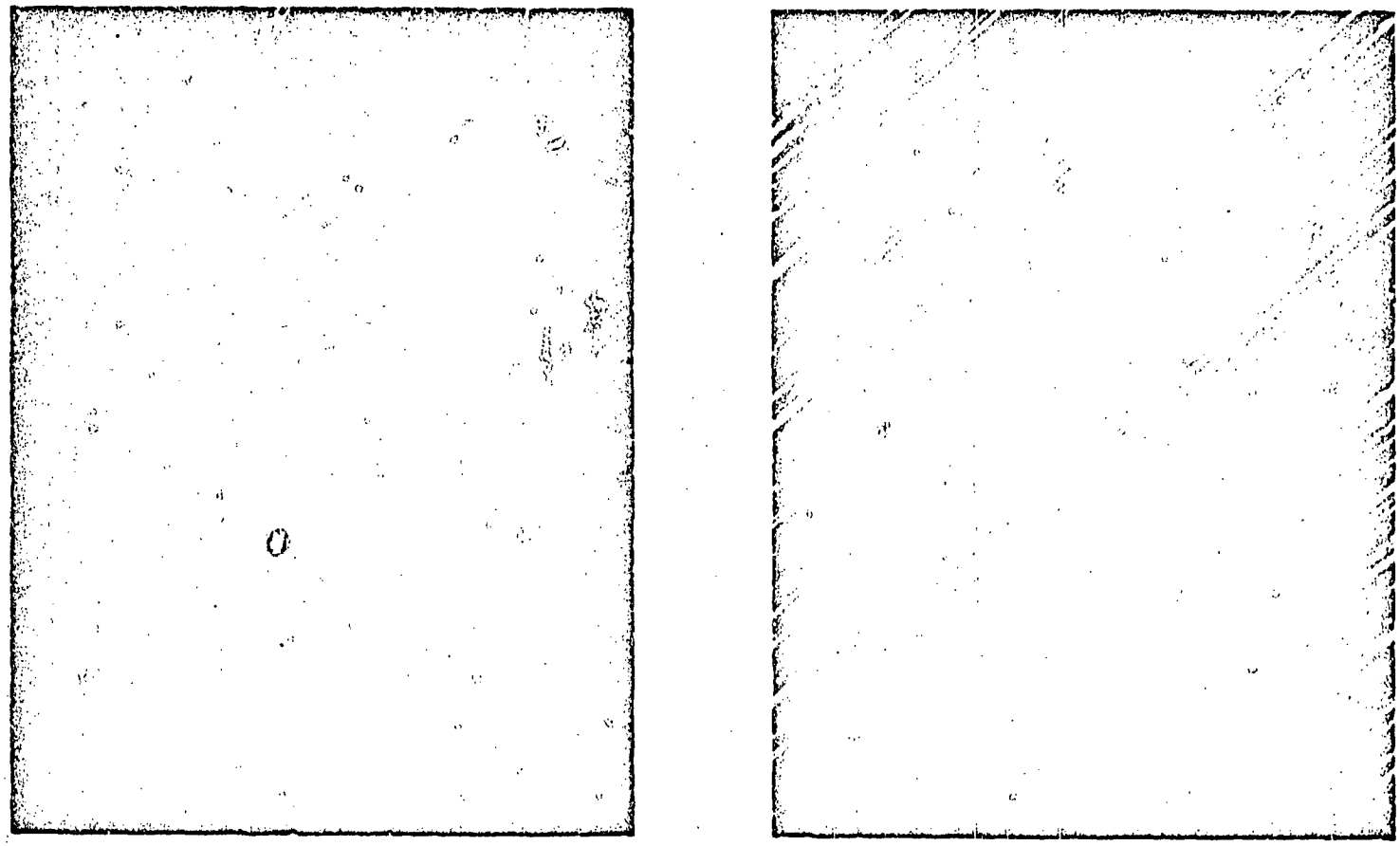

0110

0111

TA-6063-32

FIG. 23 PHOTOMICROGRAPHS OF ENDS OF SPECIMENS AFTER STORAGE (53X). (0110) 347 stainless steel plus Rulon coating; (0111) 6A1-4V titanium alloy plus Pulon coating.

RE-ORDER No. 67-3

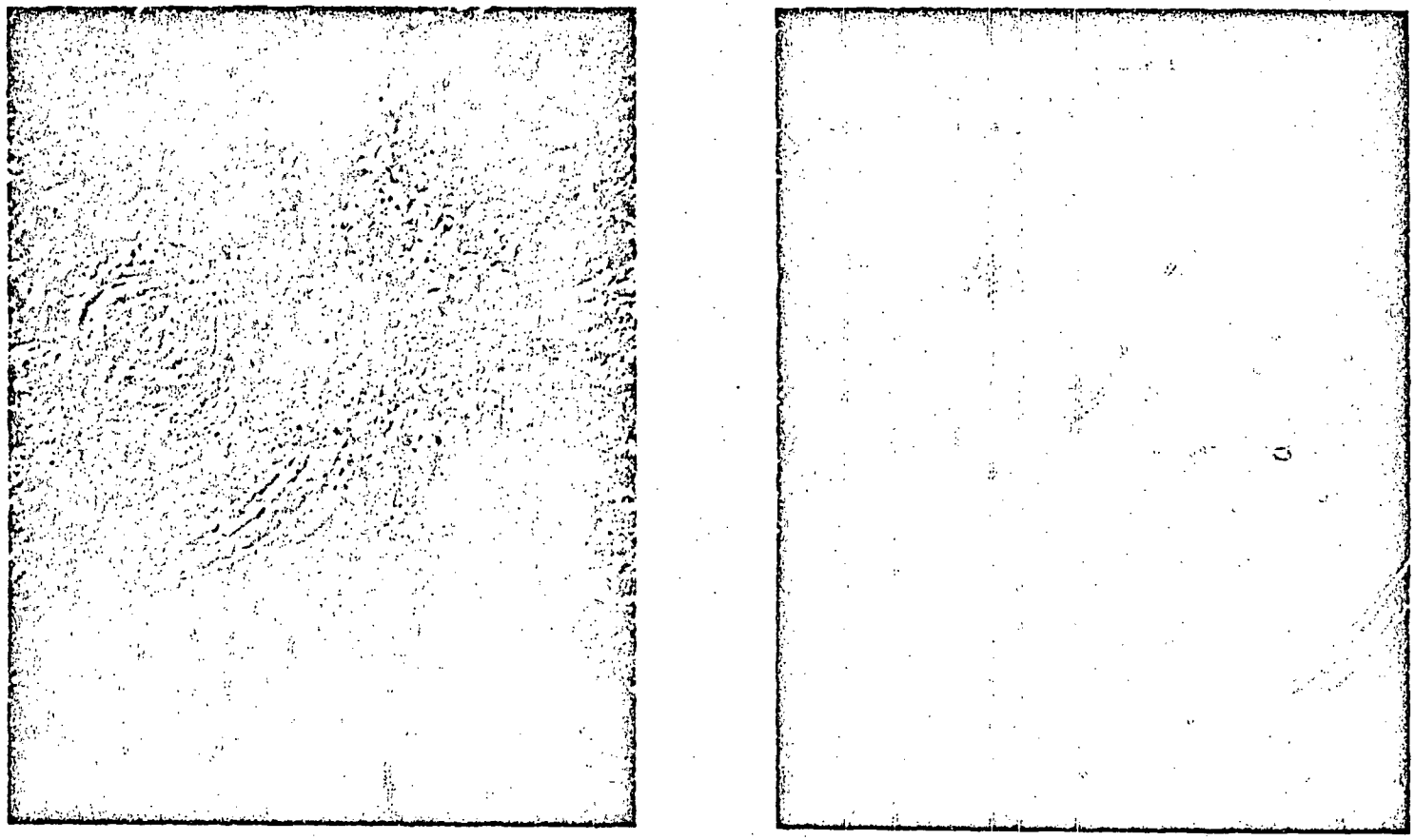

0112

0115

TA-6063-33

FIG. 24 PHOTOMICROGRAPHS OF ENDS OF SPECIMENS AFTER STORAGE (53X). (0112) 6061-T6 aluminum alloy plus Rulon coating; (0115) 6061-T6 aluminum alloy plus Kel-F grease coating.

0116

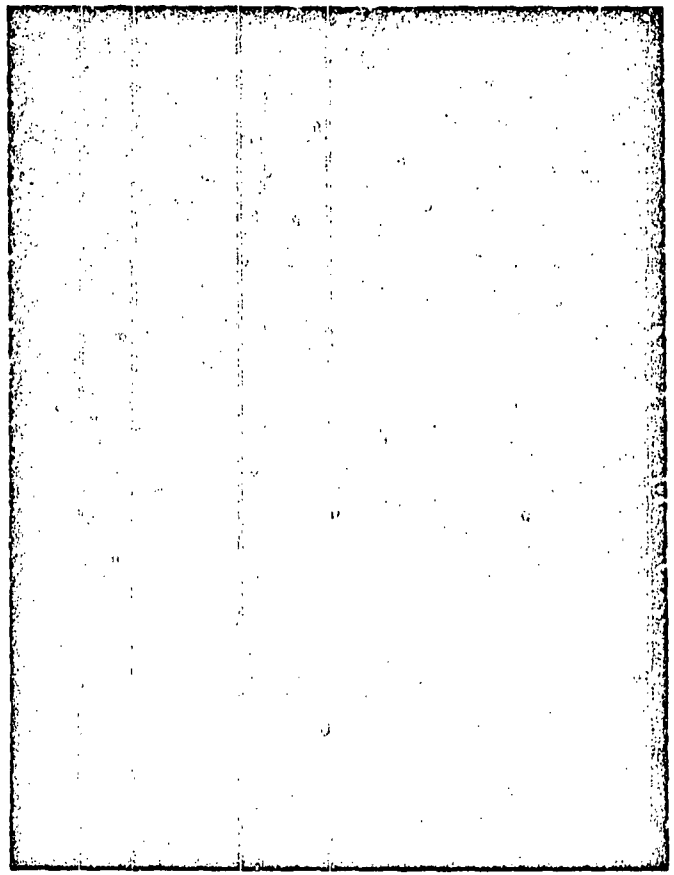

246

TA-6063-34

FIG. 25 PHOTOMICROGRAPHS OF ENDS OF SPECIMENS AFTER STORAGE (53X). (0116) 6A1-4V titanium alloy plus Kel-F grease coating; (246) 356-T6 aluminum alloy.

RE-ORDER NO. 67-34

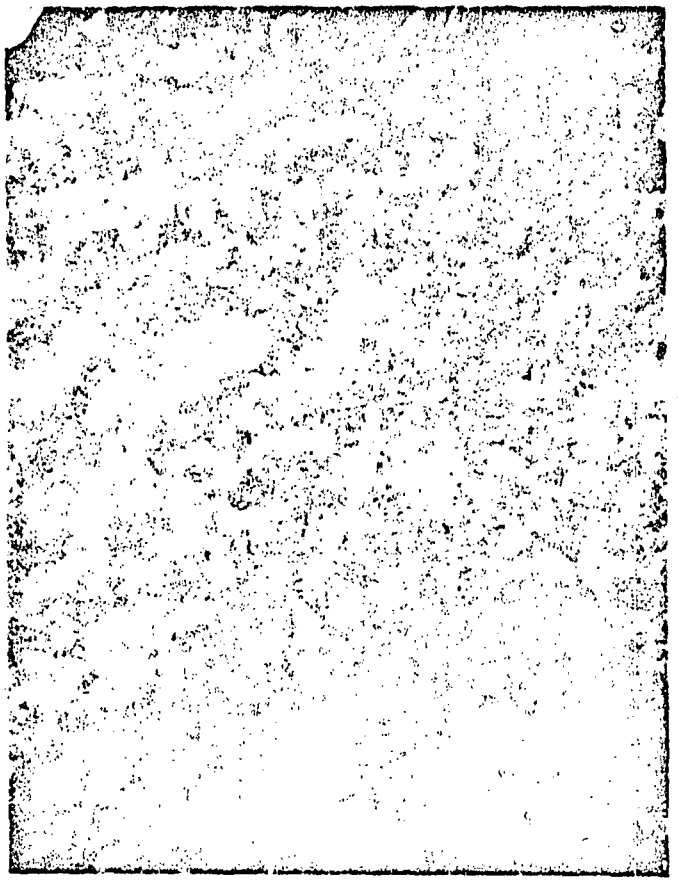

247

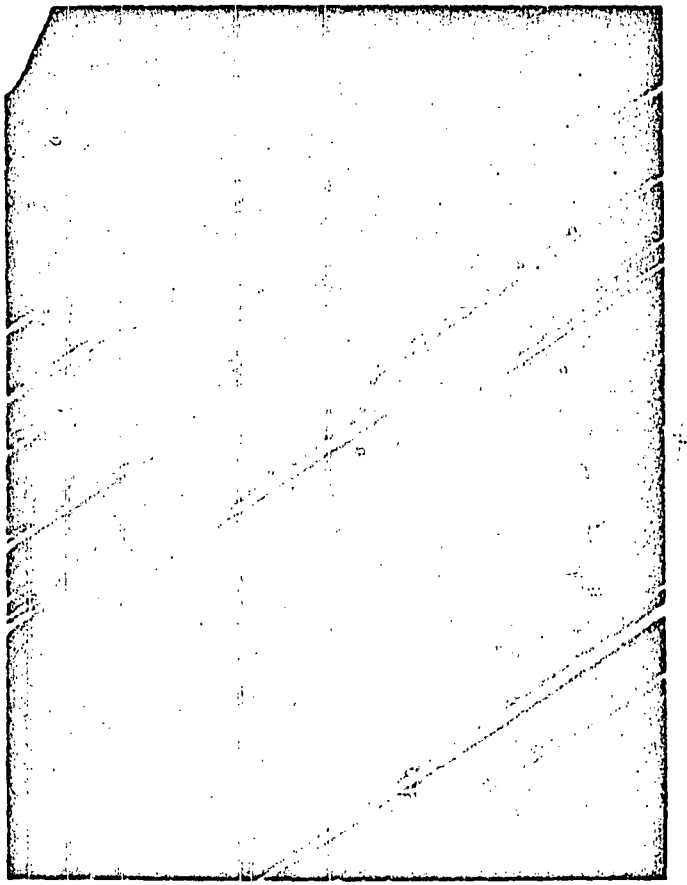

251

TA-6063-35

FIG. 26 PHOTOMICROGRAPHS OF ENDS OF SPECIMENS AFTER STORAGE (53X). (247) 356-T6 aluminum alloy; (251) 6A1-4V titanium alloy.

RE-ORDER No. 67-347

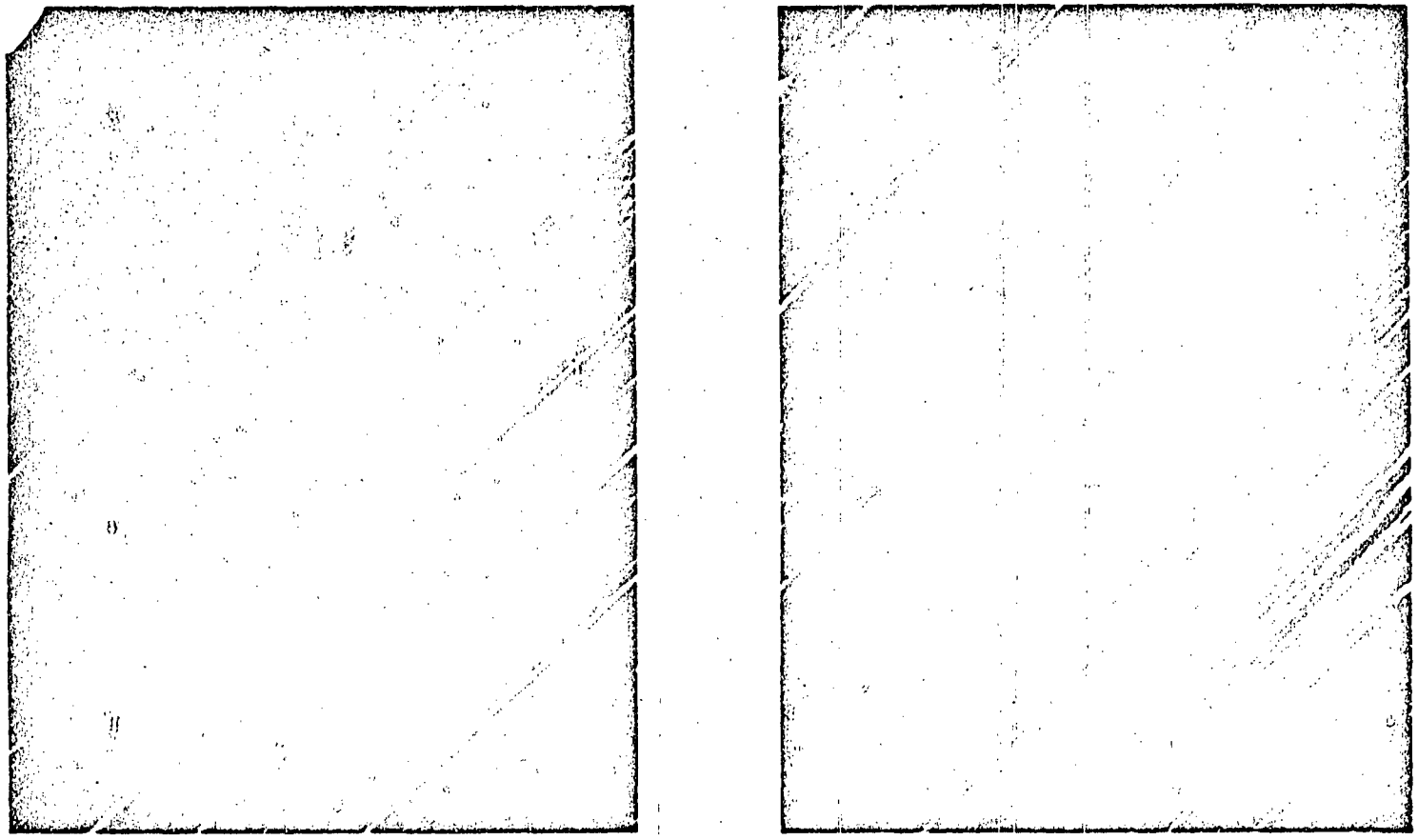

252

253

TA-6063-36

FIG. 27 PHOTOMICROGRAPHS OF ENDS OF SPECIMENS AFTER STORAGE (53X). (252) 6A1-4V titanium alloy; (253) 6A1-4V titanium alloy.

RE-ORDER No. 67-

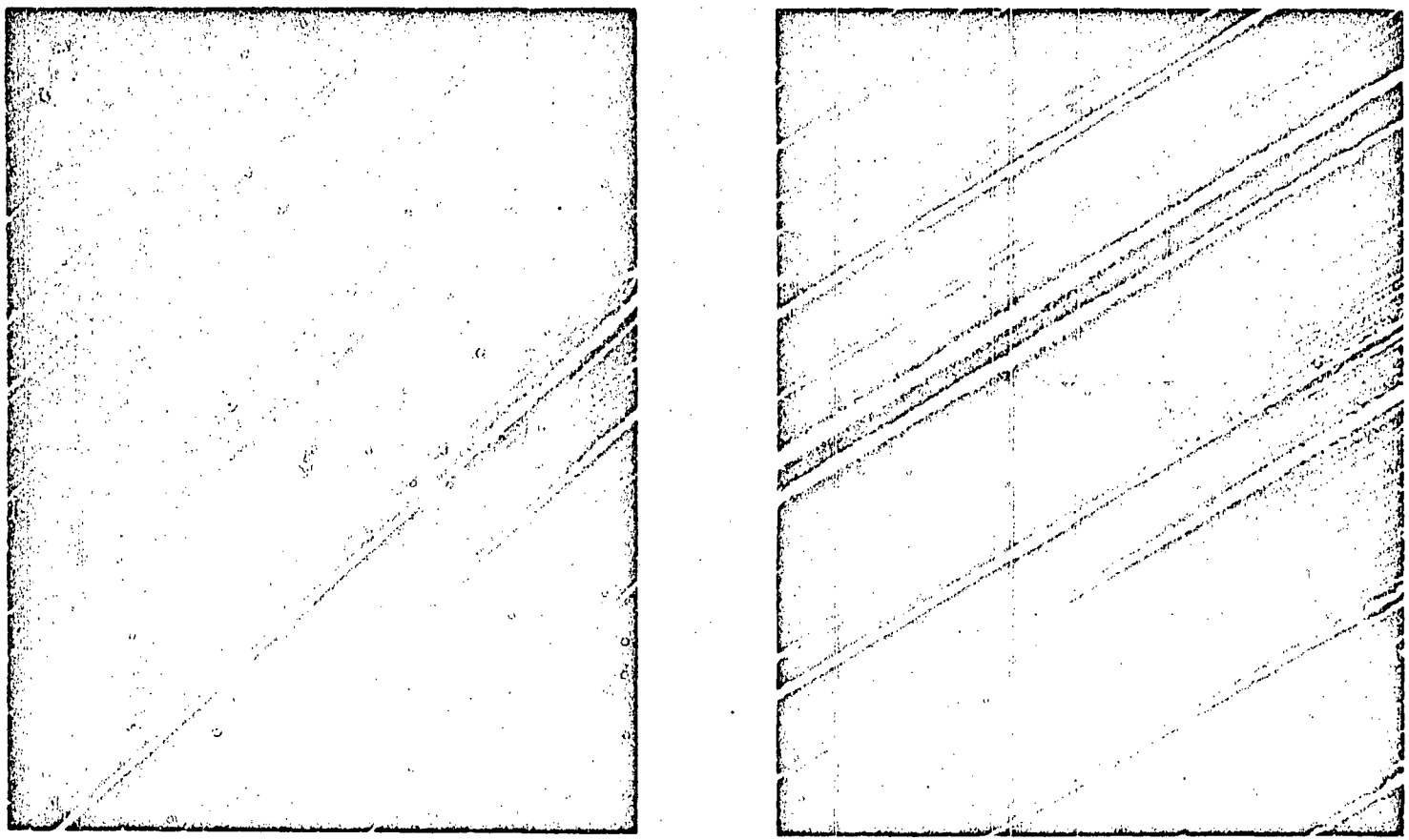

254

255

TA-6063-37

FIG. 28 PHOTOMICROGRAPHS OF ENDS OF SPECIMENS AFTER STORAGE (53X). (254) 6A1-4V titanium alloy; (255) 6A1-4V titanium alloy.

RE-ORDER No. 67-347

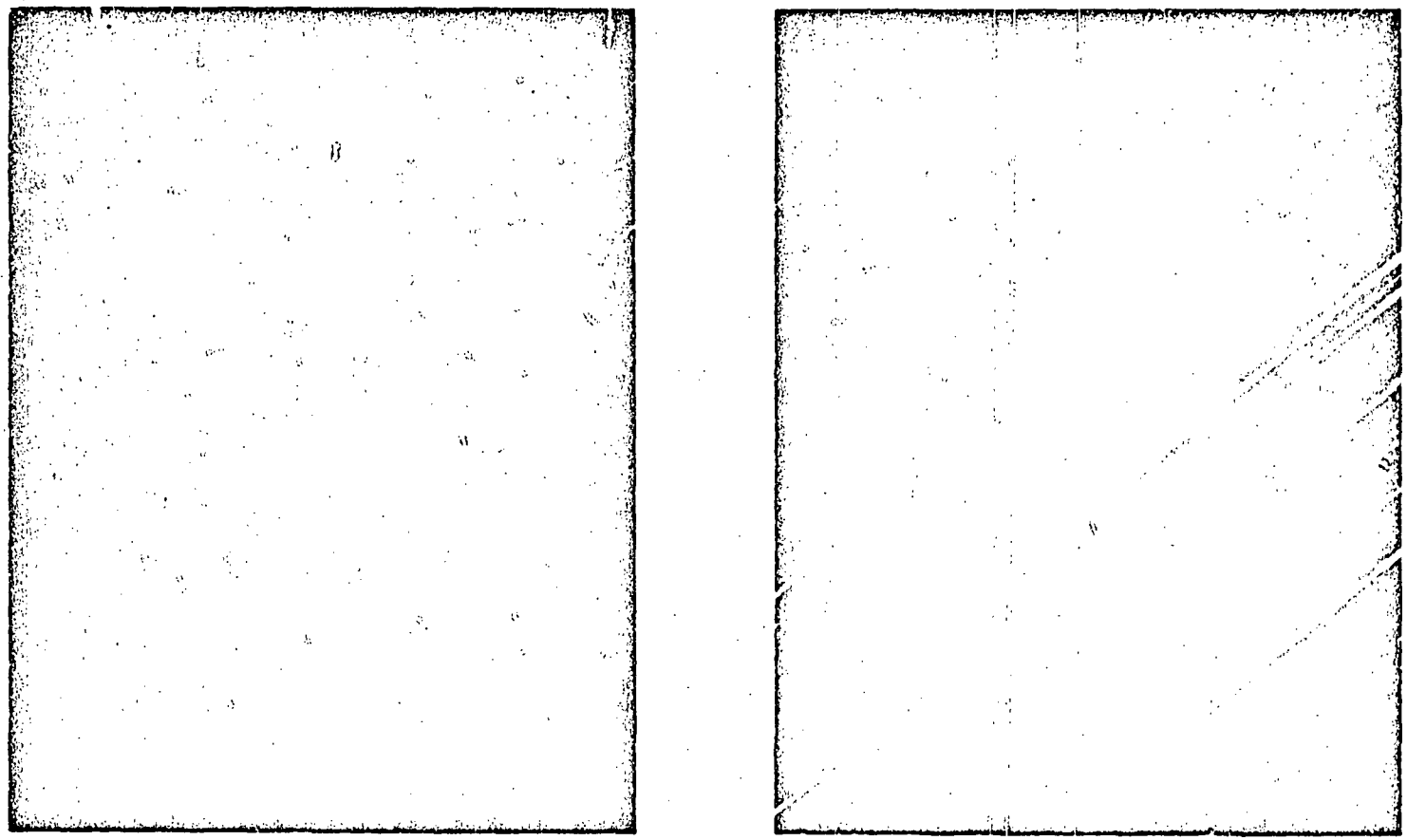

256

257

TA-6063-38

FIG. 29 PHOTOMICROGRAPHS OF ENDS OF SPECIMENS AFTER STORAGE (53X). (256) 6A1-4V titanium alloy; (257) 6A1-4V titanium alloy.

RE-ORDER NO. 67-3

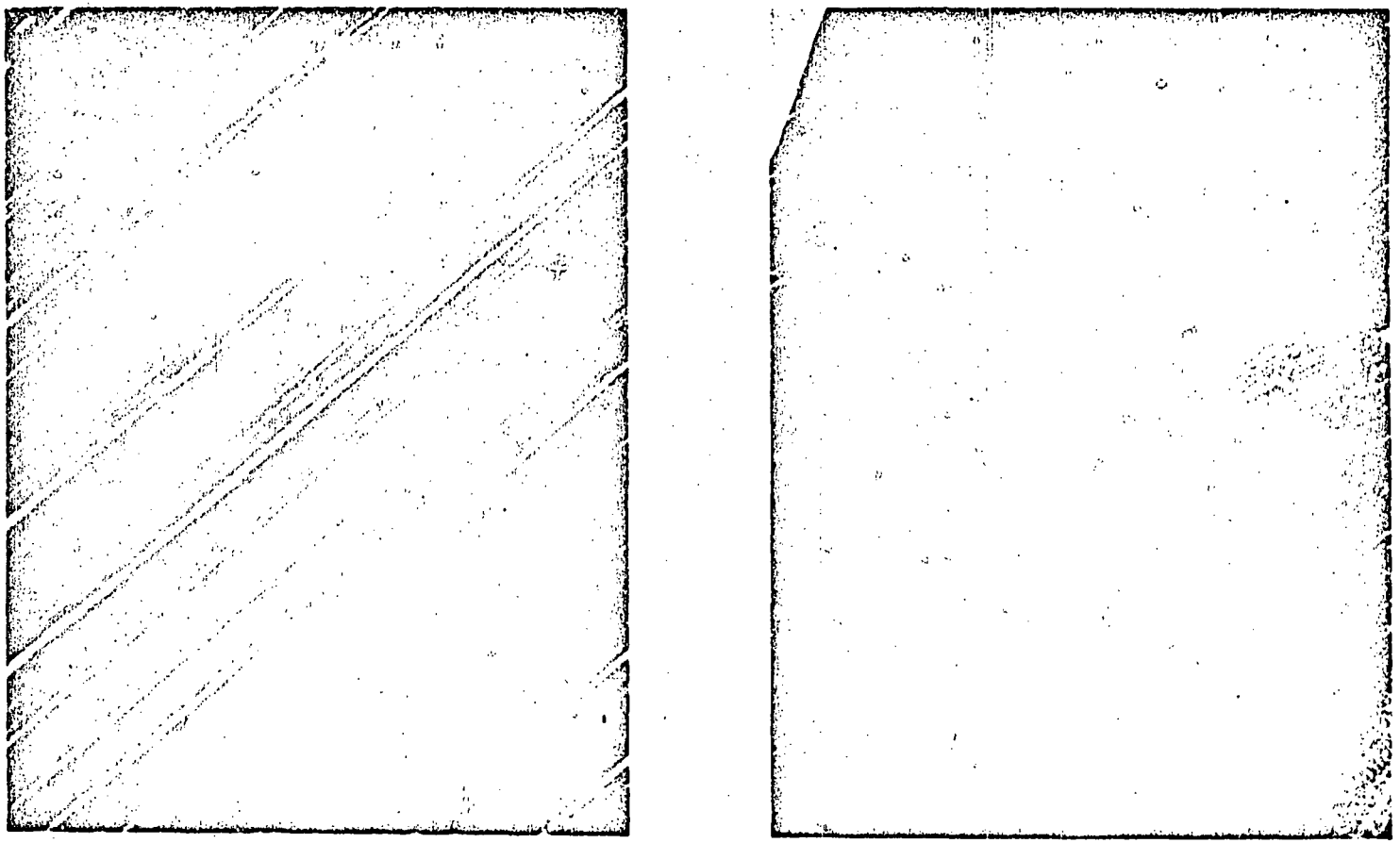

258

259

TA-6063-39

FIG. 30 PHOTOMICROGRAPHS OF ENDS OF SPECIMENS AFTER STORAGE (53X). (258) 6A1-4V titanium alloy; (259) 6A1-4V titanium alloy.

RE-ORDER NO. 67-317

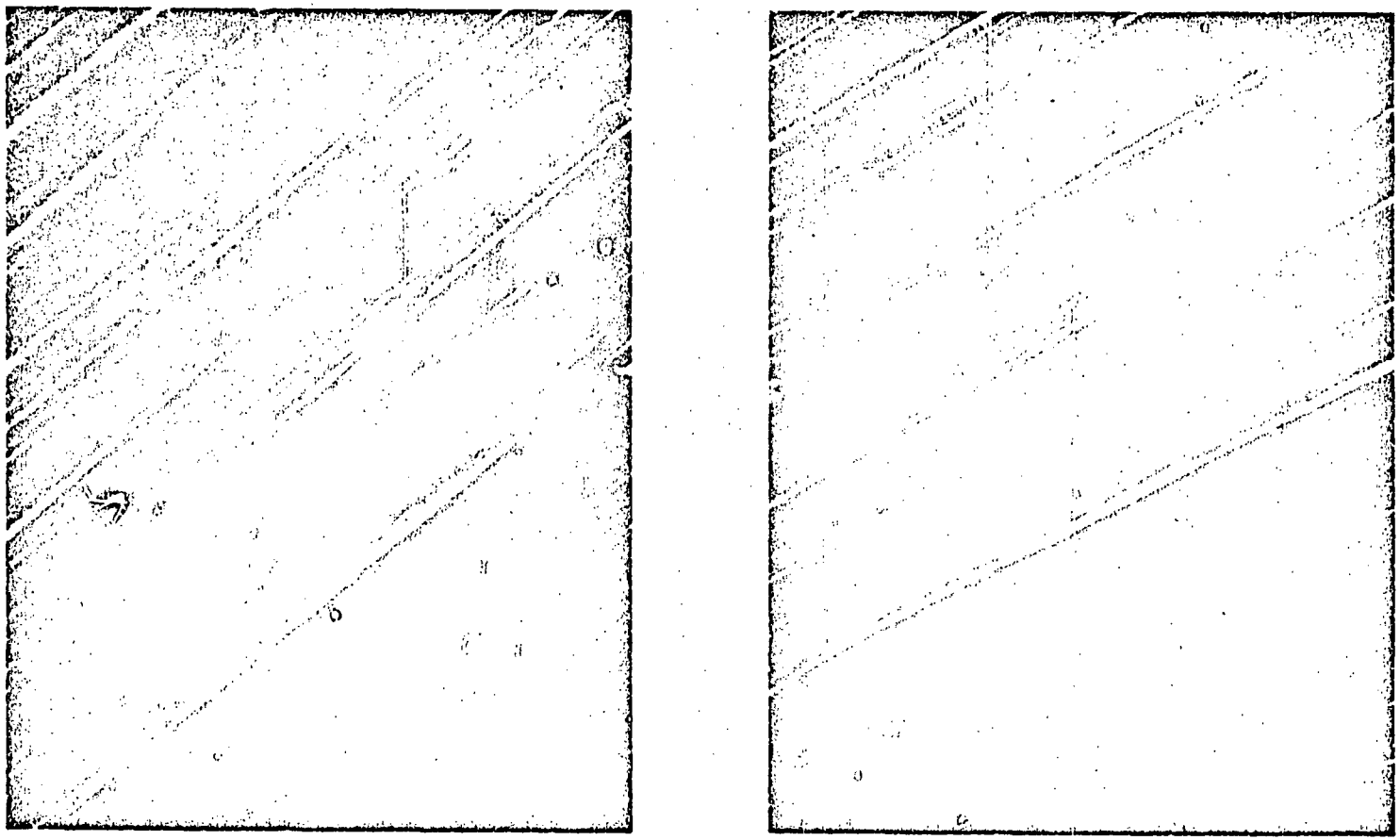

260

261

TA-6063-40

FIG. 31 PHOTOMICROGRAPHS OF ENDS OF SPECIMENS AFTER STORAGE (53X). (260) 6A1-4V titanium alloy, (261) 6A1-4V titanium alloy.

RE-ORDER No. 67

262

TA-6063-41

FIG. 32 PHOTOMICROGRAPH OF END OF SPECIMEN AFTER STORAGE (53X). (262) 6Al-4V titanium alloy.

RE-ORDER NO. 67-347

RE-ORDER No. 67-347

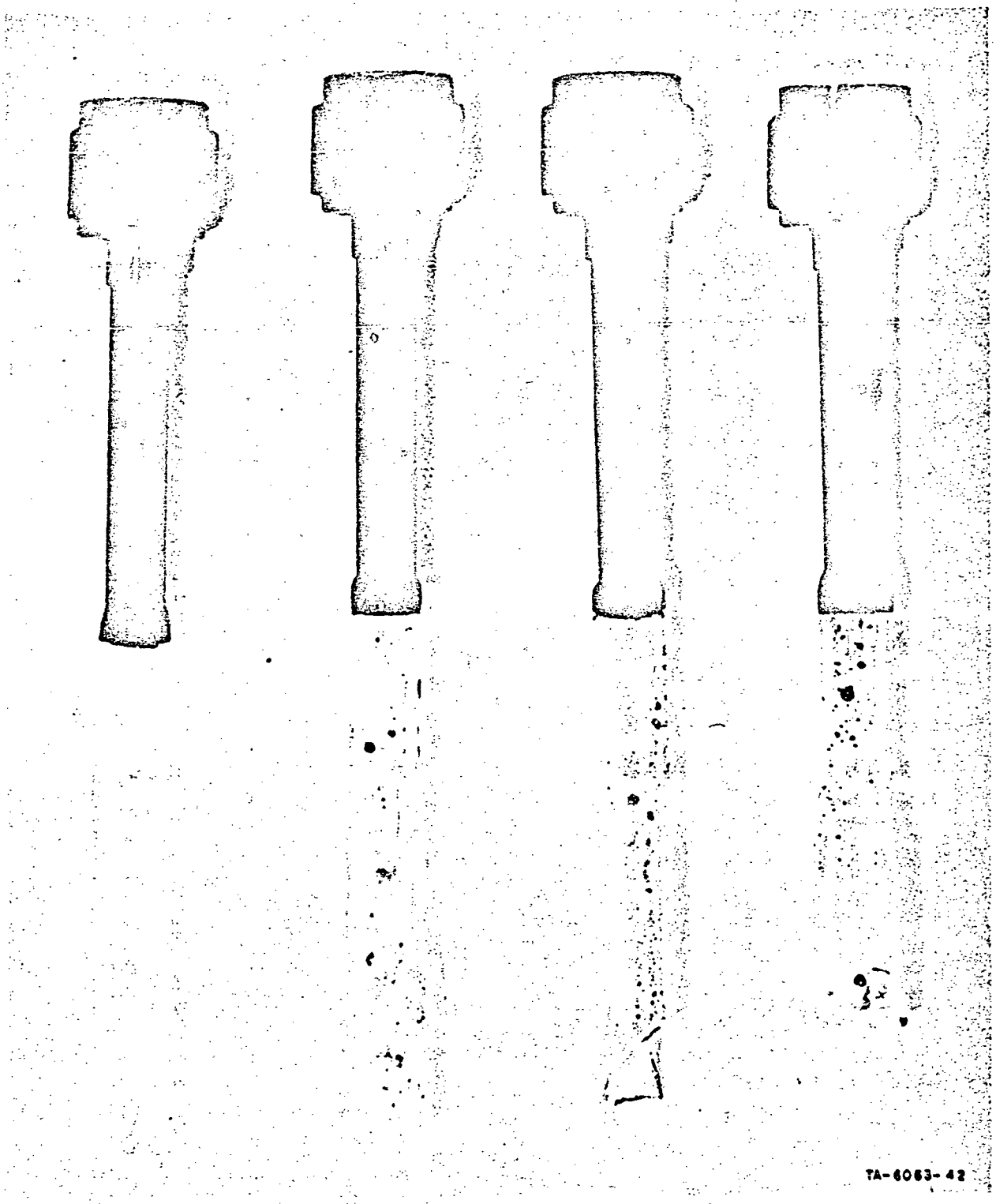

FIG. 33 PHOTOGRAPH OF TYPICAL DEPOSITS RESULTING FROM CORROSION OF KOVAR METAL USED TO CONNECT THE SAMPLE CAPSULES TO THE PRESSURE GAGES

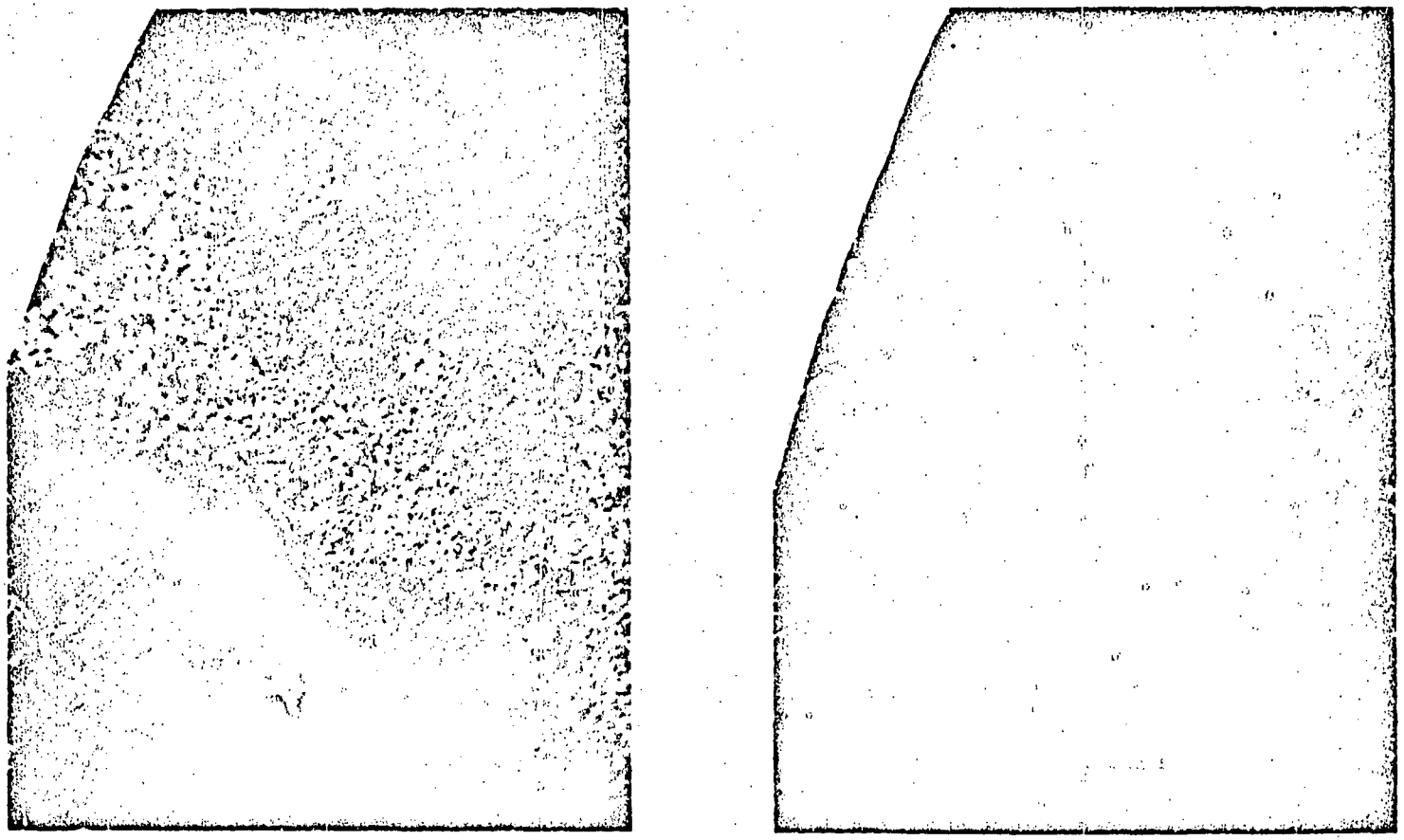

FIG. 34 PHOTOMICROGRAPH OF KOVAR TUBING (53X) SHOWING MILD ATTACK (1) inner surface; (2) exterior surface for comparison

RE-ORDER No 67-347

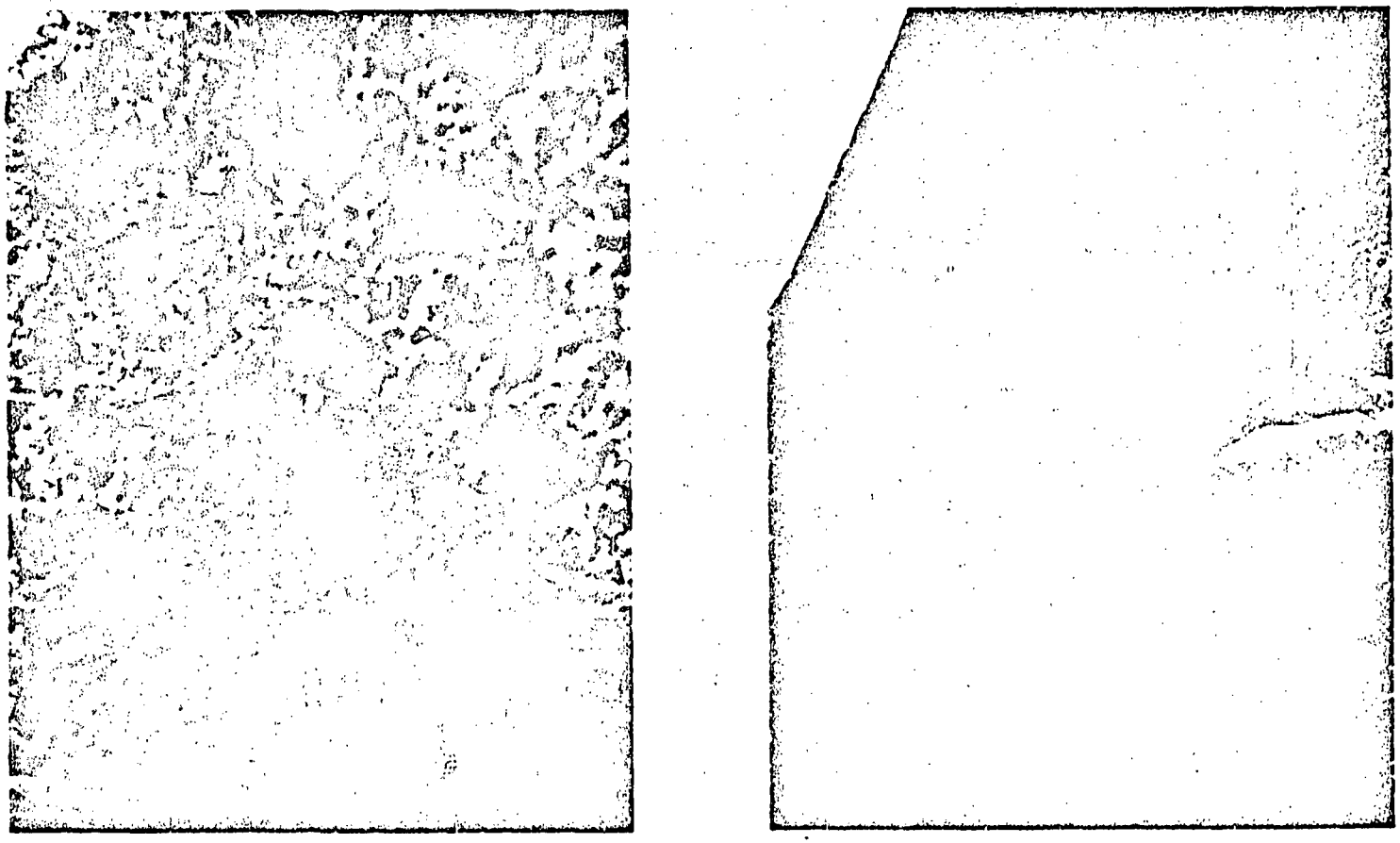

FIG. 35 PHOTOMICROGRAPH OF KOVAR TUBING (53X) SHOWING MODERATE ATTACK. (1) inner surface; (2) exterior surface for comparison.

RE-ORDER NO. 67-3

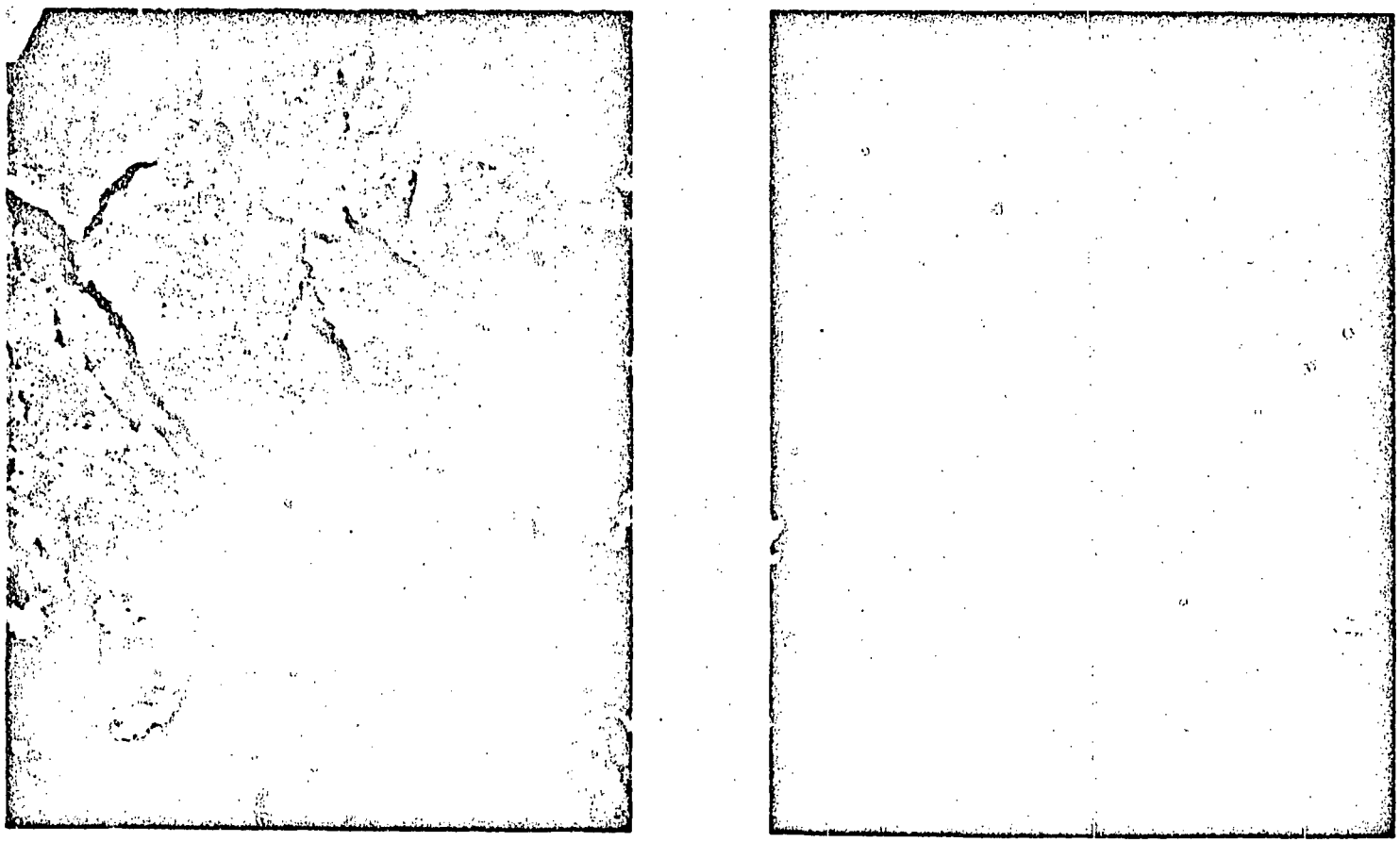

FIG. 36 PHOTOMICROGRAPH OF KOVAR TUBING (53X) SHOWING STRONG ATTACK. (1) inner surface; (2) exterior surface for comparison.

RECORDED AS ORNL-3747

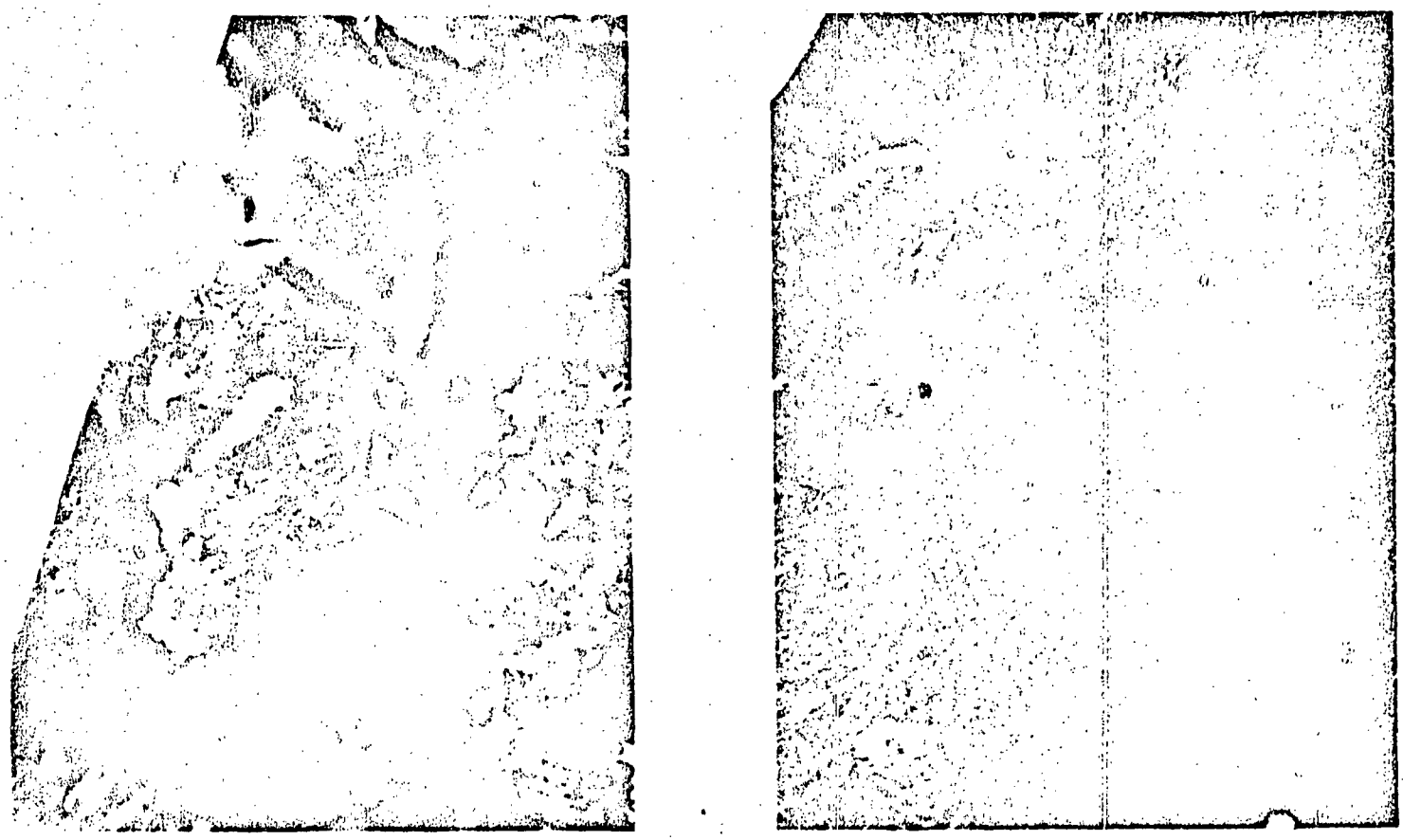

FIG. 37 PHOTOMICROGRAPH OF KOVAR TUBING (53X) SHOWING VERY STRONG ATTACK. (1) inner surface; (2) exterior surface for comparison.

RECORD NO. 67-3

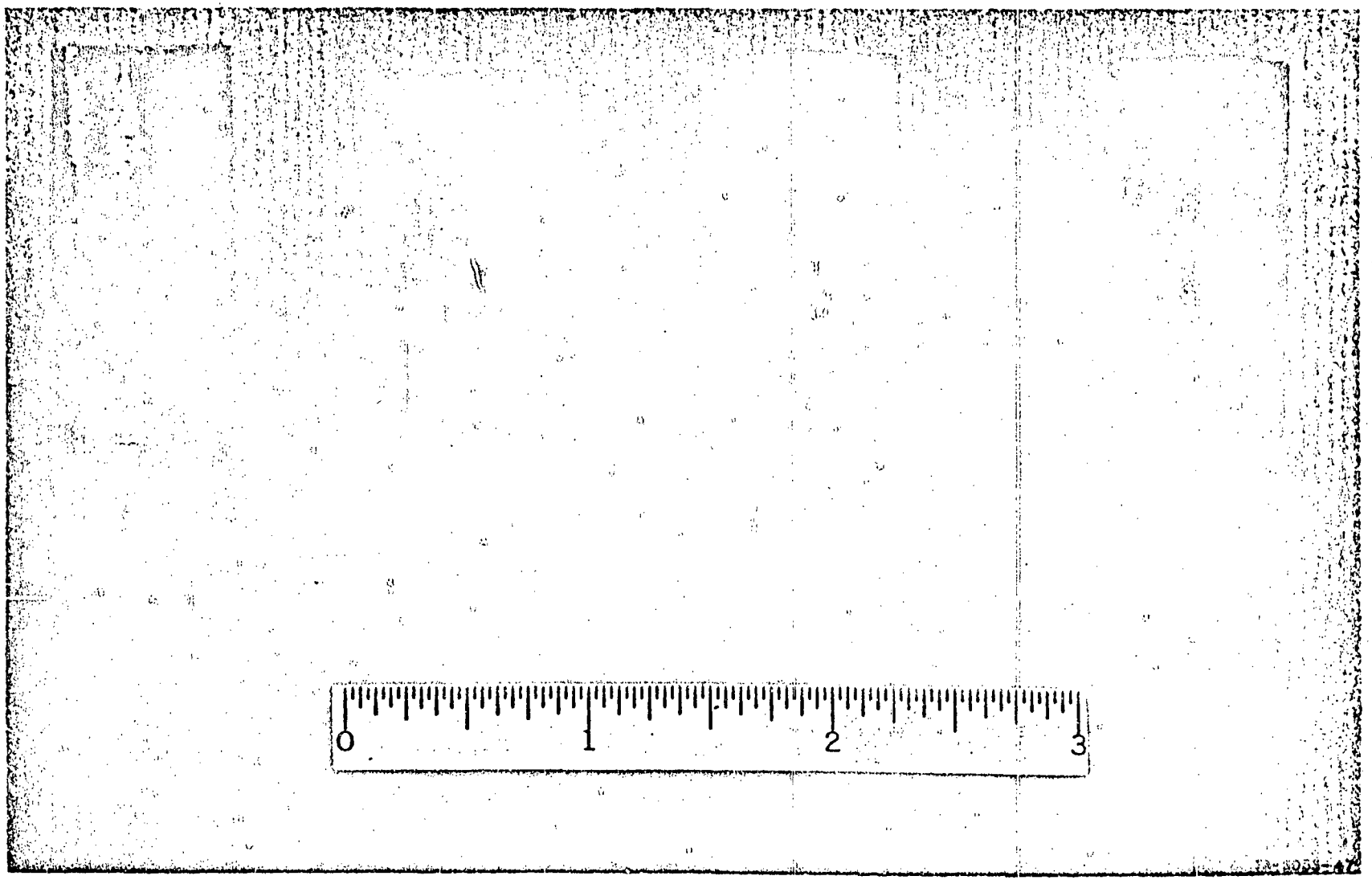

FIG. 38 PHOTOGRAPH OF INTERIOR SURFACES OF FOUR KOVAR SEALS USED IN NITROGEN TETROXIDE STORAGE TESTS, SHOWING EXTENT OF CORROSION FROM MILD TO SEVERE

RE-ORDER NO. 67-347

(Page 80).

This page was missing from the report when received by NTIS. Repeated efforts to obtain a replacement page have been unsuccessful.

This report is being made available in its present form with the hope it will be of sufficient value to justify its announcement and distribution.

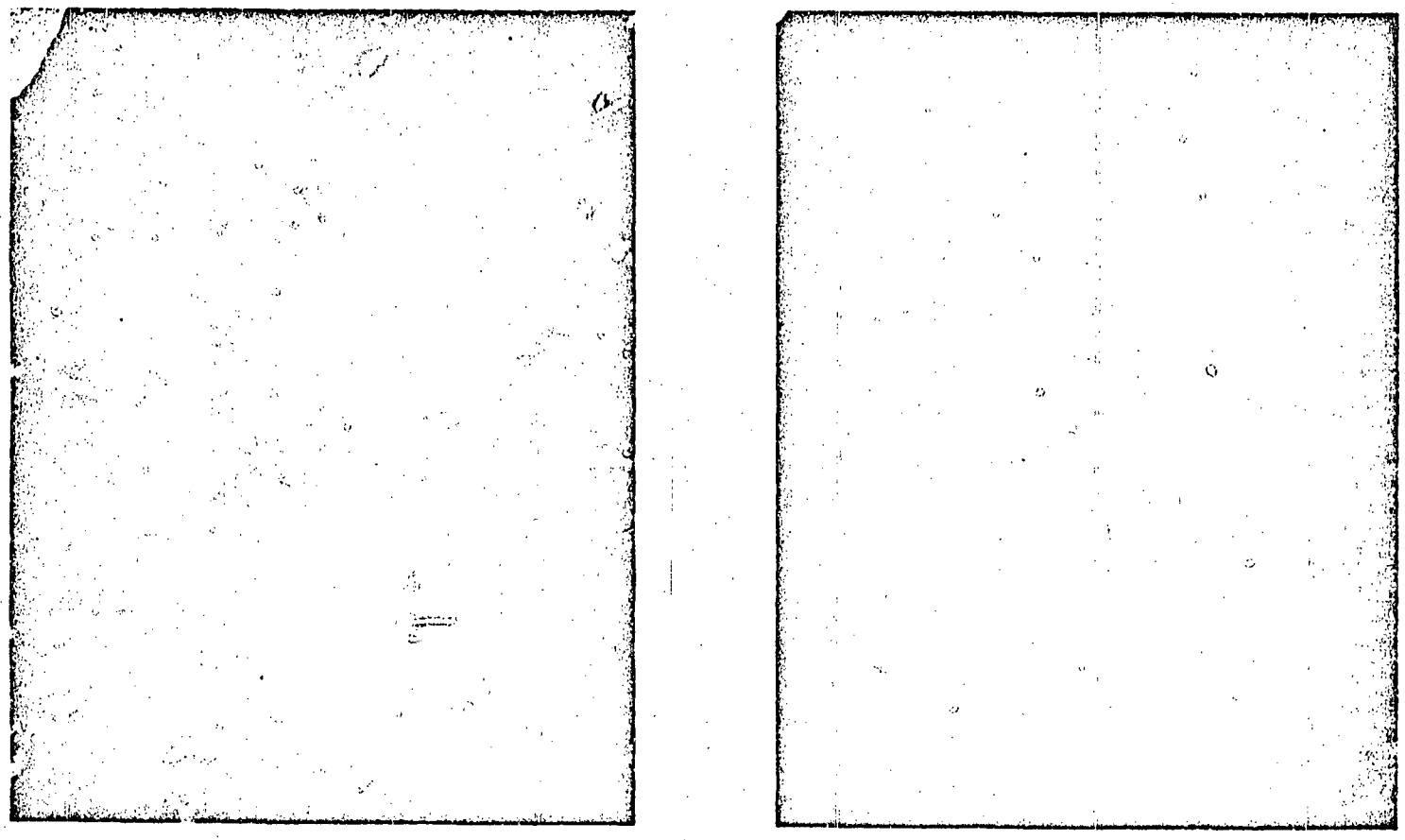

1

2

TA-6063-48

FIG. 39 PHOTOMICROGRAPHS OF INTERNAL AND EXTERNAL SURFACES OF BOURDON TUBE FROM TEST GAGE NO. 0072 (45X). (1) inner surface; (2) exterior surface for comparison

RE ORDER NO. 67-34

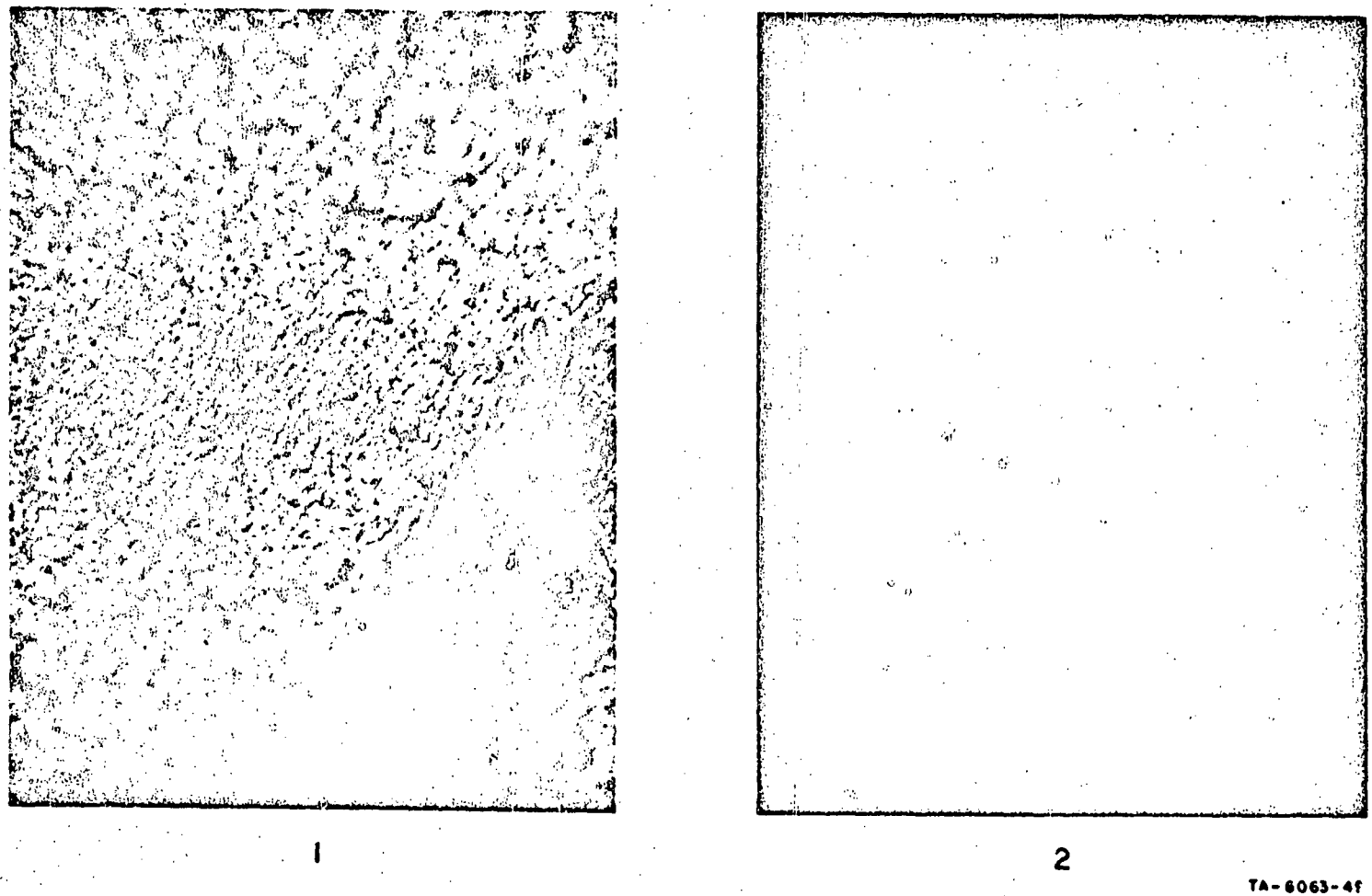

1 2

TA-6063-41

FIG. 40 PHOTOMICROGRAPHS OF INTERNAL AND EXTERNAL SURFACES OF BOURDON TUBE FROM TEST GAGE NO. 0078 (45X). (1) inner surface; (2) exterior surface for comparison.

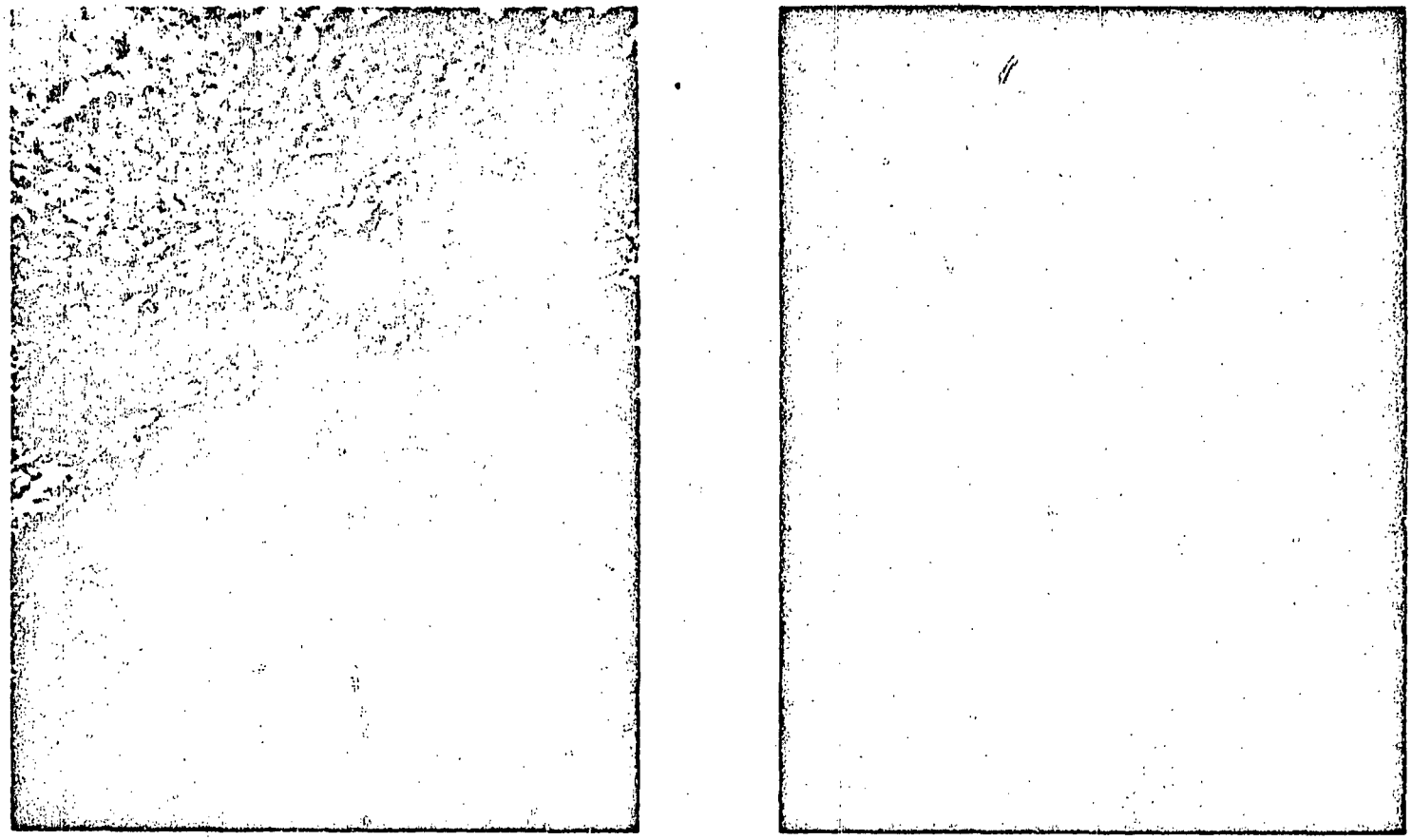

1 2

TA-6063-50

FIG. 41 PHOTOMICROGRAPHS OF INTERNAL AND EXTERNAL SURFACES OF BOURDON TUBE FROM TEST GAGE NO. 0082 (45X). (1) inner surface; (2) exterior surface for comparison.

RE-ORDER NO. 67-349

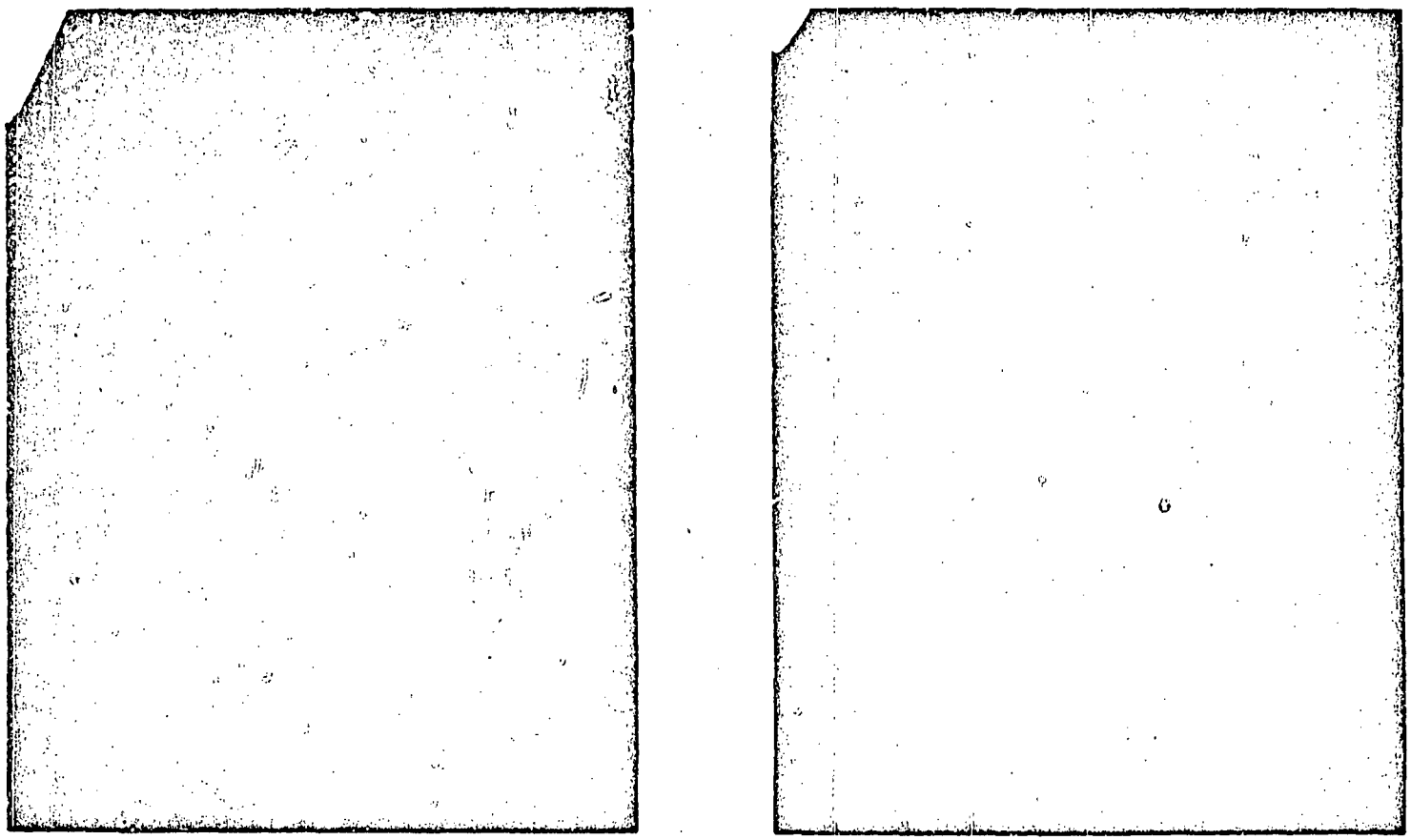

FIG. 42 PHOTOMICROGRAPHS OF INTERNAL AND EXTERNAL SURFACES OF BOURDON TUBE FROM TEST GAGE NO. 0083 (45X). (1) inner surface; (2) exterior surface for comparison.

RE-ORDER NO. 67-347

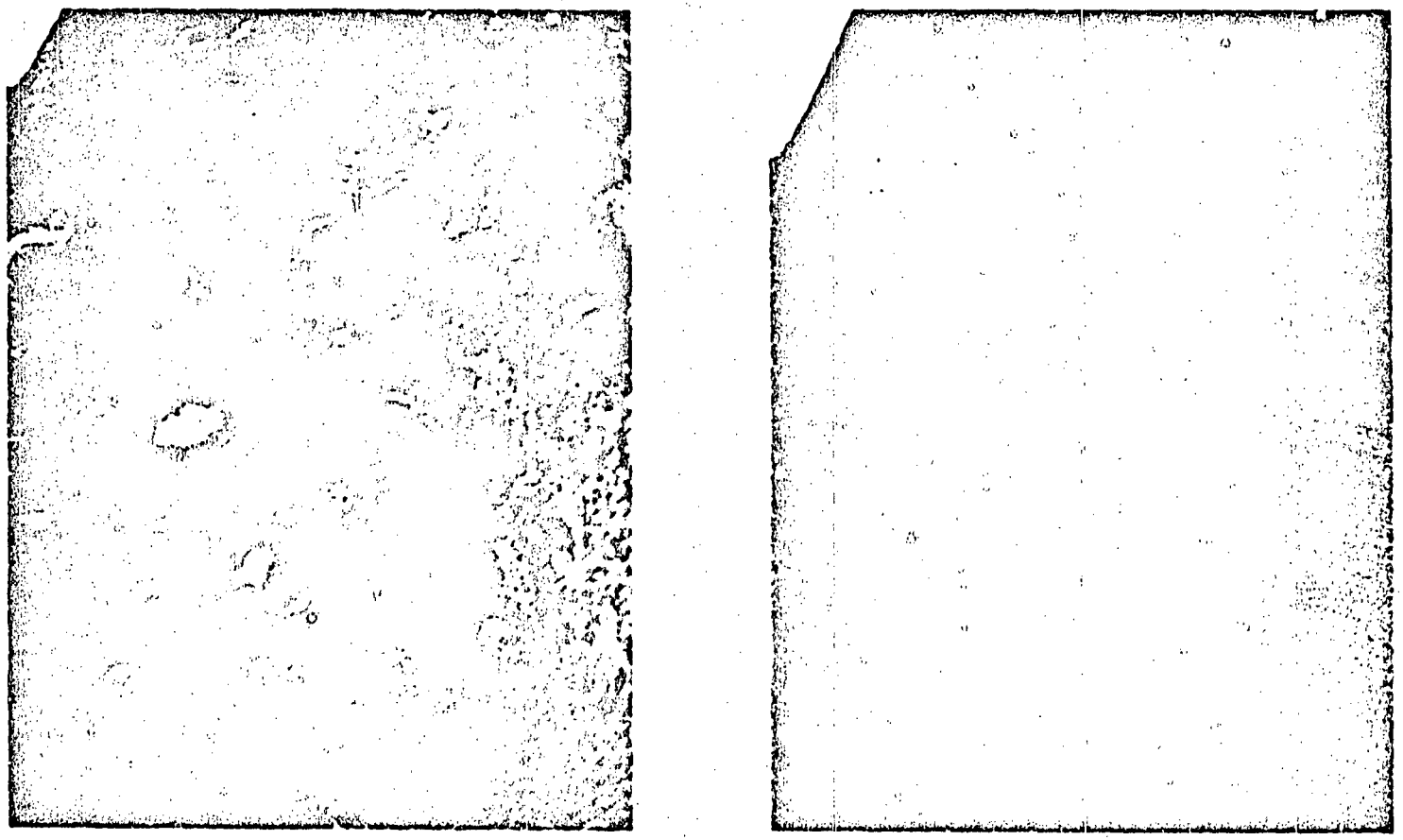

FIG. 43 PHOTOMICROGRAPHS OF INTERNAL AND EXTERNAL SURFACES OF BOURDON TUBE FROM TEST GAGE NO. 247 (45X). (1) inner surface; (2) exterior surface for comparison.

RECORDED AS 67-34

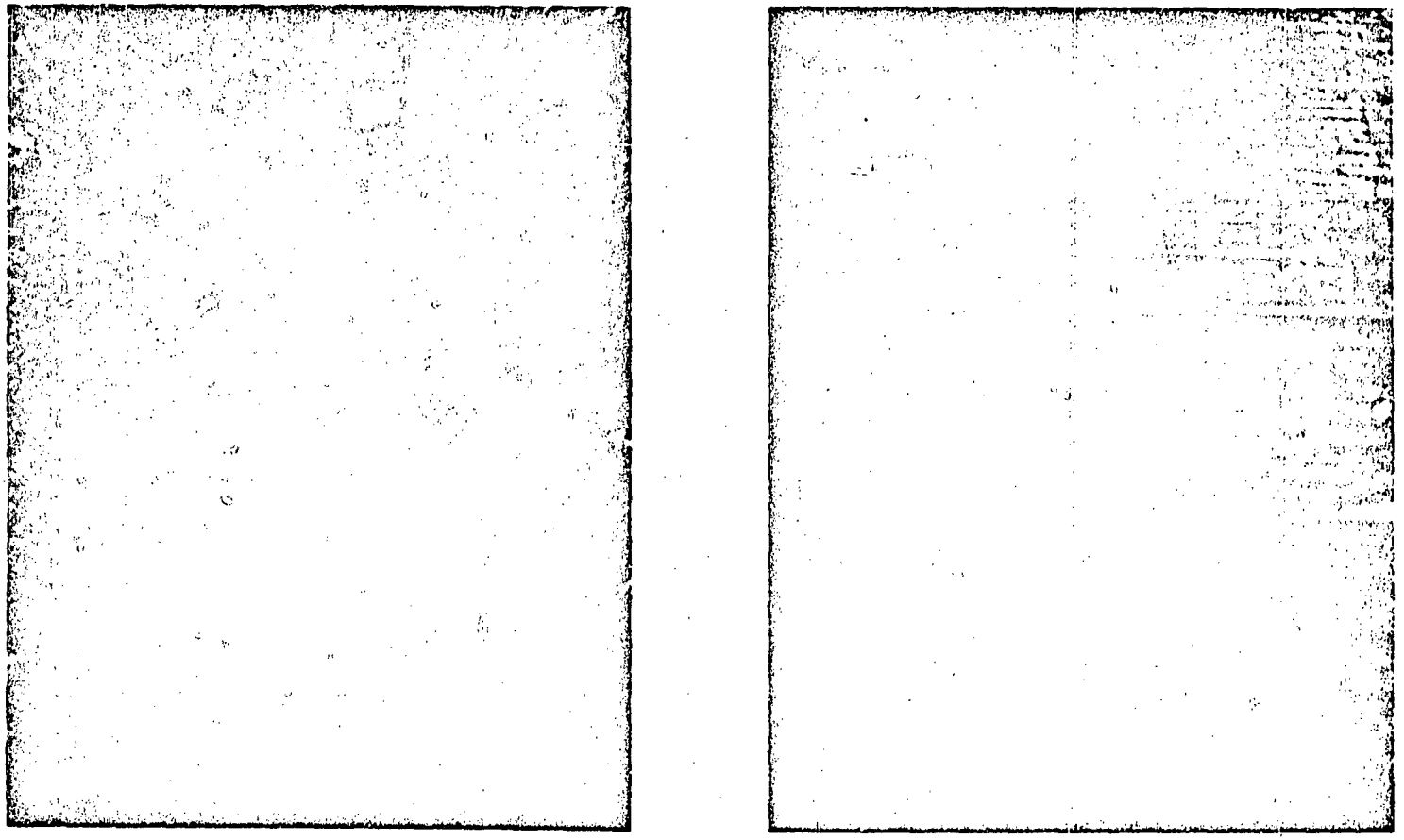

1 2

TA-6063-53

FIG. 44 PHOTOMICROGRAPHS OF INTERNAL AND EXTERNAL SURFACES OF BOURDON TUBE FROM TEST GAGE NO. 252 (45X). (1) inner surface; (2) exterior surface for comparison.

RE-ORDER No. C7-347

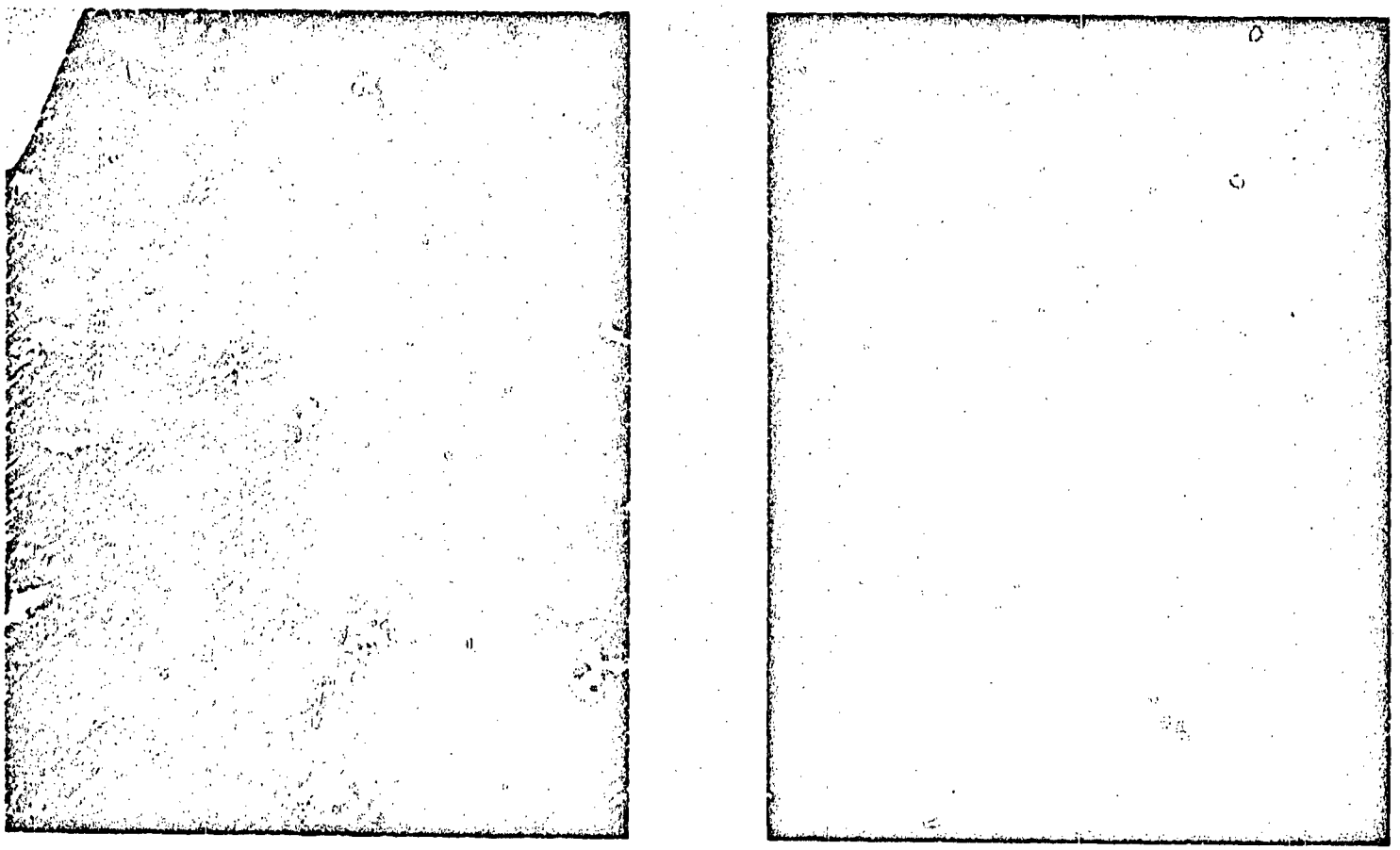

1 2

TA-6063-54

FIG. 45 PHOTOMICROGRAPHS OF INTERNAL AND EXTERNAL SURFACES OF BOURDON TUBE FROM TEST GAGE NO. 260 (45X). (1) inner surface; (2) exterior surface for comparison.

RE-ORDER NO. 67-3

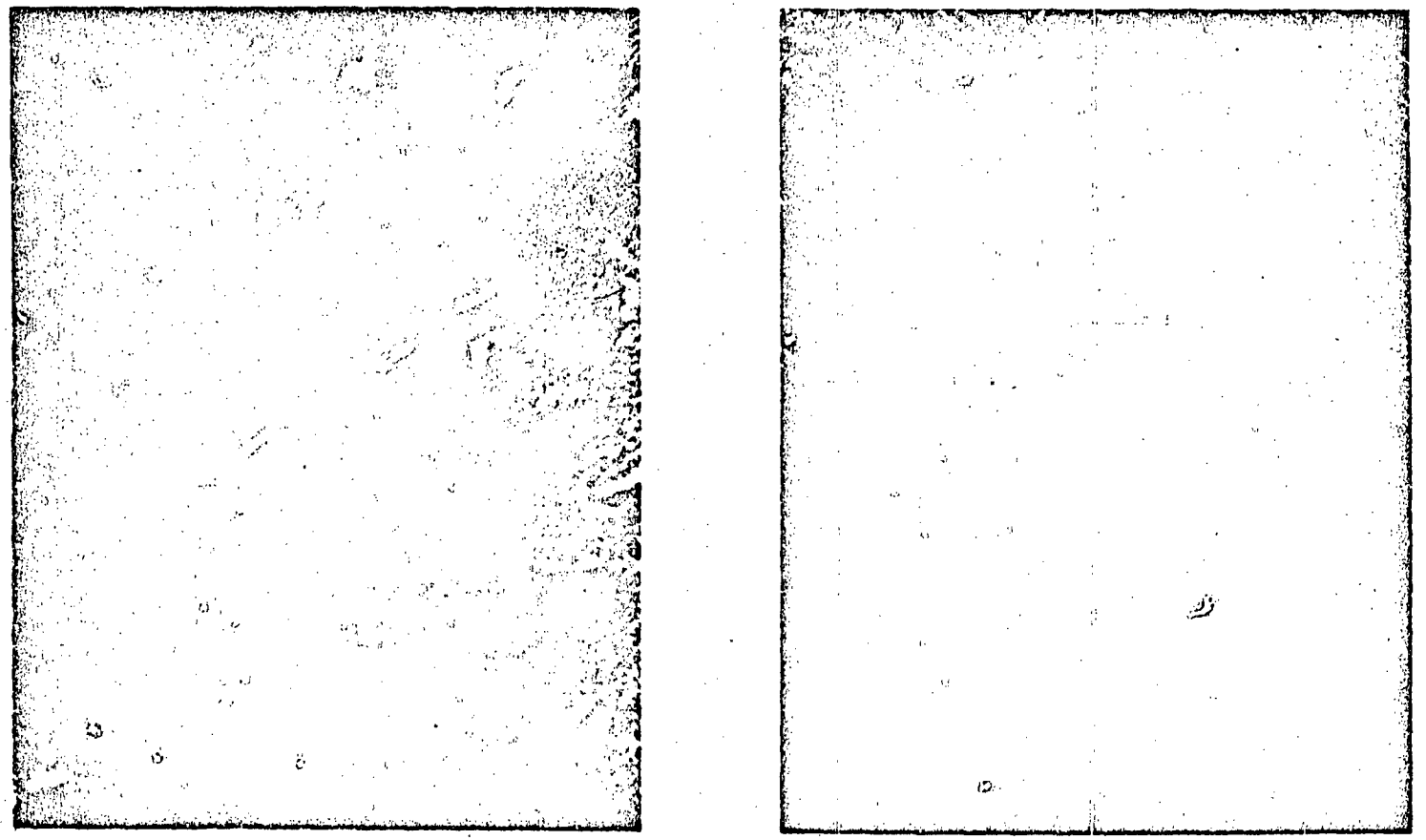

1 2

TA-6063-55

FIG. 46 PHOTOMICROGRAPHS OF INTERNAL AND EXTERNAL SURFACES OF BOURDON TUBE FROM TEST GAGE NO. 262 (45X). (1) inner surface; (2) exterior surface for comparison.

RELEASED NO 67-347

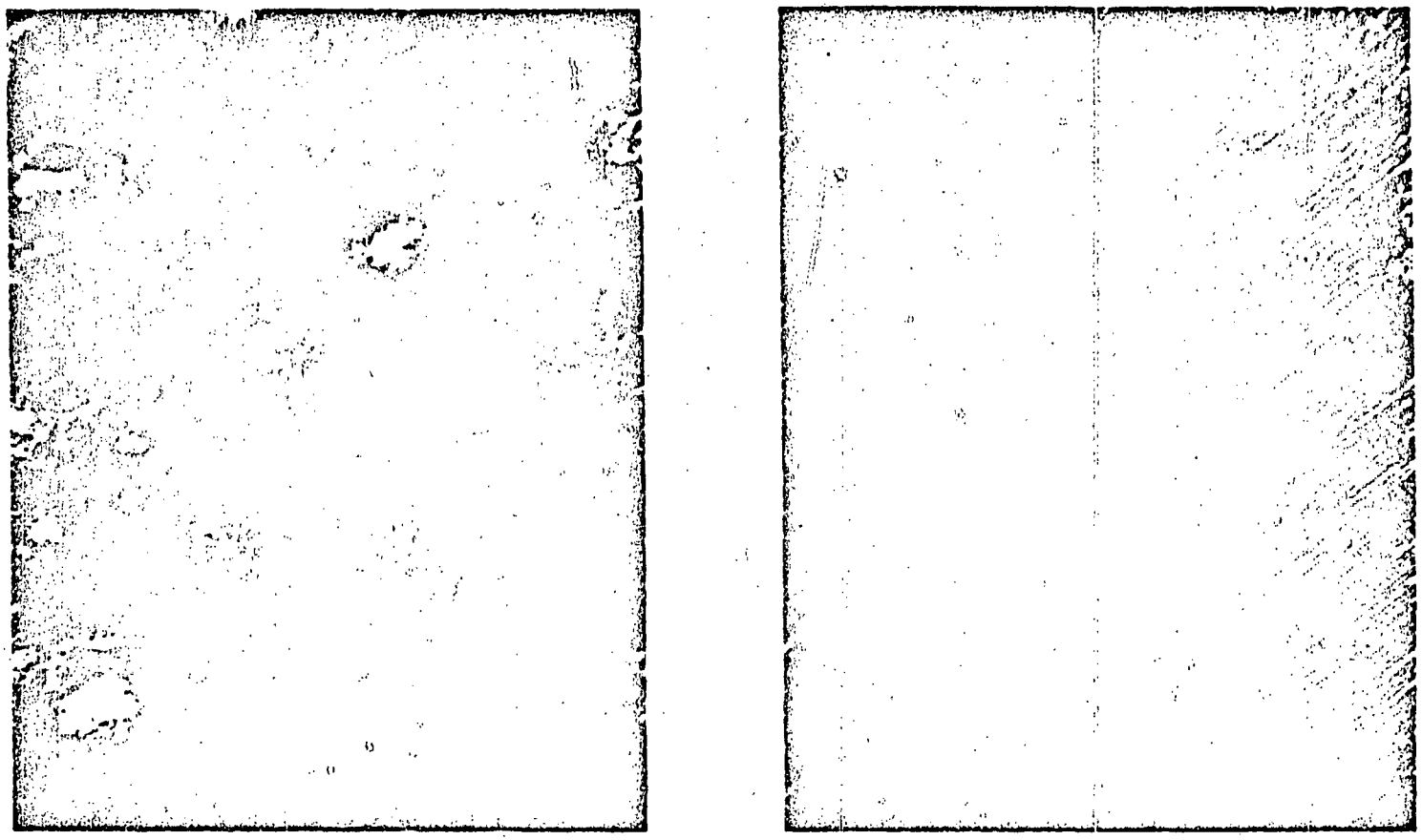

1 2

TA-6063-56

FIG. 47 PHOTOMICROGRAPHS OF INTERNAL AND EXTERNAL SURFACES OF BOURDON TUBE FROM GAGE "A" NOT EXPOSED TO N_2O_4 (53X). (1) inner surface; (2) exterior surface for comparison.

RE-ORDER NO. 67-34

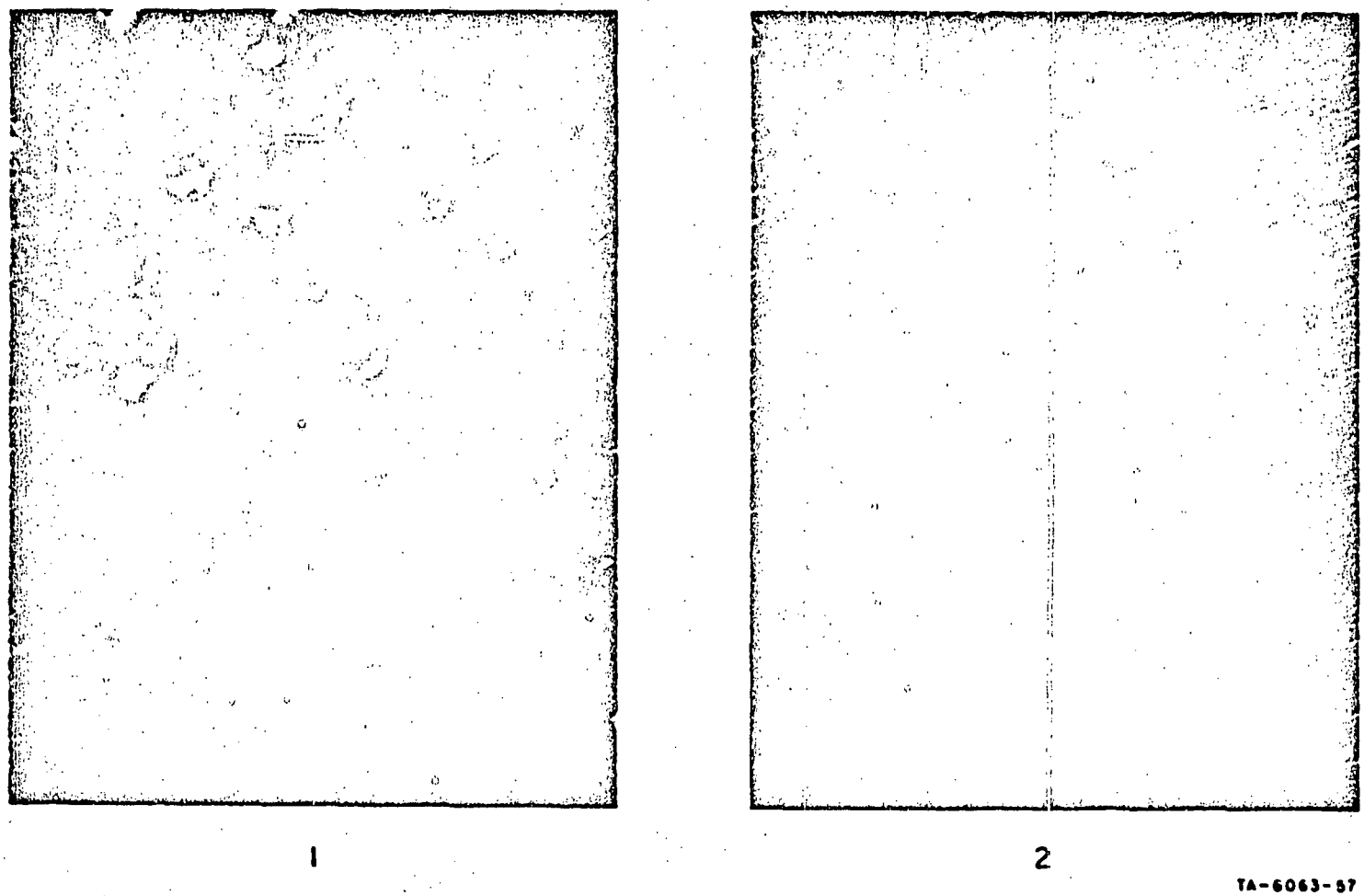

FIG. 48 PHOTOMICROGRAPHS OF INTERNAL AND EXTERNAL SURFACES OF BOURDON TUBE FROM GAGE "B" NOT EXPOSED TO N_2O_4 (53X). (1) inner surface; (2) exterior surface for comparison.

RE-ORDER No. 67-347

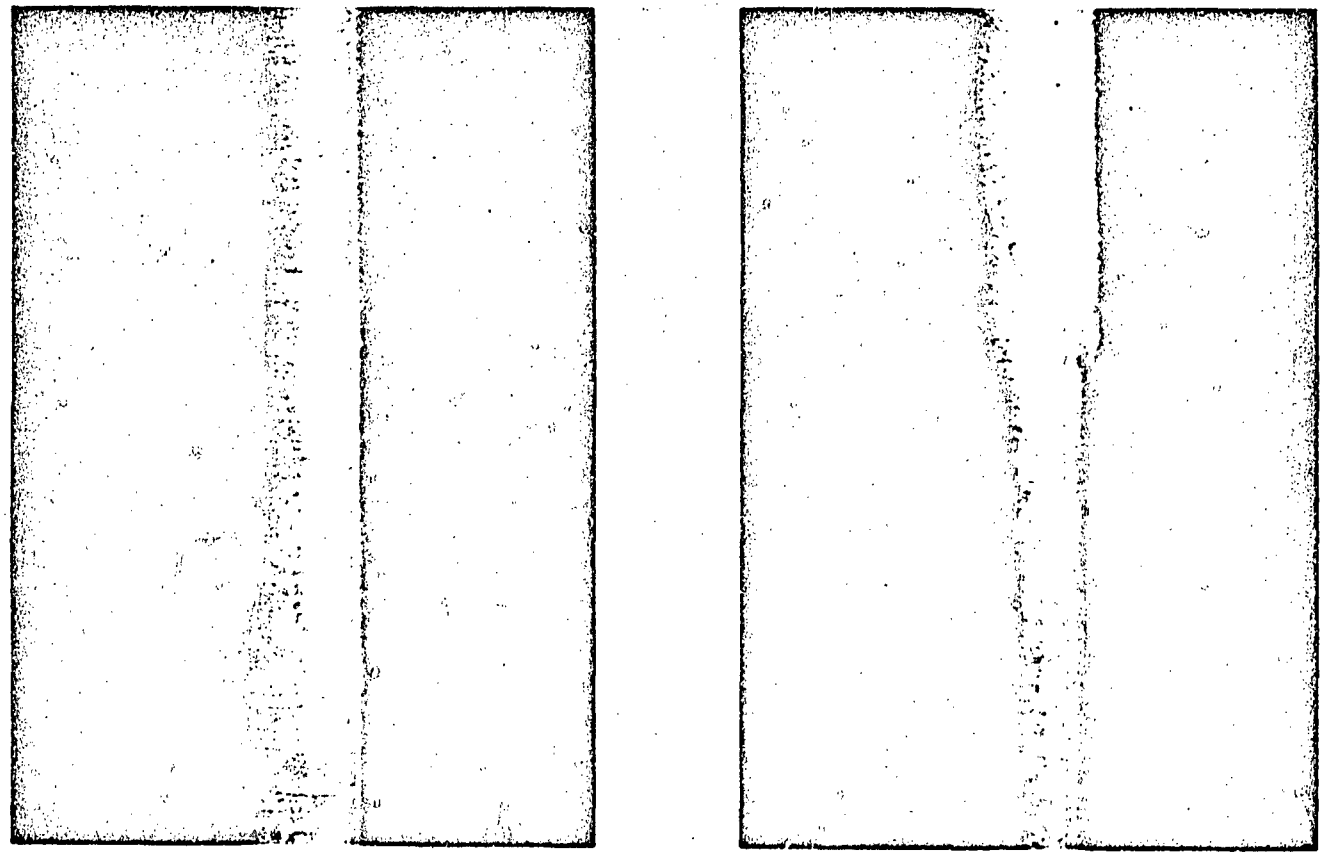

FIG. 49 ENLARGED PHOTOMICROGRAPH OF TEST SPECIMENS AFTER REMOVAL OF CORROSION PRODUCTS (10X). (246) 356-T6 aluminum alloy; (247) 356-T6 aluminum alloy.

BE ORDER NO. 67-34

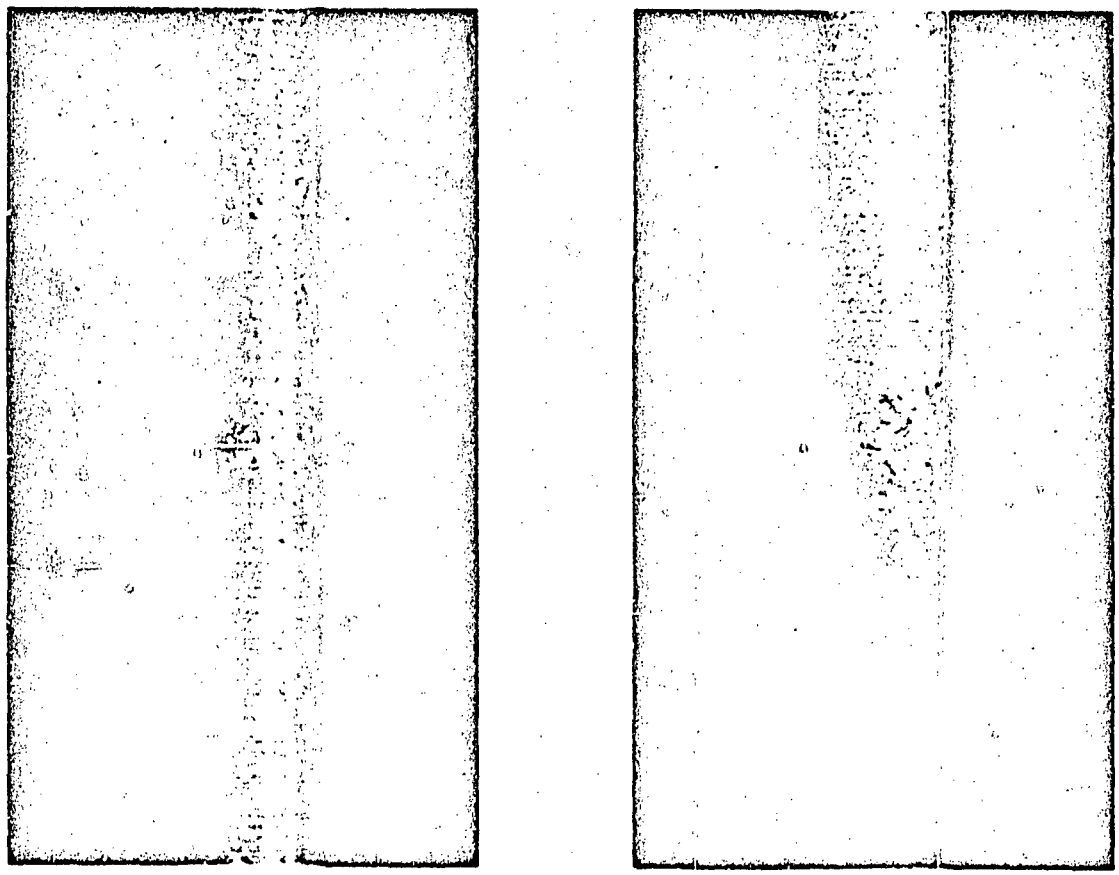

FIG. 50 ENLARGED PHOTOMICROGRAPHS OF TEST SPECIMENS AFTER REMOVAL OF CORROSION PRODUCTS (10X). (0082) Hastelloy B; (0076) magnesium A231C.

RE-ORDER NO. 67-347

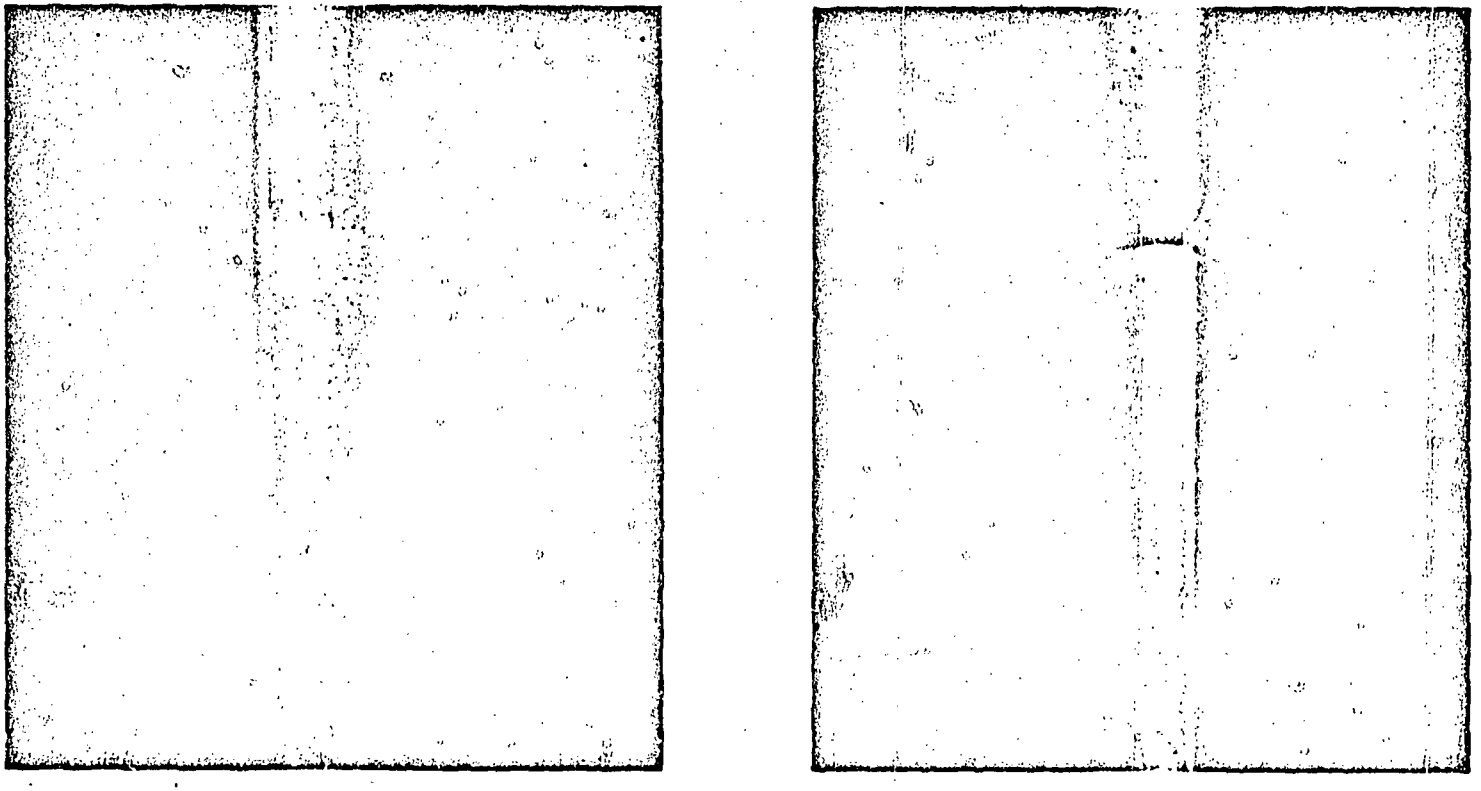

FIG. 51 ENLARGED PHOTOMICROGRAPH OF TEST SPECIMENS AFTER REMOVAL OF CORROSION PRODUCTS (10X). (0078) sintered molybdenum; (0079) arc-cast molybdenum.

RECORDED IN NEL-UNCLAS 67-34

RE-ORDER No. 67-347

VI. RECOMMENDATIONS FOR STORAGE PROCEDURES

Several observations were made during the course of the analyses which lead to suggestions which may improve the validity of similar storage tests.

Storage Vessel Design

As pointed out in Section V, minor to gross contamination was traced to the corrosion products of the Kovar metal tubing used to affix a metal pressure gage to the glass test capsule. However, since the presently-reported storage tests were initiated, JPL has been converting to all-glass capsules with external strain gages for pressure measurements. Indeed, it is questioned whether pressure measurements are necessary, since a 3-component system diagram pressure vs temperature could be used to deduce the pressure after the test system has been dismantled and the N_2O_4 composition ascertained. Data obtained in other studies (and corroborated by these tests) suggests that only NO and H_2O are the major products (volatile) of corrosion of metals.

Labeling

It is suggested that the storage capsules be scribed with a fluoride-etchant or fused-on marking ink for ultimate identification. The inks used to mark gage faces faded or were washed away when the capsules were cooled by dry ice. Tags are not suggested; scribed marks on glass are to be shunned because the localized strains may lead to breakage.

Specimens

The reliability of microscopic examination for evidences of corrosion and photomicrography would be improved if the ends of the cylindrical specimens were finished to a uniform high polish. The flat surfaces presented by the ends of specimens are ideal for photomicrography.

Preceding page blank

RE-ORDER No. 67-347

Tests should be set up at least in quadruplicate. In spite of great care, storage capsules may be broken or, in freak incidents, burst. Further, data have little statistical value when less than three determinations are performed.

Cleanliness, that is, preparation of test specimens (and capsules) without organic contamination, such as fingerprints, grease, and solvents, is absolutely essential to successful storage tests. The chloride content of fingerprints is dramatically effective in inducing corrosion of metals.

RE-ORDER No. 67-347

Appendix A

JPL PASSIVATING PROCEDURES

Log No. 0088 Passivating Procedure for Wrought Aluminum Alloys

Step	Solution/Treatment	Temp., °F	Time
1.	5 oz Na_3PO_4/gal water	180-200	Until bright appearance (1-3 min)
2.	Distilled water rinse		Until pH of run-off water equals pH of source water within pH 0.5
3.	1% HF, 1% HNO_3, 98% H_2O		1 minute
4.	Same as Step 2		
5.	Dry by blowing moisture off with oil-free, moisture-free nitrogen gas, or bake in vacuum oven at 120°F/5 min		

Log No. 0090 Passivating Procedure for Stainless Steel Alloys

Step	Solution/Treatment	Temp., °F	Time
1.	HNO_3:H_2O at 1:4,	120	20 min
	or HNO_3:H_2O 1:1	Rm. temp.	1-2 hours
2.	Distilled water rinse	Rm. temp.	Until pH of run-off water equals pH of source water within pH 0.5
3.	Dry by blowing moisture off with oil-free, moisture-free nitrogen gas or bake in vacuum oven at 120°F/5 min		

RE-ORDER No. 67-347

Log. No. 0092 Passivating Procedure for Wrought Magnesium Alloys

Step	Solution/Treatment	Temp., °F	Time
1.	24 oz CrO_3/gal H_2O, 4 oz $NaNO_3$/gal H_2O, 1/8 oz CaF_2/gal H_2O	Room	20 sec
2.	Distilled water rinse	Room	Until pH of run-off water equals pH of source water within pH 0.5
3.	Dry by blowing moisture off with oil-free, moisture-free nitrogen gas or bake in a vacuum oven at 120°F/5 min		

Log No. 0093 Passivating Procedure for Titanium Alloys

Step	Solution/Treatment	Temp., °F	Time
1.	HNO_3, 1-1/2 pints/gal; HF, 3 oz/gal; H_2O, remainder	Room	1 min
2.	Distilled water rinse	Room	Until pH of run-off water equals pH of source water within pH 0.5
3.	Dry by blowing moisture off with oil-free, moisture-free nitrogen gas or bake in a vacuum oven at 120°F/5 min		

Log. No. 0094 Passivating Procedure for Nickel and Nickel Alloys

Step	Solution/Treatment	Temp., °F	Time
1.	1 part HCl: 2 parts H_2O	180	2 min
2.	Distilled water rinse, immediately	160-180	
3.	2 parts H_2SO_4, 1 part HNO_3, 5 parts H_2O	Room	2 min
4.	Distilled water rinse	Room	Until run-off water pH equals source water pH within pH 0.5
5.	Dry by blowing moisture off with oil-free, moisture-free nitrogen gas or bake in a vacuum oven at 120°F/5 min		

RE-ORDER No. 67-347 34

Log. No. 0095 Passivating Procedure for Pure Molybdenum

Step	Solution/Treatment	Temp., °F	Time
1.	Hot chromic acid cleaning solution: Dissolve 100 g $Na_2Cr_2O_7 \cdot 2H_2O$ in 1 liter H_2SO_4 with heating	160	2 min
2.	Distilled water rinse		Until run-off water pH equals source water pH within pH 0.5
3.	Dry by blowing moisture off with oil-free, moisture-free nitrogen gas or bake in a vacuum oven at 120°F/5 min		

Log. No. 0096 Passivating Procedure for Tantalum

Step	Solution-Treatment	Temp., °F	Time
1.	Hot chromic acid cleaning solution: Dissolve 100 g $Na_2Cr_2O_7 \cdot 2H_2O$ in 1 liter H_2SO_4 with heating	160	2 min
2.	Distilled water rinse	Room	Until run-off water pH equals source water pH within pH 0.5
3.	Dry by blowing moisture off with oil-free, moisture-free nitrogen gas or bake in vacuum at 120°F/5 min		

Log. No. 0097 Passivating Procedure for Mild Steel Alloys

Step	Solution/Treatment	Temp., °F	Time
1.	5-10% HCl with distilled water	Room	5-15 sec
2.	Distilled water rinse	Room	Until run-off water pH equals source water pH within pH 0.5
3.	Dry by blowing moisture off with oil-free, moisture-free nitrogen gas or bake in vacuum at 120°F/5 min		